

 M 2014

**U. PORTO**  
**FEUP** FACULDADE DE ENGENHARIA  
UNIVERSIDADE DO PORTO

# **NEUROKINECT**

**KINECT-BASED SYSTEM FOR MOTION ANALYSIS AND QUANTIFICATION IN  
NEUROLOGICAL DISEASES**

**HUGO MIGUEL PEREIRA CHOUPINA**

DISSERTAÇÃO DE MESTRADO APRESENTADA  
À FACULDADE DE ENGENHARIA DA UNIVERSIDADE DO PORTO EM  
ENGENHARIA BIOMÉDICA





**FEUP** FACULDADE DE ENGENHARIA  
UNIVERSIDADE DO PORTO

# **NeuroKinect: Kinect-based System for Motion Analysis and Quantification in Neurological Diseases**

**Hugo Miguel Pereira Choupina**

Supervisor: PhD João Paulo Trigueiros Silva Cunha

Mestrado em Engenharia Biomédica

July, 2014





Faculdade de Engenharia da Universidade do Porto

**NeuroKinect: Kinect-based System for Motion Analysis  
and Quantification in Neurological Diseases**

**Hugo Miguel Pereira Choupina**

Dissertation submitted to Faculdade de Engenharia da Universidade do Porto  
to obtain the degree of

**Masters in Biomedical Engineering**

President: PhD Ana Maria Mendonça

Referee: PhD João Paulo Vilas-Boas

Referee: PhD João Paulo Cunha

---

July, 2014



*Ao meu falecido Tio-Avô Francisco, aos meus Pais e ao meu Irmão.*



# Abstract

Many neurological diseases, such as Parkinson's disease (PD) and epilepsy, can significantly affect patients' motor function, often leading to a dramatic loss of their quality of life. Human motion analysis is undoubtedly regarded as fundamental towards an early diagnosis and an enhanced follow-up in this type of diseases. In this contribution, NeuroKinect, a markerless system for human motion analysis in neurological diseases is presented. This system includes an RGB-D camera (Microsoft Kinect XBOX 360 and Kinect v2 for XBOX One) and two applications, *KiT* (KinectTracker) and *KiMA* (Kinect Motion Analyzer), running in a portable PC, which enable the acquisition, visualization and management of RGB, depth, infrared, body-index and 3D tracking data provided by the sensor. The presented system is a portable, low-cost solution, suitable for use in a clinical environment, which has already been deployed in an Epilepsy Monitoring Unit (in Munich, Germany) and used in multiple healthcare scenarios. In addition, in the Epilepsy scenario, a new tool named KiSA (Kinect Seizure Analyzer) makes use of the RGB-D information from *KiT* and *KiMA* to track and quantify uncoordinated seizure movements.

**Keywords:** RGB-D camera. Kinect. motion quantification, movement-related diseases, Parkinson's disease, epilepsy.



# Resumo

Várias doenças neurológicas, tais como a doença de Parkinson ou a Epilepsia, podem afectar de forma significativa as capacidades motoras de um paciente, levando a uma perda significativa da sua qualidade de vida. A Análise do movimento humano é reconhecidamente considerada como fundamental na obtenção de um diagnóstico precoce e no acompanhamento ao longo do tempo deste tipo de doentes. Nesta contribuição, o NeuroKinect, um sistema não-vestível para análise de movimento humano em doenças neurológicas é apresentado. O sistema inclui um sensor RGB-D (Microsoft Kinect XBOX 360 e Kinect v2 XBOX One) e duas aplicações, o *KiT* (KinectTracker) and *KiMA* (Kinect Motion Analyzer), que aquando instaladas num computador, permitem a aquisição, visualização e manipulação de informação RGB, profundidade, infra-vermelho, presença de um corpo e dados de esqueleto 3D providenciados pelo sensor. O sistema apresentado é portátil, e é uma solução low-cost, adequada á prática clínica, que foi já implementado numa unidade de monitorização de Epilepsia (em Munique, Alemanha) e usado em diversificados contextos hospitalares. Além disso, no cenário da Epilepsia, uma nova ferramenta chamada *KiSA* (Kinect Seizure Analyser) utiliza a informação RGB-D do *KiT* e do *KiMA* para acompanhamento e quantificação de movimentos descoordenados em crises epiléticas.

**Keywords:** câmara RGB-D. Kinect. quantificação de movimento. doenças do movimento. Parkinson's. epilepsia.





# Acknowledgments

Uma caminhada tem sempre um início, meio e fim. Os últimos 5 anos da minha vida foram riquíssimos em todos os aspectos. Ultrapassei obstáculos que nunca até então tinha tido coragem de enfrentar, e conheci pessoas que de certa forma fazem de mim aquilo que sou hoje. Mais do que obter um grau ou ter um currículo, a faculdade é efectivamente uma Escola para a vida. Neste trajecto, muita gente contribuiu, de forma directa ou indirecta, aos quais passo a agradecer.

Primeiro de tudo, a minha maior palavra de agradecimento e gratidão ao Professor João Paulo Cunha. Aquilo que eu era há dois anos atrás em nada se compara com aquilo que sou hoje. A minha evolução praticamente seguiu uma linha exponencial ao longo do tempo que tive a oportunidade de trabalhar, ouvir e acima de tudo aprender sob a sua orientação. Deu-me um enorme voto de confiança quando me aceitou para integrar a sua unidade de investigação. Obrigado por todo o acompanhamento científico prestado, e por tentar tirar de mim sempre mais e melhor, sempre com aquela pergunta difícil e com desafios constantes. Aproveite aqui também para publicamente agradecer o financiamento da viagem à Alemanha.

À Ana Rocha, por ter sido quase que como uma co-orientadora para mim: obrigado por todos os momentos de troca de informação, inter-ajuda e acima de tudo de aprendizagem constante. Foi um prazer enorme ter trabalhado em constante parceria contigo.

Ao grupo BRAIN em geral, mas em especial à Nadia e ao Pedro Pinto, obrigado por partilharem comigo diversos momentos ao longo dos dois últimos anos.

Ao Filipe Monteiro e ao Pedro Costa, deixo uma palavra particular por todo o brainstorm que fizeram comigo sempre que precisei, e por serem duas pessoas impecáveis em todos os aspectos. O meu muito obrigado.

Aos meus amigos, aqueles que fiz na FEUP, Ivo Silva, Mario Espinoza, Raquel Alves, Cláudia Tonelo, Maria Ramalho, e aos meus restantes amigos da Católica, Francisco Pereira, Diogo Borges, Joana Silva, Carla Pereira, Ana Sofia Neto, Tiago Heitor, Joana Silva, parte desta minha conquista deve-se a tudo aquilo que vivi ao vosso lado de alguma maneira e agradeço-vos por isso. Da mesma forma, os meus amigos de sempre, que eu não esqueço, apesar de mais ausentes mas sempre presentes, Diogo Pinto, Tatiana Lima, Diana Costa e Filipa Gregório, obrigado.

À minha família, em especial aos meus primos Armindo e Ana Isabel Costa, porque são e sempre serão um modelo para mim em todos os aspectos. Ao meu irmão, por ser um miúdo incrível e por me ajudar em tudo o que preciso. E aos meus pais, porque são pessoas únicas, que lutam todos os dias para que o nosso futuro seja risonho, para que tenhamos mais oportunidades do que aquelas que eles tiveram. Aos três, amo-vos do fundo do coração.

À Diana Silva. Por não me deixares cair. Por me motivares e seres uma pessoa especial para mim. Por me teres ensinado a lutar e a não desistir, por seres a minha companhia e a minha alegria constante ao longo dos últimos três anos e meio. És um orgulho para mim, e grande parte desta conquista é tua. @. Obrigado.



*“Few things can help an individual more than to place responsibility on him, and to let him know that you trust him.”*

Sir Booker T. Washington



# Contents

<b>List of Figures</b>	<b>xvi</b>
<b>List of Tables</b>	<b>xvii</b>
<b>List of Abbreviations</b>	<b>xix</b>
<b>1 Introduction</b>	<b>1</b>
1.1 Motivation . . . . .	2
1.2 Objectives . . . . .	2
1.3 Resulted Publications . . . . .	3
<b>I State of the Art</b>	<b>5</b>
<b>2 Neurological Diseases</b>	<b>7</b>
2.1 Parkinson’s Disease . . . . .	7
2.1.1 Background . . . . .	7
2.1.2 Modern Definition . . . . .	7
2.1.3 Health and Social Implications . . . . .	8
2.1.4 Symptoms . . . . .	8
2.1.5 Diagnosis . . . . .	9
2.1.6 PD Rating Scales . . . . .	11
2.1.7 Gait Disturbances in PD . . . . .	11
2.1.8 Treatment . . . . .	11
2.2 Epilepsy . . . . .	12
2.2.1 Background . . . . .	12
2.2.2 Modern Definition . . . . .	12
2.2.3 Types of Seizures . . . . .	13
2.2.4 Semiology of Epileptic Seizures . . . . .	14
2.2.5 Epilepsy Triggers . . . . .	15
2.2.6 Diagnosis . . . . .	16
2.2.7 Treatment . . . . .	20
<b>3 Movement Analysis and Quantification</b>	<b>23</b>
3.1 Passive marker-based motion capture systems . . . . .	24
3.2 RGB-D Sensors . . . . .	26
3.3 Kinect XBOX 360 . . . . .	29
3.3.1 Kinect Basic Principles . . . . .	29
3.3.2 Sensor Properties . . . . .	31

3.4	Kinect for Windows (K4W) v2 . . . . .	34
3.5	Gait Quantification in Parkinson Disease . . . . .	36
3.6	Movement Quantification in Epilepsy . . . . .	36
<b>4</b>	<b>Summary and Proposed Methodology</b>	<b>43</b>
<b>II</b>	<b>NeuroKinect: A Kinect-based System for Movement Analysis and Quantification in Neurological Diseases</b>	<b>45</b>
<b>5</b>	<b>NeuroKinect: A Kinect-based System for Movement Analysis and Quantification</b>	<b>47</b>
5.1	NeuroKinect, KiT and KiMA . . . . .	47
5.1.1	KiMA Requirements . . . . .	48
5.1.2	NeuroKinect Architecture . . . . .	49
5.1.3	KiMA Application . . . . .	49
5.1.4	KiMA for Kinect v2 . . . . .	57
5.2	Kinect 2 Matlab Dynamic Linked Library (DLL) . . . . .	59
5.2.1	KinectforMatlab.dll . . . . .	59
<b>6</b>	<b>NeuroKinect usage in the Healthcare Context: Practical Examples</b>	<b>61</b>
6.1	Parkinson's Disease . . . . .	61
6.2	Epilepsy . . . . .	62
6.2.1	Physical Constraints in the Epilepsy Routine . . . . .	63
6.2.2	Bed Subtraction Algorithm . . . . .	66
6.2.3	Optical Flow Approach . . . . .	68
6.2.4	3D Motion Tracking Algorithm based on Optical Flow . . . . .	74
6.2.5	Quantification Results . . . . .	77
6.2.6	KiSA: Kinect Seizure Analyzer . . . . .	84
6.3	Other usages of NeuroKinect . . . . .	89
6.3.1	Familial Amyloid Polyneuropathy (FAP) and Movement Rehabilitation Strategies in Patients that suffered Strokes . . . . .	89
<b>7</b>	<b>Discussion and Future Work</b>	<b>91</b>
	<b>Bibliography</b>	<b>95</b>
	<b>Index</b>	<b>101</b>
<b>A</b>	<b>Steps for KinectforMatlab.dll instalation</b>	<b>101</b>
<b>B</b>	<b>Portuguese Annual Biomedical Students Conference</b>	<b>105</b>
<b>C</b>	<b>Microsoft Kinect for Windows Developer Preview Conference</b>	<b>109</b>
<b>D</b>	<b>Reference Letter from LMU</b>	<b>113</b>
<b>E</b>	<b>Parkinson's Disease Assessment Based on Gait Analysis Using an Innovative RGB-D Camera System - EMBC 2014</b>	<b>117</b>

# List of Figures

2.1	Parkinson’s Disease Flowchart on the Health Systems Requirements throughout the disease progression <a href="#">WHO [2006]</a> . . . . .	8
	10figure.caption.9	
2.3	Epileptic Seizures electroencephalography (EEG) pattern. . . . .	13
	14figure.caption.11	
2.5	Semiological Seizure Classification (Adapted from: <a href="#">Noachtar and Peters [2009]</a> ). . . . .	15
2.6	Normal electrocardiography (ECG) + EEG Signal. . . . .	16
	17figure.caption.14	
2.8	"‘Stills from video-EEG recording. 1) Micturating; 2) forward flexion of upper trunk and extension of upper extremities, and a beta burst (arrow) at Cz electrode; 3) fall and attenuation of the EEG activity (arrow); and 4) rhythmic 2 Hz spike and wave discharges at Cz electrode during postictal phase" <a href="#">Rathore et al. [2008]</a> . . . . .	17
2.9	"Ictal video/EEG recording during a typical episode of yawning. The EEG of the episode shows low-to medium-voltage fast activity over bilateral central areas lasting a few seconds, followed by rhythmic spikes and polyspikes involving bilateral central and frontal areas during which the patient yawns. Multiple artifacts related to mouth movement and tongue protrusion are also evident. A prolonged subclinical sequence of spike-and wave complexes is evident over frontal and central areas after the artifacts. Arrows indicate the correlation with the snapshot of the video." <a href="#">Specchio et al. [2011]</a> . . . . .	18
	19figure.caption.17	
2.11	PET Scan <a href="#">Spencer [1994]</a> . . . . .	19
	20figure.caption.19	
3.1	Anterior and posterior view of markers placement general scheme (red – fixed markers for dynamic full body analysis; green – markers for static view; yellow posterior view). . . . .	25
3.2	VICON F40 motion capture system. . . . .	26
3.3	Classification of Depth Measurement Techniques <a href="#">Castaneda and Navab [2011]</a> . . . . .	26
3.4	Time-of-Flight Cameras Depth Estimation Process <a href="#">Fuchs and Hirzinger [2008]</a> . . . . .	27
3.5	DepthSense DS325. . . . .	27
3.6	DepthSense DS311. . . . .	28
	28figure.caption.26	
3.8	Asus Xtion Pro Live. . . . .	29
3.9	Kinect v1 Joint List. . . . .	30
3.10	Kinect XBOX 360 Vision Sensor. . . . .	31
3.11	Kinect Color and Depth acquisition: IR and RGB physical locations <a href="#">Zollhöfer et al. [2011]</a> . . . . .	31
3.12	Shadow formation process using Kinect <a href="#">Andersen et al. [2012]</a> . . . . .	33

3.13	The object in the figure blocks the path of the laser. Since the depth estimate is based on the pattern projected by the laser, Kinect cannot estimate depth outside the line of sight of the laser <a href="#">Andersen et al. [2012]</a> . . . . .	33
3.14	Kinect for Windows version 2 available for the project thesis. . . . .	35
3.15	Kinect for Windows version 2: 25 Joints Collection Enumeration. . . . .	35
3.16	The setup of QMovES System. A CCD camera acquires video sequences into a PC where a digital video-EEG system and the QMovES software tool are installed <a href="#">Li et al. [2002]</a> . . . . .	38
3.17	22 landmark positions defined for the full-body marker positioning system <a href="#">Li et al. [2002]</a> . . . . .	38
3.18	Schematic representation of the procedure for movement quantification used in QMovES <a href="#">Li et al. [2002]</a> . . . . .	39
3.19	Video setup geometric model. Adapted from <a href="#">Cunha et al. [2003]</a> . . . . .	40
3.20	System setup with the 4 high-speed SVCams to achieve a 3D motion tracking system for seizure movements. A data-station processes the massive information coming from the cameras and feeds pre-processed data to the workstation where the MOIs are analyzed <a href="#">Cunha et al. [2012]</a> . . . . .	42
5.1	KinecTracker v1 UI. . . . .	48
5.2	KiMA Use-Case Diagram for Kinect v1. . . . .	49
5.3	NeuroKinect Use-Case Diagram. . . . .	50
5.4	NeuroKinect Architecture <a href="#">Rocha A [2014]</a> . . . . .	50
5.5	Main Window UI of KiMA application, including the display of color, depth and skeleton data and the mouse-binded Context menu. . . . .	51
5.6	KiMA activity diagram. . . . .	52
5.7	KiMA UI: At the right-side, the tree-view information regarding all labels and events. . . . .	53
5.8	KiMA New Label Example: the user must name the event, but an additional description is optional. . . . .	54
5.9	KiMA XML Example: XML organization after the analysis of an acquisition. . . . .	55
5.10	KiMA v2 Use-Case Diagram, with the two new streams: Infrared and BodyIndex . . . . .	56
5.11	KiMA v2: Depth, Color and Body streams . . . . .	57
5.12	KiMA v2: BodyIndex, Infrared and Body streams . . . . .	58
5.13	KiMA v2: Folder data Organization when exporting Events . . . . .	58
6.1	Experimental setup used for data acquisition, including the coordinate system associated with the Kinect. . . . .	62
6.2	KiMA v1: Field-of-view of the Epilepsy Room. Typical distances range between 1.9m-2.1m from the sensor to the patient. . . . .	63
6.3	Epilepsy Activity Diagram for KiMA: KiMA is used to segment and export the seizure Events, which are then made available via a secure FTP server. . . . .	64
6.4	KiMA v2 Infrared, Body and BodyIndex. . . . .	65
6.5	KiMA v2 Infrared, Body and Depth. . . . .	65
6.6	KiT v2 from LMU Bed: Trial tests to assess the new sensor robustness. . . . .	66
6.7	Seizure first depth frame. . . . .	67
6.8	Study to evaluate the difference between mask and color image using MATLAB <a href="#">H [2013]</a> . . . . .	68
6.9	Mean Variation of the Square Root Distance vs Depth of each frame of the training image set. . . . .	68



6.10	Result of Bed Subtraction over the first frame, after alignment between color and depth. . . . .	69
6.11	UML Activity Diagram of the Bed Subtraction Algorithm. . . . .	70
6.12	Schematic Representation of the conducted trial to perceive and validate the performance of the Optical Flow Algorithms. . . . .	71
6.13	Tracings of the 2D golf-ball movement in terms of the X and Y coordinates for the slowest movement. . . . .	72
6.14	Tracings of the 3D golf-ball movement in terms of the real depth value (provided by the Kinect) and the calculated theoretical one for the slowest movement. . . .	73
6.15	Tracings of the 2D golf-ball movement in terms of the Optical flow velocities for the slowest movement. . . . .	73
6.16	Epilepsy Seizure Frame, with bed subtraction performed and OF lines drawn in the frame. The orange arrow represents the actual lines (which represent the detected movement by the algorithm) that are intended to be tracked, whereas the red arrow represents the upper body movement. Note that the original image was rotated 90° for visualization purposes only. . . . .	75
6.17	UML Activity Diagram of the designed algorithm. . . . .	76
6.18	KiMA UI: Seizure initial frame. . . . .	77
6.19	Representation of the motion pattern experienced by the patient during the quantified seizure. . . . .	78
6.20	MaxTRAQ 2D motion software UI. In the represented frame there is a marker with the centroid of the head at a certain moment in time. The green line represents the head movement throughout the frames. . . . .	79
6.21	Tracings of the body motion in X coordinate (anterior-posterior view), non-filtered and filtered, in function of time with the corresponding body positions. . . . .	79
6.22	Tracings of the body motion in Y coordinate (vertical), non-filtered and filtered, in function of time with the corresponding body positions. . . . .	80
6.23	Tracings of the optical flow magnitude velocity in function of time with the corresponding body positions. . . . .	80
6.24	Tracings of the optical flow magnitude horizontal velocity in function of time with the corresponding body positions. . . . .	81
6.25	Tracings of the optical flow vertical velocity in function of time with the corresponding body positions. . . . .	81
6.26	Tracings of the depth values, non-filtered and filtered, in function of time with the corresponding body positions. . . . .	82
6.27	Tracings of the velocity values filtered, in function of time with the corresponding body positions. . . . .	82
6.28	Tracings of the velocity values non-filtered and filtered of the Head, in function of time. . . . .	83
6.29	Tracings of the acceleration values filtered, in function of time with the corresponding body positions. . . . .	83
6.30	KiSA Use-Case Diagram . . . . .	84
6.31	KiSA activity diagram. . . . .	86
6.32	Main Window UI of KiSA application, including the display of color and optical flow images. In yellow: the menu bar; In red: the current timestamp; In orange: the elapsed time; In blue: the current frame number; In green: the video manipulation buttons. . . . .	87
6.33	UI of KiSA Parameters. . . . .	87

6.34	UI of KiSA Analysis. Representation of the depth tracing and the 3D position, as well as the statistics of the depth Head variation. . . . .	88
A.1	KinectforMatlab.dll Pipeline Procedure . . . . .	103

# List of Tables

3.1	Kinect Requirements Overview . . . . .	34
3.2	Kinect v2 overview. . . . .	35
6.1	Characteristics of the ball movement in terms of initial velocity, acceleration and the angle of the incline plane . . . . .	71
6.2	Results obtained on the Optical Flow algorithms: Maximum and Minimum Optical Flow velocities values of the ball, for the two algorithms. . . . .	72



# List of Abbreviations

CBF	Cerebral Blood Flow
CGD	Continuous Gait Disturbances
DBS	Deep Brain Stimulation
DLL	Dynamic Link Libraries
ECG	Electrocardiography
EEG	Electroencephalography
EGD	Episodic Gait Disturbances
FEUP	Faculdade de Engenharia da Universidade do Porto
GPI	Internal Globus Pallidus
MOI	Moment Of Interest
MRI	Magnetic Resonance Imaging
IR	Infrared
K4W	Kinect For Windows v2
KiMA	Kinect Motion Analyzer
KiSA	Kinect Seizure Analyzer
KiT	KinectTracker
JPC	PhD João Paulo Cunha
JMF	PhD José Maria Fernandes
OF	Optical Flow
PET	Positron Emission Tomography
PD	Parkinson's Disease
ROI	Region Of Interest
SDK	Software Development Kit
SPECT	Single Photon Emission Computed Tomography
STN	Subthalamic Nucleus
ToF	Time-of-Flight
UI	User-Interface



# Chapter 1

## Introduction

Technologies are now worldwide spread and became an intrinsic part of society. Technology is also constantly changing and, by now, new types of devices that have different properties than their antecessors (smaller size, wearable, wireless) are emerging. Everyone can now be a Q-Selfie (Quantified Self, QS), meaning that an individual can monitor, for instance, its own heart rate during one night using a wearable t-shirt [Cunha et al. \[2010\]](#). The QS movement is based on the self-tracking of any kind of biological, physical, behavioral, or environmental information. The continuous monitoring of such variables have already been done in high-performance teams and players, but with a high cost associated. By using this recent and free applications, available online, everyone can monitor almost everything [Swan \[2013\]](#).

Nowadays, in Healthcare, several medical devices and high powerful processing techniques are being used, followed by continuous improvements in the DNA research, which is flourishing new frontiers for disease treatment and diagnosis.

The need for better quality and personalization of the medical care provided by clinical institutions to patients spiked this interest in medical devices that brought up valuable clinical information that until now was not available.

Technology takes a big role in healthcare and by now, besides the state-of-art imaging modalities (magnetic resonance imaging (MRI) or computed tomography (CT)), numerous hospitals have their owns gait-labs, as well as video-EEG systems to enhance the diagnosis process.

Besides data acquisition, new developments on algorithms for signal processing and methodologies for data analysis will allow the extraction of other clinical relevant parameters than can be interpreted by physicians. With the increase of life expectancy and elderly population, much attention should be given to the need of constant care provision and follow-up.

Therefore, information technology associated with Healthcare greatly enhances the amount of information available for the physicians, improving both the efficiency and quality of healthcare [Wu et al. \[2006\]](#). In order to provide the best care possible to a patient, the amount of information available for the physicians should be as much as possible. In diseases where the movement is impaired, accurate information regarding that same impairment is critical to the diagnosis process.

## 1.1 Motivation

Many neurological diseases are characterized by movement impairments that affect the patients quality of life. Often, this patients are carefully followed up by physicians and therefore, accurate information of the disease progress throughout time is critical.

Most of the times, this information is based on the visual analysis provided by a video-recording, which only allows a qualitative instead of an accurate quantitative analysis. Movement analysis of movement-related diseases is typically achieved by using wearable passive-marker systems, under a controlled environment. Performing such analysis within the normal routine of an Hospital is a very demanding task (it is necessary room availability, the physicians presence and overall it is a time-consuming activity), that makes them unsuitable and unpractical for many healthcare routine environments. For that specific problem, the emergent 3D RGB-D cameras have already shown greater ability for the development of a markerless based system.

RGB-D cameras are sensing systems that capture RGB images along with per-pixel depth information, as well as 3D subject tracking data: all of this information is obtained in the most comfortable way to the patient, since that, for this data acquisition, the sensor only needs to be placed in front of the patient.

RGB-D cameras characteristics makes them suitable for enhancing the diagnosis process by supporting the physicians with quantitative information, besides the qualitative analysis that is already performed by video (visual inspection). The opportunity of using RGB-D cameras for human motion analysis and quantification, in a markerless way, would be of great value for the biomedical engineering field as well as for the routine healthcare systems.

## 1.2 Objectives

In this thesis, the aim is to make a contribution to the development of a markerless based video-system, based on a low-cost RGB-D camera, that: can be used in the clinical neurology environment, in multiple scenarios; allows the acquisition and tracking of the movement and is also unobstructive to the patients given their health conditions. Thus, systems that use markers or reflectors, for example, attached to the patient's body are out of scope of the goal of this thesis.

Firstly, in this document, the state of the art regarding two targeted neurological diseases will be reviewed and then focus will be pointed onto motion tracking sensors, with particular incidence on Kinect. Further examples of existing technologies based on the same premise will be also covered without so much detail. Finally, attention will be drawn to movement quantification, with particular emphasis in Parkinson's and epilepsy movement analysis. Chapter 5 addresses KiMA software and chapter 6 the use of the NeuroKinect system in the healthcare context, whereas in the final chapter the work developed is reviewed and analyzed.



### 1.3 Resulted Publications

The present thesis resulted in the following publications:

- Ana Patrícia Rocha, Hugo Choupina, José Maria Fernandes, Maria José Rosas, Rui Vaz, João Paulo Silva Cunha. *Parkinson's Disease Assessment Based on Gait Analysis Using an Innovative RGB-D Camera System*. In 36th Annual International IEEE EMBS Conference Chicago, USA: 2014 - Accepted for Publication (see Appendix E).
- João Paulo Silva Cunha, Ana Patrícia Rocha, Hugo Choupina, José Maria Fernandes, Maria José Rosas, Rui Vaz. *Sistema de quantificação 3D de movimento portátil e de baixo custo para estimativa do sub-score de marcha em doentes parkinsónicos*. In Sinapse no. 1 volume 14 (2014): 67.
- Ana Patrícia Rocha, Hugo Choupina, José Maria Fernandes, Maria José Rosas, Rui Vaz, João Paulo Silva Cunha. *Estimativa do sub-score UPDRS de marcha em doentes parkinsónicos usando um sistema de quantificação 3D de movimento portátil e de baixo custo*. In 30º Congresso Nacional da Sociedade Portuguesa de Neurocirurgia.

Some other publications are also being prepared based on some of the contributions here reported.



## **Part I**

# **State of the Art**



## Chapter 2

# Neurological Diseases

Several neurological diseases produce motion impairments in patients. In the present thesis we have focused on two of them: Parkinson's and Epilepsy.

### 2.1 Parkinson's Disease

#### 2.1.1 Background

Parkinson's disease (PD) is named after the London general practitioner, James Parkinson, who was the first person to describe the “paralysis agitans”, a condition that lately was renamed Parkinson Disease by Jean-Martin Charcot.

In his work, where it was described many of the clinical features of the condition (“An Essay on the Shaking Palsy (1817)”) [James Parkinson Essay \[1817\]](#), James Parkinson refers the medical condition by the term said above which captures a peculiar characteristic of the disease: the combination of movement loss (also known as hypokinesia) with stiffness (i.e. rigidity) and tremor [James Parkinson Essay \[1817\]](#).

#### 2.1.2 Modern Definition

PD is an idiopathic progressive neurodegenerative disease that results from the death and degeneration of brain cells responsible for producing dopamine. Dopamine [Bernheimer et al. \[1973\]](#) is a neurotransmitter, released by the brain, that is responsible for a number of important physiological functions in the bodies of animals, such as movement, memory or behavior and cognition.

The deficiency or excess of this vital chemical molecule is the main cause of several disease conditions. Dopamine is produced in the dopaminergic neurons in the ventral tegmental area (VTA) of the mid-brain, in the *substantia nigra pars compacta*, and also in the *arcuate nucleus* of the hypothalamus.

This lack of dopamine results in a dysregulated motion action, which is controlled by the basal ganglia (responsible for the movement function), that depends on a certain amount of dopamine to function at peak efficiency. The process occurs via dopamine receptors, and, every time that

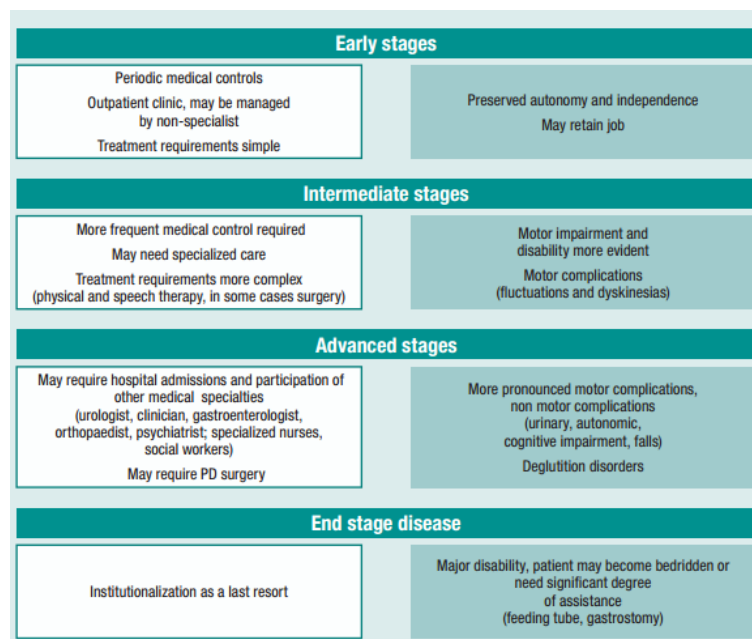


Figure 2.1: Parkinson's Disease Flowchart on the Health Systems Requirements throughout the disease progression WHO [2006].

there is a deficiency of the molecule in the brain, movements may become impaired Schultz [2007] Fellous and Suri.

### 2.1.3 Health and Social Implications

An estimated seven to ten million individuals worldwide have PD<sup>1</sup>. This number is expected to rise significantly in the future Dorsey et al. [2007], with 60,000 new cases being currently reported every year only in the U.S.

Information from WHO WHO [2006] states that there is a higher prevalence and incidence of PD in males. Incidence increases with age, but an estimated four percent of people with PD are diagnosed before the age of 50.

The progression of the disease varies among different individuals, meaning that symptoms continue and worsen over a period of years. Over this time, patients autonomy is lost and that affects themselves as well as their carers quality of life. The left-side of Figure 2.1 provides a flowchart on health systems requirements as the disease progresses.

### 2.1.4 Symptoms

PD is characterized primarily by movement dysfunctions and with time cognitive functions are also affected. People that present Parkinsonism symptoms often demonstrate hypokinesia, akinesia, bradykinesia, rigidity and tremor NCC [2006]. Impaired postural balance is often frequently reported.

<sup>1</sup>Parkinson's Disease Foundation <http://www.pdf.org/>

The most debilitating ones are hypokinesia and akinesia. Studies reported that other impairments could also include dystonia and dyskinesias [NCC \[2006\]](#) [Hausdorff \[2009\]](#).

Hypokinesia is characterized by the decrease in body movement, and its effect is more noticeable when the individual is requested to do movement sequences such as walking, writing and speaking or even when performing multiple tasks that require self-coordination.

Akinesia is the inability to initiate movement due to the degeneration of the brain cells responsible for selecting and activating the correct motor programs. The impact in the patient life is tremendous since he loses autonomy in routine tasks such as standing, dressing and even speaking.

Bradykinesia is referred to the slowness of movement and it is also associated to other disorders of the basal ganglia. It is also associated to what is normally referred as “stone face”, typical in PD patients.

Tremor is an involuntary muscular contraction often seen in PD and its one of the earliest symptoms to arise. It is very tricky to assess since tremor does not affect tremendously the patient life and it easily disappears during voluntary's movements. Resting tremor in PD can occur as an isolated symptom or can be seen accompanied by others.

Rigidity is also one of the primary symptoms of PD and refers to stiffness and resistance of movement in a body part. Rigidity may occur in the neck, shoulders, hips, ankles or hands [NCC \[2006\]](#) [Hausdorff \[2009\]](#) [Jankovic \[2008\]](#). [Figure 2.2](#) presents some of the symptoms describe above, as well as other typical impairments, such as the shuffling gait.

### 2.1.5 Diagnosis

The initial symptoms of the disease usually manifest after mid-age of the individual. PD can also be caused by drugs and less common conditions such as multiple system atrophy (MSA) or progressive supranuclear palsy (PSP) [NCC \[2006\]](#). The disease is mainly a movement disorder, but in fact other impairments frequently develop, such as the ones seen on the right side of [Figure 2.1](#).

Medical imaging is a tool that cannot be applied in diagnosis, since MRI and CT scans of the patients appear normal. In addition, there are no definitive biological or imaging markers that can be used in the imaging process [WHO \[2006\]](#).

The brain changes that occur are microscopic, on a chemical level, and they are not revealed by these scans [NCC \[2006\]](#). Physicians assessment is then based on the patient history and also stringent clinical criteria. Expert physicians are intimately familiar with the characteristic history, signs and symptoms found when examining a person with PD. They then must judge how closely the history of symptoms and the neurological findings (from the physical examination) of any specific person match those of typical PD.

A specific exam that is often made is the evaluation of movement after the intake of PD medication (i.e. carbidopa-levodopa). If significant improvement happens, the diagnosis of PD will be



Figure 2.2: Parkinson's Disease Systematic Symptoms <sup>2</sup>



confirmed NCC [2006]. Additional exams may be also realized, but to exclude other diseases that imitate Parkinson's disease, such as stroke or hydrocephalus<sup>3</sup>.

### 2.1.6 PD Rating Scales

The progress of PD is different in each individual, and, physicians have tools that helps them understand the evolution during continuous follow-up consults, using rate-scales. This analysis is critical to assess the severity of the movements impairments and how much the disease affects a person's daily activities.

The state of motor function in patients with PD is commonly characterized by the Unified Parkinson Disease Rating Scale (UPDRS), whereby motor functions such as tremor, hypo-bradyakinesia, rigidity of hand and arm movements are examined and classified on five discrete levels of severity ranging from 0 to 4. The scale is divided in five levels, each one regarding different aspects of the patient life and autonomy. There is one section fully dedicated to the gait impairments (part III). The UPDRS scale is used to follow the progression of the disease and also to measure possible benefits of specific treatments and medications<sup>4</sup>.

### 2.1.7 Gait Disturbances in PD

PD is characterized by movement dysfunctions, usually the continuous (CGD) and episodic gait disturbances (EGD). EPD are occasional and intermittent, which act in a random way. Still there is no scientific explanation for their occurrence.

EGD includes festination (i.e. involuntary tendency to take short accelerating steps), hesitation and also freezing of gait.

CGD are alterations on the normal movement pattern that are persistent and easily spotted over time. Increase of stride length and gait variability are some of the normal alterations associated to this impairment Ebersbach et al. [1999] Morris et al. [1996] Morris et al. [2000]. Hausdorff Hausdorff [2009] reports that the mechanisms responsible for both continuous and episodic events are in some way independent of each other even though they result from the dysfunctions of the basal ganglia.

### 2.1.8 Treatment

Nowadays, there is still no cure for PD, but there are ways to help control the disease. The goal of the treatment is to provide a better quality of life for as long as possible. Patient quality of life deteriorates quickly if no treatment is applied after a positive diagnosis.

Pharmacological treatment help in controlling acuties directly related to the motor symptoms. This therapy can be classified into: symptomatic and neuroprotective. Usually, the Pharmacological treatment is based on levodopa (combined with a dopadecarboxylase inhibitor or with COMT

<sup>3</sup>Parkinson's Disease Foundation <http://www.pdf.org/>

<sup>4</sup>European Parkinson's Disease Association: Unified Parkinson's Disease Rating Scale (UPDRS)<http://www.epda.eu.com/en/parkinsons/indepth/parkinsonsdisease/rating-scales/updrs/>

inhibitor), dopamine agonists and MAO-B inhibitors [Fellous and Suri Fahn et al. \[2004\]](#) [Hausdorff \[2009\]](#).

These drugs should be used in the early stages of the disease, in the hope of delaying the frequency of dyskinesias. Improvements of symptoms might occur during this treatment but over-time, the benefit of using drugs frequently becomes less consistent.

Physicians recommend that, in the early stages, lifestyle changes should be implemented towards helping the improvement mainly of the motor symptoms, such as increasing the physical activity. Aerobic exercises not only improve balance and postural control but can make the patient feel more relaxed, and overall, provide a sense of comfort [Hausdorff \[2009\]](#). When medication is not effective anymore, other available solution is the DBS surgery. DBS is a surgical treatment where electrodes(or neurostimulators) are implanted inside the brain for stimulating specific zones of the brain. Two areas may be stimulated: the subthalamic nucleus (STN) or the internal globus pallidus (GPI) [Hausdorff \[2009\]](#). These structures are the ones involved in motor control. After the implantation of DBS, patients have a much greater control over their body movements.

DBS does not cure the disease, but it can help managing some of the symptoms and therefore improve the patient quality of life <sup>5</sup>. Other breakthrough treatment strategies involve gene therapy's, stem cells treatment, neural transplants or even brain infusions <sup>6</sup>.

## 2.2 Epilepsy

### 2.2.1 Background

Epilepsy is a neurological condition which affects the nervous system. Epilepsy is commonly referred as seizure disorder. Seizures are caused by disturbances in the electrical activity of the brain. The cause of this seizures may be related to a brain injury or a family history, but most of the time it is unknown. An estimated 65 million people have epilepsy, with 150.000 new cases being reported each year in the USA <sup>7</sup>, whereas in the European Country the number of people that suffers from the disease is above 5 million <sup>8</sup>.

### 2.2.2 Modern Definition

An epileptic seizure is a temporary and transient occurrence of signs due to abnormal brain activity. This disease is characterized by a person's predisposition to generate epileptic seizures, and by the neurobiological, cognitive, psychological, and social consequences of this disease. Seizures origin's is believed to be an electrochemical disorder in the brain cells, causing an imbalance of the regions of the brain which are excited or inhibited by the same brain cells. The seizure is then

<sup>5</sup>European Parkinson's Disease Association: Deep Brain Stimulation <http://www.epda.eu.com/en/parkinsons/in-depth/surgery/deep-brain-stimulation/>

<sup>6</sup>Surgical Treatments from the European Parkinson's Disease Association: <http://www.epda.eu.com/en/parkinsons/in-depth/surgery/>

<sup>7</sup>An introduction to Epilepsy <https://www.epilepsy.com/start-here/introduction-epilepsy>

<sup>8</sup>Statistics by Country for Epilepsy <http://www.rightdiagnosis.com/e/epilepsy/stats-country.htm>.

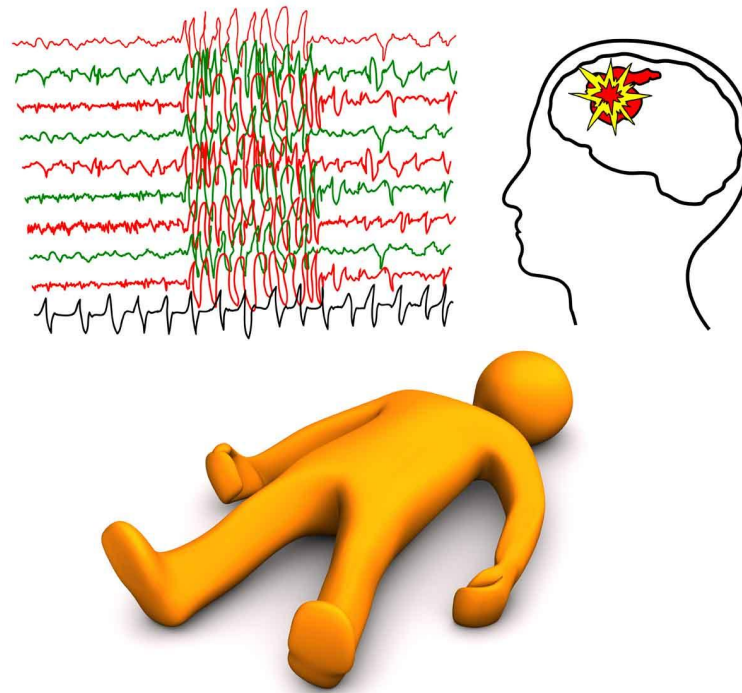


Figure 2.3: Epileptic Seizures electroencephalography (EEG) pattern.

characterized by the sudden appearance of uncontrolled electrical activity in the brain, affecting the way the people feel's and acts during, typically, a short amount of time. Some seizures might go unnoticed by the patient, where numbness might be felt, whereas in the most common seizures, the person might go unconscious, and experience uncontrolled body movement [Fisher and Saul \[1997\]](#).

### 2.2.3 Types of Seizures

Seizures have been classified in terms of the patient behavior during the seizures. Typically, they are divided first into two categories: partial (focal) and generalized.

Partial seizures have onset on one side of the brain, resulting in focal symptomatology such as twitching in an arm or face, a sensory change, or even the focal type of change in memory that occurs with temporal lobe seizures and frontal lobe seizures. This kind of seizure can alter the patient memory or even its consciousness over a short period of time. They are usually characterized by twitching, abnormal sensations, distortions of perceptions and uncontrolled body movement [Fisher and Saul \[1997\]](#).

On the other hand, generalized seizures apparently start on both sides of the brain. In fact, this kind impairs consciousness and distorts the electrical activity of the whole or a larger portion of the brain. Typically, generalized seizures are associated to seizures with sudden and very short

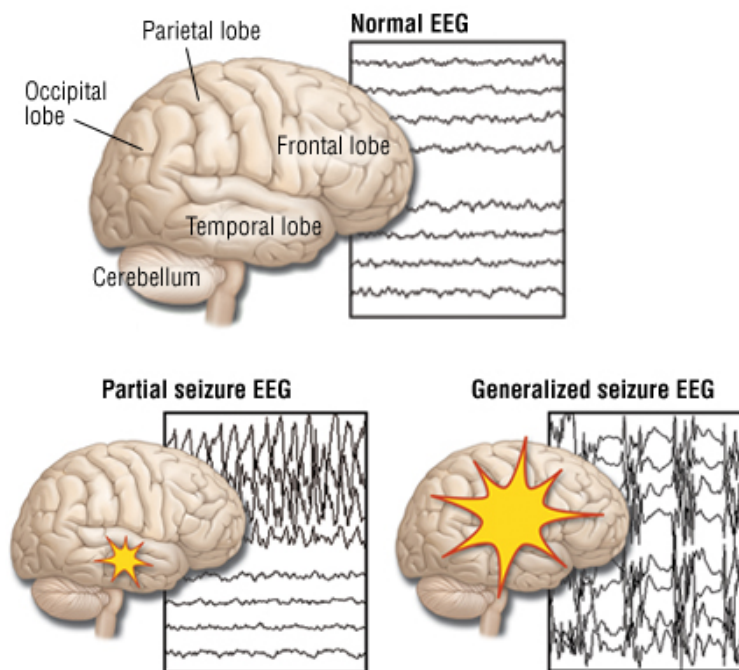


Figure 2.4: Epileptic Seizures EEG patterns depending on the type of seizures: Partial or Generalized <sup>9</sup>.

duration of jerking in the body extremities Fisher and Saul [1997] <sup>10</sup>.

### 2.2.4 Semiology of Epileptic Seizures

The state-of-art classification of epileptic seizures is based exclusively on the ictal seizure semiology, and was divided into five branches: aura, autonomic, dialeptic, motor and special seizure. This classification was performed only by 2D video analysis Lüders et al. [1998] Noachtar and Peters [2009].

Each kind of seizure is characterized by certain phenomena and so, seizures in which the main manifestations are motor activity were named as motor seizures. Figure 2.5 shows the full table of the semiological seizure classification.

Within the motor seizures, two major groups are differentiated: the simple and the complex motor seizures. On one hand, the simple motor seizures movements are relatively "simple", unnatural and are characterized by movements similar to the ones obtained when electrically stimulating the primary areas of the brain responsible for the motor functions.

On the other hand, the complex motor seizures are named after the complexity of the movements being presented, which simulates natural movements, but are inappropriate, unexpected and unintended from the patient Lüders et al. [1998] Noachtar and Peters [2009].

Each simple and complex motor seizures are then divided into subgroups, whereas each subgroup is characterized by a different muscle activity of the individual. The simple (myoclonic,

<sup>10</sup>Epilepsy Health Center <http://www.webmd.com/epilepsy/guide/types-epilepsy>

Epileptic seizures
Auras
Somatosensory aura <sup>a</sup>
Visual aura <sup>a</sup>
Auditory aura <sup>a</sup>
Olfactory aura
Gustatory aura
Autonomic aura
Abdominal aura
Psychic aura
Autonomic seizures <sup>a</sup>
Dialeptic seizures <sup>b</sup>
Typical dialeptic seizure <sup>b</sup>
Motor seizures <sup>a</sup>
Simple motor seizures <sup>a</sup>
Myoclonic seizure <sup>a</sup>
Epileptic spasm <sup>a</sup>
Tonic-clonic seizure
Tonic seizure <sup>a</sup>
Clonic seizure <sup>a</sup>
Versive seizure <sup>a</sup>
Complex motor seizures <sup>b</sup>
Hypermotor seizure <sup>b</sup>
Automotor seizure <sup>b</sup>
Gelastic seizure
Special seizures
Atonic seizure <sup>a</sup>
Astatic seizure
Akinetic seizure <sup>a</sup>
Negative myoclonic seizure <sup>a</sup>
Hypomotor seizure <sup>b</sup>
Aphasic seizure <sup>b</sup>
Paroxysmal events

<sup>a</sup> Left/right/axial/generalized/bilateral asymmetric.  
<sup>b</sup> Lateralizing signs occurring during this seizure type are listed separately.

Figure 2.5: Semiological Seizure Classification (Adapted from: Noachtar and Peters [2009]).

tonic, epileptic spasms, clonic, tonic-clonic and versive seizures) are all characterized by short periods of muscle activity, whereas the complex motor seizures (hypermotor, automotor and gelastic seizures) are known for complex movements, with considerable duration, involving the proximal segments of the limbs and trunk Lüders et al. [1998] Noachtar and Peters [2009].

### 2.2.5 Epilepsy Triggers

Seizure occurrence is unpredictable and therefore, a seizure can occur at any time. Nevertheless, keeping track of biological and environmental factors that may trigger a seizure can help in the process of identifying when a seizure will arise.

Some triggers are easily perceived and can arise at any time, even during sleep or when waking up. Others may be triggered by highly stressful situations, alcohol, drug abuse or sleeping deprivation <sup>11</sup>.

Common epilepsy triggers are:

- Specific time of day or night;
- Flashing bright lights or patterns (gaming for long hours, which is very common in younger ages);
- Specific foods, excess caffeine or other products that may aggravate seizures;

<sup>11</sup>Epilepsy Triggers <http://www.drugs.com/health-guide/epilepsy.html>

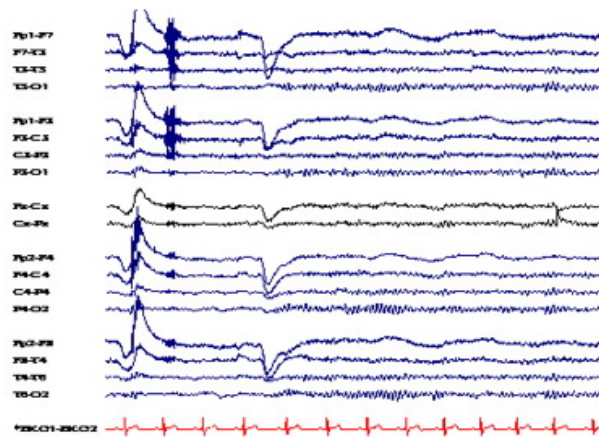


Figure 2.6: Normal electrocardiography (ECG) + EEG Signal.

### 2.2.6 Diagnosis

Knowing if a person is having a seizure and diagnosing the type of seizure can be extremely difficult. There are many other disorders that can be easily confused with epilepsy. Nevertheless, accurate descriptions of seizure events are insufficient to clearly attest epilepsy, and so, imaging tools are critical in order to learn more about the brain, what is causing the events and where is the source of the problem.

Epilepsy is usually diagnosed after a person has had at least two seizures that were not caused by some known medical condition [Fisher and Saul \[1997\]](#). Besides this criteria, information of the medical history, blood tests, EEG analysis, and brain imaging tests such as CT and MRI scans are fundamental in providing physicians with critical information for an accurate diagnosis.

EEG (electroencephalography) is the tool for the analysis of the brain's electrical activity. Electrodes are attached to the patient scalp and connected by wires, which allow the recording of the brain's electrical activity as a series of squiggles called traces. Each trace corresponds to a different region of the brain. EEG shows patterns of normal or abnormal brain electrical activity. Figure 2.6 shows the typical output from an EEG recording and figure 2.7 presents the unusual electrical activity during a generalized seizure. When an EEG test picks up unusual electrical activity, it shows the areas of your brain where it is coming from.

EEG acquisition is now frequently associated and synchronized with video-recording of the seizure, namely Video-EEG systems [Specchio et al. \[2011\]](#). This modality provides the EEG signal combined with the video, which is tremendously important in case of epileptic seizures. When using such a system, besides the typical EEG signal, the seizure can be also qualitatively analyzed in terms of the motion pattern. This pattern can be visually perceived by an experienced physician [2.8](#).

Analyzing the motion pattern of the seizure can provide the physicians with critical information towards an accurate diagnosis: the motion pattern may reveal the seizure onset point or source (location inside the brain responsible for the seizure), as well as identify the presence of an actual seizure and also the type of seizure (see Figure 2.9).



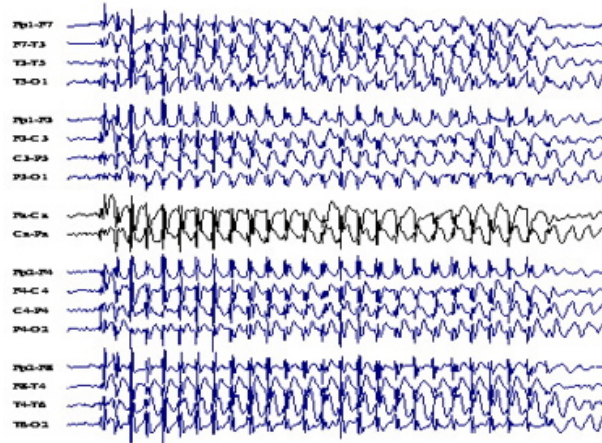


Figure 2.7: Normal EEG Signal of Generalized Epilepsy <sup>12</sup>.

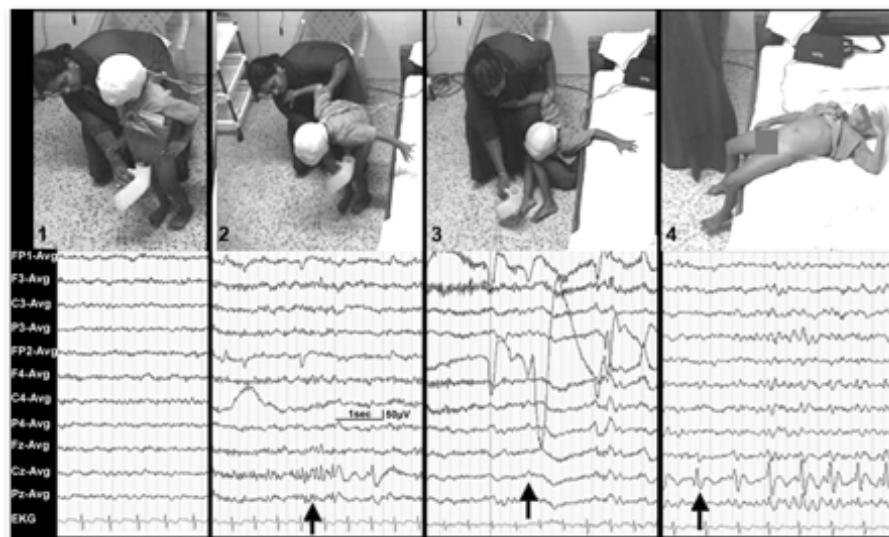


Figure 2.8: "Stills from video-EEG recording. 1) Micturating; 2) forward flexion of upper trunk and extension of upper extremities, and a beta burst (arrow) at Cz electrode; 3) fall and attenuation of the EEG activity (arrow); and 4) rhythmic 2 Hz spike and wave discharges at Cz electrode during postictal phase" [Rathore et al. \[2008\]](#).

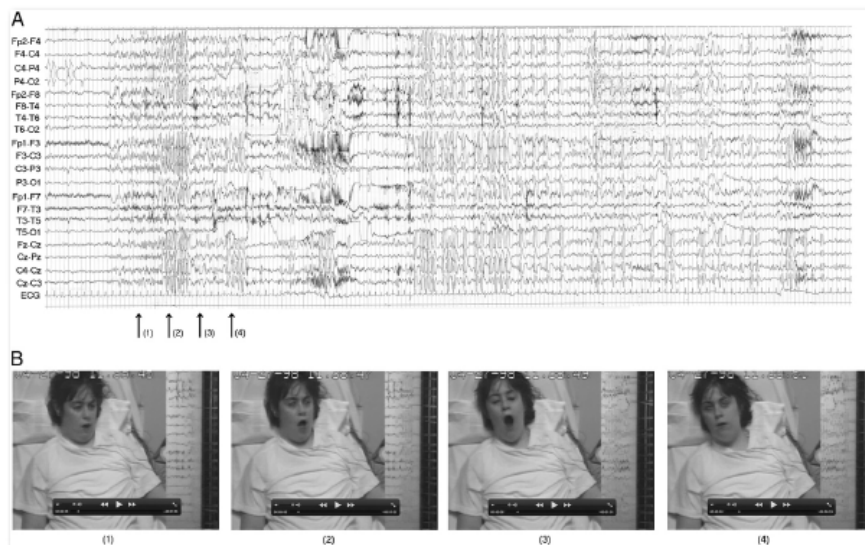


Figure 2.9: "Ictal video/EEG recording during a typical episode of yawning. The EEG of the episode shows low-to medium-voltage fast activity over bilateral central areas lasting a few seconds, followed by rhythmic spikes and polyspikes involving bilateral central and frontal areas during which the patient yawns. Multiple artifacts related to mouth movement and tongue protrusion are also evident. A prolonged subclinical sequence of spike-and wave complexes is evident over frontal and central areas after the artifacts. Arrows indicate the correlation with the snapshot of the video." [Specchio et al. \[2011\]](#).

Medical Imaging is another critical tool in a clear assessment of Epilepsy. Magnetic Resonance Imaging (MRI) is used to visualize the brain's internal structures in detail, producing high resolution images of the brain.

MRI imaging can be used as an extremely precise imaging tool, for the detection of brain aneurisms, strokes or brain tumors. Besides that, this imaging technique is often used for studying the brain's anatomy and also as a reference for the mapping and spatial co-registering with others imaging modalities [Warach et al. \[1996\]](#).

Positron Emission Tomography (PET) is an functional imaging technique which makes use of radioactive tracers (i.e. radiotracers) to produce three-dimensional images of functional processes in the body. Pairs of gamma rays emitted indirectly by the tracers, which is introduced into the body on a biologically active molecule, are detected and used to construct high-resolution images.

PET is often used in Epilepsy due to greater spatial resolution and versatility in tracking multiple tracers and therefore, imaging various aspects of cerebral function at the same time [Spencer \[1994\]](#).

SPECT (Single photon emission computed tomography) is an imaging technique used to localize the region of seizure onset for epilepsy surgery planning, using ictal and interictal scans. SPECT has recently emerged as a valuable adjunct to standard techniques in clinical nuclear radiology, in which SPECT can help in significantly improving the scintigraphic localization and characterization of a region, which is tremendously important in this era of minimally invasive





Figure 2.10: MRI Brain Scan <sup>13</sup>

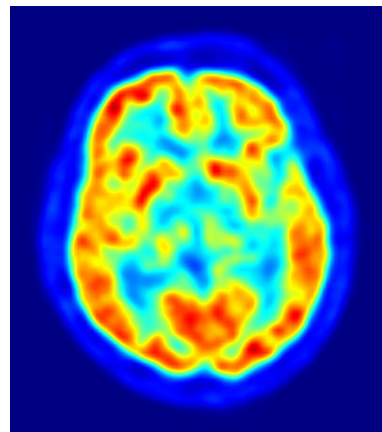


Figure 2.11: PET Scan [Spencer \[1994\]](#)

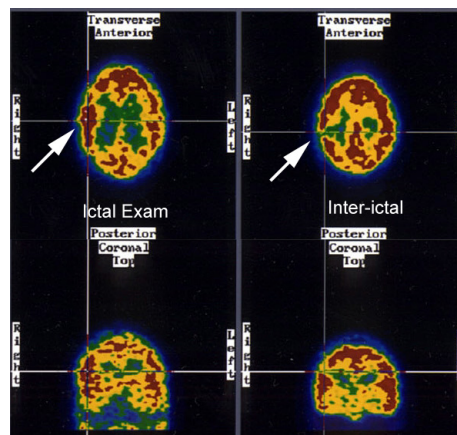


Figure 2.12: SPECT images <sup>14</sup>

surgery and targeted radiotherapy. This technique has the outstanding and unique advantage of mapping the brain activity when the radiotracer is injected, at the time of the seizure, and the actual imaging can be done later on when the patient is stable. The radiotracer is rapidly taken up by the brain based on the cerebral blood flow (CBF) and does not spread itself through the brain [McNally et al. \[2005\]](#) [Kim et al. \[2001\]](#). CBF is very important since it is closely related to the neuronal activity, and so, the SPECT injection provides a living proof of the brain activity at that specific time [McNally et al. \[2005\]](#). ISAS (Ictal – Interictal Spect Analysis by SPM) basic idea is to compute the difference between an ictal and interictal SPECT scan for a patient [Kim et al. \[2001\]](#).

Ictal images represent the brain activity at the moment of seizure and the interictal are obtained within 24hours of the seizure end, being images that portrait the brain activity during a stable phase of the patient. Significant increases and decreases in CBF between the two moments can then be detected, and the differences are computed against a healthy normal database to determine the variation [Kim et al. \[2001\]](#), providing information in the localization of the epileptogenic region [McNally et al. \[2005\]](#).

### 2.2.7 Treatment

The majority of epileptic seizures are controlled through drug therapy. These are sometimes called anti-epileptic drugs or anti-seizure drugs. They will successfully control seizures for about 7 out of 10 people with epilepsy. The type of treatment prescribed will depend on several factors including the frequency and severity of the seizures as well as the person's age, overall health, and medical history.

Surgery is an alternative for some people whose seizures cannot be controlled by medication. The benefits of surgery should be weighed carefully against its risks because there is no guarantee that it will be successful in controlling seizures. The surgery goal is to remove the brain part

which is thought to be responsible for the rise of the epileptic seizures and therefore, by removing it, seizure frequency is expected to diminish <sup>15</sup>.

---

<sup>15</sup>Epilepsy Treatments <https://www.epilepsy.com/learn/treating-seizures-and-epilepsy/surgery>



## Chapter 3

# Movement Analysis and Quantification

Movement analysis is the study of movement, and in a more specific case, study of human motion, using visual perception of people and also complex video-systems (with sensors measuring body movements and body mechanics) to study the biomechanical activity. Human motion analysis is normally used when there is a need to assess, for instance, the walking acuties of an individual and, based on the information retrieved, set a treatment plan to enhance their ability to walk [Gavrila \[1999\]](#).

With the continuous developments of technology, more areas started to use the information retrieved from the body and so, such analysis can also be used, for example, in sports Biomechanics to help professional athletes improve their overall performance. Movement analysis consists mainly in two different aspects: quantification and interpretation of movement. Quantification is related to the specific parameters, for instance speed, acceleration or cadence, and interpretation enables to draw different conclusions based on the subject information (i.e. age, height, size, disease) [Gavrila \[1999\]](#) [Lee and Grimson \[2002\]](#).

The introduction of video-systems, which enabled detailed studies of patients with relatively good accuracy, it led to the development of treatment strategies, mainly involving different departments, from the neurosurgeons to the orthopedic and rehabilitation physicians. Nowadays, several hospitals have their owns gait labs, as well as video-EEG systems, to perform routine consults and follow-up monitoring, besides designing treatment plans [Davis III et al. \[1991\]](#). Computers are now becoming a crucial element in such analysis, since that, provided with a video-recording of barely any kind, it can put out critical information regarding certain features that can be of extreme relevance for that specific scenario. Despite this developments in technology, such systems are still not an essential tool in diagnosis and rehabilitation that had the potential to be [Baker \[2007\]](#). Numerous factors contributed to this: prohibitive costs in technology, time consuming tests, results lack of clinical interpretation and validation.

Biomedical engineering has sought to address these same problems by creating new techniques that can capture data in a much more rapidly and efficient way. The result of this effort has resulted in evolving from the traditional kinematical systems (film analysis, chronophotography) to modern techniques such as video-based systems and more recently the new modern optoelectronics,

beyond the typical force platforms<sup>1</sup>.

Movement can be affected by many factors, and these acuties can be temporary or even permanent. The factors can be of several types: extrinsic (i.e. footwear, clothing), intrinsic (i.e. sex, weight, height, age), physical, psychological or even pathological (i.e. neurological diseases, musculoskeletal anomalies). The common features that can be extracted from human movement analysis are: velocity and accelerations of body parts, angles, distances between body parts and many others. In the specific case of gait, the typical features are: stride length, cadence, gait speed, acceleration, foot angle, joint angles, stride-to-stride variability and swing timeLee and Grimson [2002].

The analysis of the movement patterns can be performed in 3 different ways: a biomechanical anthropometric analysis, Kinematical analysis and Electromyography. Recently, thermography is emerging as a promising way to also quantify movements.

### 3.1 Passive marker-based motion capture systems

Active and passive markers are used when a multi-camera system is implemented. The cameras utilize infrared signals and then, based on the angle and time delay between the original and reflected signals, triangulation of the marker in space is possible. It also enables the computation of joint angles Morris et al. [1999] Sofuwa et al. [2005]. Such devices can measure the position, may be portable and may even transmit data in real-time, however and are prone to noise and interference from metal objects, besides being expensive. On the other hand, marker-based approaches are very precise and highly accurate but also very expensive. In this case, the subject is surrounded by cameras that, additionally, need to be calibrated. It is an adaptable and minimally intrusive but it is physically limited because of the need of a gait laboratory.

Passive marker-based tracking systems use reflective-markers - small plastic support covered with retro-reflecting material and its goal is the skeleton reconstruction of the 3D motion of a set of markers. Those markers do not require any powering, are hardly sensed by the subjects and appear much brighter than the background allowing their detection, on the video images. Nevertheless, the system is quite robust, not portable, and expensive that involves cameras, connections, computers and displays. Current commercially available full body motion capture systems (e.g. Vicon<sup>2</sup> and Qualysis<sup>3</sup>) usually rely on a predefined skeleton model with a small number of markers, which have fixed positions on the tracked subjects. Correct placing markers at anatomical landmarks minimizes sliding and allows regression based methods for the localization of joints, as it can be depicted in Figure 3.1.

In such systems like the Qualysis or the Vicon, as referred before, multiple cameras observe a target moving around a pre-determinaded path. Features on the target are identified in each image. Triangulation or disparity can be used to compute each feature's 3D position. The pipeline of the

---

<sup>1</sup>AMTI Force Platforms <http://www.anti.biz/fps-overview.aspx>

<sup>2</sup>Vicon System <http://www.vicon.com/>

<sup>3</sup>Qualysis Motion Capture Systems <http://www.qualisys.com/>

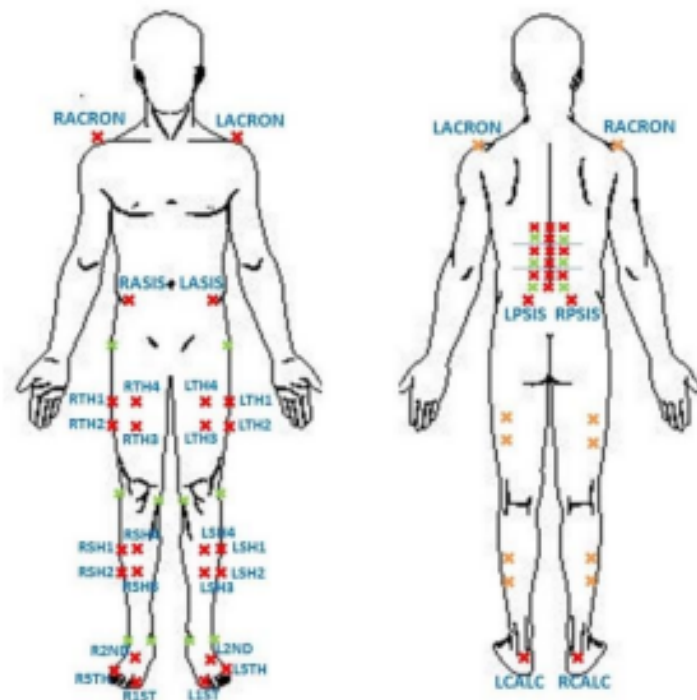


Figure 3.1: Anterior and posterior view of markers placement general scheme (red – fixed markers for dynamic full body analysis; green – markers for static view; yellow posterior view).

analysis consists of 1) Camera set-up and calibration; 2) Recording; 3) Marker identification; 4) 3D Reconstruction where the multiple set of 2D data have to be correctly labeled and associated to their corresponding 3D markers; and 5) Clean-up post-processing [Moeslund et al. \[2006\]](#).

The drawbacks of such systems in terms of performance can come from two major sources: low resolution which results in poor features identification; and occlusion which results in failure to see the feature. Occlusion may be due to either the target itself or other objects in the scene, for instance, when a marker is hidden to the cameras by any body part. That is why this system use multi-cameras, so that occlusion can be reduced. Other disadvantage is the dependence on scene illumination [Moeslund et al. \[2006\]](#) [Chen and Davis \[2000\]](#). However, the main difficulty is the correct synchronization between multiple markers and multiple cameras. Also, the dense set of markers gives rise to the possibility of them coming very close to one another at times during data collection [Chen and Davis \[2000\]](#). Recently, RGB-D sensors emerged as markerless systems capable of performing motion analysis.



Figure 3.2: VICON F40 motion capture system.

### 3.2 RGB-D Sensors

The RGB-D (Red, Green, Blue, Depth) sensors are usually divided into two broad categories, depending on the depth measurement: time-of-flight cameras and structured-light systems.

The 3D Time-of-Flight (ToF) is an emerging imaging technology which adds a new dimension to the imaging world. The cameras equipped with this technology capture the lateral as well as the depth information of an imaging 3D scenario. The camera works on the principle of Time-of-Flight wherein the distance towards any imaging point in 3D space is calculated according to the travel time of the rays hitting the sensor pixel. This technology provides an easy and fast way of capturing 3D information which is of prior interest among the new generation image and video processing systems [Hansard et al. \[2013\]](#).

Basically, a ToF produces a depth image where each pixel encodes the distance to the corresponding point in the scene; it is a range imaging camera system that resolves distance based on the known speed of light, measuring the time-of-flight of a light signal between the camera and the subject for each point of the image.

These cameras can then be used to estimate a 3D structure directly, without using complex computer-vision algorithms, which is a tremendous advantage. Besides, only one camera is required, no manual depth computation is needed (it is a direct measurement), as well as it is not

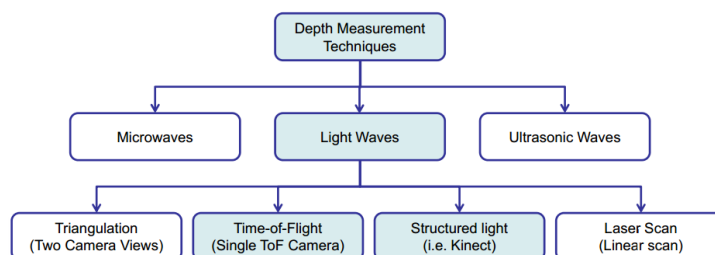


Figure 3.3: Classification of Depth Measurement Techniques [Castaneda and Navab \[2011\]](#).



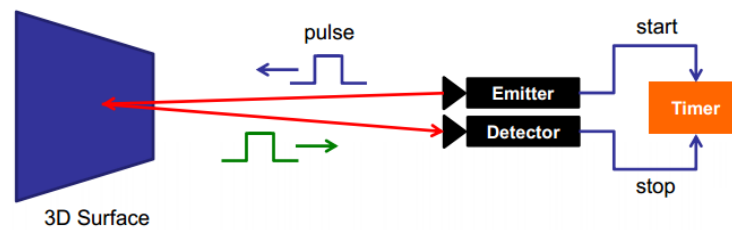


Figure 3.4: Time-of-Flight Cameras Depth Estimation Process [Fuchs and Hirzinger \[2008\]](#).

dependent of the background illumination since its influence is limited by the light pulses, and also the fact that the illumination and observation directions are collinear. As downsides of this technology, it requires high-accuracy time measurement, can be affected by light scattering and there is a difficulty in generating light pulses with fast rise and fall times [Fuchs and Hirzinger \[2008\]](#). Practical applications for this sensing modality include robot navigation, human-machine interaction and 3D reconstruction.

Examples of ToF based RGB-D sensors are the DepthSense Cameras – DS311 and DS325, as well as the Panasonic D-IMager and the recent Kinect For Windows version 2(K4W) sensor. DS311 device delivers real time 3D distance data mainly for far interaction (full body tracking), but it can also be used for close interaction. It can provide depth data at a distance of 15cm, up to 60fps. It is composed of ToF sensor, RGB sensor and two microphones. The device, combined with IISU Middleware platform, provides several functionalities that can be both implemented for commercial or scientific applications.

DS325<sup>4</sup> is the most accurate depth sensor in the market. It is aimed to be used into close interaction applications (hand and finger tracking). It has a higher RGB resolution and field-of-view comparing with DS311<sup>5</sup>.

<sup>4</sup>DS 325 [http://www.softkinetic.com/Portals/0/Documents/PDF/WEB\\_20130527\\_SK\\_DS325\\_Datasheet\\_V3.0.pdf](http://www.softkinetic.com/Portals/0/Documents/PDF/WEB_20130527_SK_DS325_Datasheet_V3.0.pdf)

<sup>5</sup>DS311 [http://www.softkinetic.com/Portals/0/Documents/PDF/WEB\\_20130527\\_SK\\_DS311\\_Datasheet\\_V3.0.pdf](http://www.softkinetic.com/Portals/0/Documents/PDF/WEB_20130527_SK_DS311_Datasheet_V3.0.pdf)



Figure 3.5: DepthSense DS325.



Figure 3.6: DepthSense DS311.

Panasonic D-IMager is another ToF 3D sensor, launched by Panasonic Electric Works. D-IMager uses a proprietary CCD along with near-infrared LEDs to sense human gestures and track full body motion allowing users a fully interactive experience. This Sensor enables precise motion capture of spatial objects with wide field-of-view by processing high precision (pixel by pixel) data. It works at an approximate rate of 15-30 fps with a  $160 \times 120$  resolution. The main advantage of this sensor is the range that varies from 1.2m to 9.0m. ToF cameras differ from structured-light systems as the Kinect<sup>TM</sup> sensor and Asus Xtion Pro Live.

At this moment, ToF cameras, even though they can provide a much more accurate depth image and are able to deal better with shadow effect, their price (i.e. hundreds of dollars), noise in depth information (substantially higher) makes it some-how not suitable in the quest of implementing a low-cost markerless video-system for movement analysis.

Asus Xtion Pro Live is an alternative hardware sensor for motion-tracking. The device is based on the same hardware as Kinect, both produced by PrimeSense. Xtion is largely similar to Kinect in its functionality. The cameras and sensors installed closely follow the movement of the person in front, extrapolating and even recognizing key spots, all in real time. Like Kinect, all this data can then be processed in PC software. A major drawback of Asus Xtion Pro Live is that due to the nature of the hardware, it needs to be placed ideally in the middle of the display length when viewed horizontally (i.e. in top of a TV or monitor). One of the differences between the two devices is the quality of the RGB camera, which is higher in Asus Xtion Pro Live<sup>7</sup>.

<sup>7</sup>ASUS Xtion PRO LIVE [http://www.asus.com/Multimedia/Xtion\\_PRO\\_LIVE/](http://www.asus.com/Multimedia/Xtion_PRO_LIVE/)



Figure 3.7: Panasonic D-IMager <sup>6</sup>.



Figure 3.8: Asus Xtion Pro Live.

### 3.3 Kinect XBOX 360

Kinect<sup>TM</sup> was launched as a non-contact motion sensing device by Microsoft for the Xbox 360 video game console back in November 2010 [Melgar and Diez [2012]]. Kinect<sup>TM</sup> is the result of combining technologies from Microsoft Game Studios owned by Microsoft and PrimeSense, an Israeli developer [Melgar and Diez [2012]]; [Webb and Ashley [2012]]; [Catuhe [2012]].

It was quickly discovered that depth sensing technology could be used for other purposes besides gaming and at a much lower cost than traditional 3D-cameras. Kinect<sup>TM</sup> sensor breakthrough technology and inherent functionalities, built-in in their SDK, were immediately noticed by everyone, resulting in being the fastest selling consumer electronics device and worthy a Guinness World Record <sup>8</sup>.

Since its release, Kinect<sup>TM</sup> sensor has been used widely in many research areas such as biomedical engineering, human-computer interface and robotics. The Kinect<sup>TM</sup> hardware would be nothing without the software that makes use of the data gathered. In June 2011, Microsoft released Kinect<sup>TM</sup> Software Development Kit (SDK), which allows the user to write Kinect applications in different languages such as C++, C# or Visual Basic. Several communities developed immediately, where users could interact and develop software open-source (i.e. OpenNI and OpenKinect).

#### 3.3.1 Kinect Basic Principles

Kinect is composed by a horizontal bar connected to a small base with a motorized pivot. The device characteristics include a RGB camera, a multi-array microphone and depth sensor. The video camera helps in facial recognition and in the detection of other features just by detecting the three color components red, green and blue.

Depth is assessed by using an infrared projector and a monochrome CMOS (complimentary metal-oxide semiconductor) sensor that combine to see the space in 3D, independently of the lighting conditions [Webb and Ashley [2012]]. The principle behind the Kinect depth sensor is the emission of an IR pattern and the image capture of the IR image with the CMOS camera that filters the image.

The image processor of the device uses the relative positions of the dots in the pattern to calculate the depth displacement at each pixel position in the image [Webb and Ashley [2012]],

<sup>8</sup>Microsoft Kinect.: World's Fastest-Selling Consumer Electronics Device [http://www.huffingtonpost.com/2011/03/09/microsoft-kinect-fastest-selling-consumer-electronics\\_n\\_833706.html](http://www.huffingtonpost.com/2011/03/09/microsoft-kinect-fastest-selling-consumer-electronics_n_833706.html)

Catuhe [2012], Andersen et al. [2012]. The depth image from the IR camera has a maximum resolution of  $640 \times 480$  pixels with 11-bits, which provides 2 048 levels of sensitivity.

The Microsoft Kinect is a RGB-D camera that provides three different types of data, at 30 fps:

- Color ( $1280 \times 960$  at 12 frames per second (fps),  $640 \times 480$  or  $320 \times 240$  resolution);
- Depth ( $640 \times 480$ ,  $320 \times 240$ , or  $80 \times 60$  resolution);
- Skeleton information of 20 body joints (Figure 3.9).

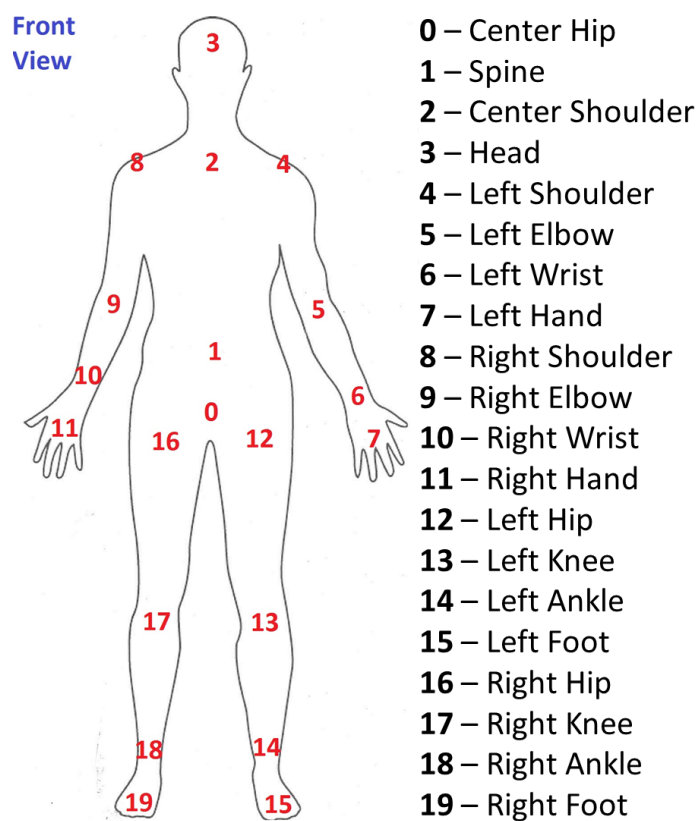


Figure 3.9: Kinect v1 Joint List.

The IR or depth camera has a field of view just like any other camera. The original purpose of Kinect is to play video games within the confines of a living room space, at a certain nominal distance. The normal depth vision ranges from around 800mm to just over 4000mm Webb and Ashley [2012]. However, a recommended usage range is 1500mm to 3500mm as the reliability of the depth values degrade at the edges of the field of view Andersen et al. [2012]. At 2m from the sensor, it is able to resolve down to 3 mm for height and 1 cm for depth. The sensing range of the depth sensor is adjustable, with the possibility of Near Mode range or Default range. Nevertheless, the depth resolution of Kinect<sup>TM</sup> coarsens as the distance increases Catuhe [2012] Andersen et al. [2012].



Figure 3.10: Kinect XBOX 360 Vision Sensor.

### 3.3.2 Sensor Properties

- Linearity

Kinect™ sensor has several properties. One of them is linearity. Linearity of the sensor can be analyzed by pointing the sensor perpendicularly to a planar surface and in the measuring range of the sensor, determine if the depth estimates are close to the actual distance. It is a fact that in the measuring range of the sensor depth estimates are accurate and that is particularly relevant when performing qualitative analysis of the acquisition using the sensor [Andersen et al. \[2012\]](#).

- Depth Accuracy and Precision

Depth accuracy and precision can be affected by errors mainly related to the lighting conditions and the imaging geometry. Light condition affects the contrast in the infrared image and imaging geometry is related to difficulties in determining the object distance and orientation relative to the sensor [Andersen et al. \[2012\]](#), [Khoshelham and Elberink \[2012\]](#).

[Khoshelham et al.](#) analyzed the accuracy and resolution of Kinect depth data for indoor mapping applications and concluded that for mapping applications the data should be acquired within 1–3m distance to the sensor and that the depth resolution decreases quadratically with an increase distance from the sensor. In addition, [Khoshelham et al.](#) proposed

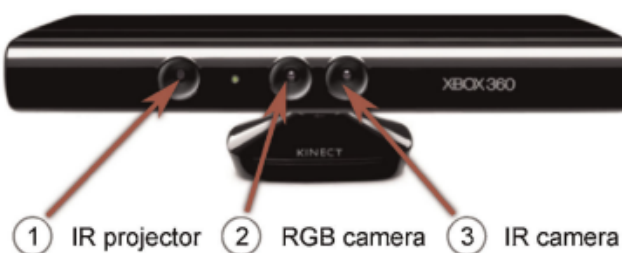


Figure 3.11: Kinect Color and Depth acquisition: IR and RGB physical locations [Zollhöfer et al. \[2011\]](#).

a mathematical model for obtaining 3D object coordinates from the raw depth image measurements [Khoshelham and Elberink \[2012\]](#) [Han et al. \[2013\]](#).

- Structural Noise

The depth estimates in the depth image describe the distance from the point to the sensor plane rather than the actual distance from the point to the sensor. This should result in the same depth estimate over the entire image if the sensor is pointed directly at a planar surface. However, there are small variations over the image.

These variations that occur mainly on the edges of the objects are called structural noise. Noisy edges are used to determine the spatial precision of the sensor, as it was done in Andersen et al. work [Andersen et al. \[2012\]](#). Structural noise is a measurement error that can affect qualitative analysis when using the sensor. Its filtering and removal is of extreme importance [Han et al. \[2013\]](#).

- Multi-Camera Setup

Depending on the type of experiment desired, there is a need for a second (or more) Kinect<sup>TM</sup> sensors. This allows a larger field-of-view and also to record an object from more than one viewpoint. Despite this possibility, many problems arise from the use of multi-cameras. One of those problems is that multiple sensors may interfere in the image formation of each other, by overlapping their IR pattern and making it impossible to estimate the depth. This overlaps are often called blind spots and unexpectedly Kinect<sup>TM</sup> can overcome this error with an error of 1-5%" of the correct value [Melgar and Diez \[2012\]](#).

The major problem when using multi-sensors is the low response that the computer provides the user. Each sensor requires USB connection + external power. If both sensors are connected in the same USB controller the device might not work correctly. In order to effectively use two Kinect<sup>TM</sup> devices, multiple USB Controllers are required. Normal laptops only have one USB Port. When both devices are connected into a single laptop, the USB bandwidth is exceeded and that disables the device abilities.

- Shadows in the depth image

The quality of the depth-map image can be affected by light conditions. One of the recurrent problem is related with the creation of shadows due to the distance between the illuminator and the IR camera illuminated objects. The appearance of this shadow hampers the ability of the sensor to estimate the depth and therefore the pixels in that particular area are set to zero depth. Figure 3.12 explains the formation of this shadow [Andersen et al. \[2012\]](#) [Han et al. \[2013\]](#).

Figure 3.13 explains shadow formation in the depth image. The presence of this shadow does not allow the sensor to estimate the depth and therefore the pixels in that particular area are not assigned to any specific value [Andersen et al. \[2012\]](#). Table 3.1 presents a table with an overview on the Kinect XBOX 360 sensor.

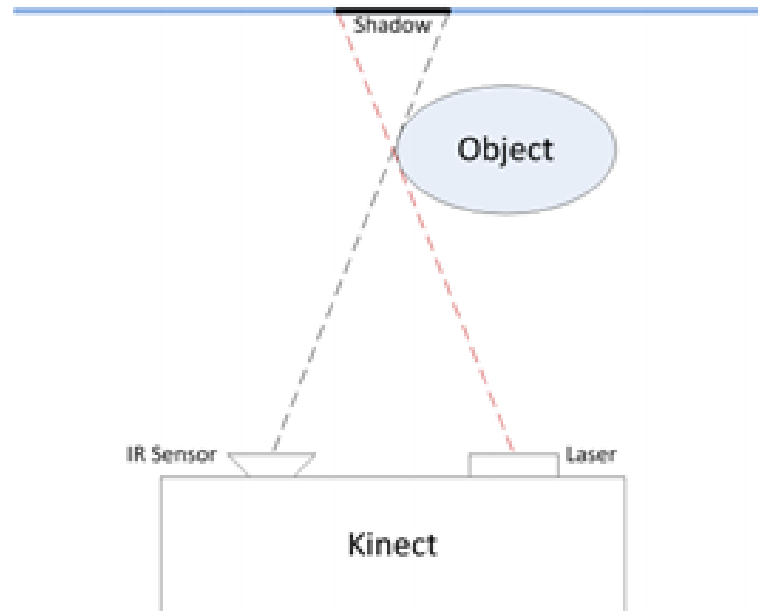


Figure 3.12: Shadow formation process using Kinect Andersen et al. [2012].

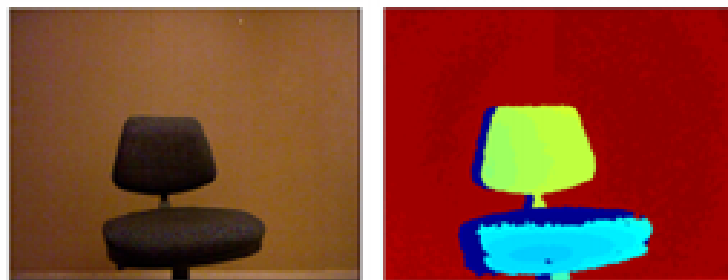


Figure 3.13: The object in the figure blocks the path of the laser. Since the depth estimate is based on the pattern projected by the laser, Kinect cannot estimate depth outside the line of sight of the laser Andersen et al. [2012].

Table 3.1: Kinect Requirements Overview

<b>External Power Required</b>	Yes
<b>Angular Field of View</b>	Horizontal 57°   Vertical 43°
<b>Sensorization</b>	RGB and Depth Sensors, Microphone Array, Accelerometers
<b>Resolution</b>	RGB and Depth: 640 x 480 pixels @ 30 Hz
<b>Platform</b>	At least dual-core 2.66-GHz processor, 32/64 bit, 2GB RAM
<b>Interface</b>	Dedicated USB 2.0
<b>Software</b>	Microsoft Kinect SDK , OpenKinect, OpenNI and OpenCV
<b>Programming Language</b>	C#, C++, Visual Basic, Java, Python, ActionScript
<b>Dimensions</b>	30 cm x 7.6 cm x 6.4 cm
<b>Notes</b>	Motor tilt from -27° to 27°

### 3.4 Kinect for Windows (K4W) v2

Kinect for Windows Developer Program Preview enabled research groups and developers to be provided with the alpha version of the new Kinect sensor, expected to be released to the market by the end of 2014. BRAINlab was one of the first 500 selected groups being granted with one such sensor, which can be depicted in figure 3.14<sup>9</sup>.

The recent sensor is still under development, with monthly releases of updated SDK's and so far, not much information can be released on the physical, as well as inner properties of the sensor (BRAINlab signed a non-disclosure agreement). Nevertheless, the new sensor has been re-engineered with major enhancements in the near mode, wider field-of-view, optimized skeletal tracking algorithm (built-in inside the SDK), API improvements, improved USB support, and two new different streams from XBOX 360: besides the normal color, depth and skeleton (now referred as body) stream (available with the SDK), the new Kinect v2 includes the infrared (IR) and also the "bodyindex" (per-pixel position of the player) stream.

The sensor is optimized for use with computers running Windows 8.0 or 8.1. The major developments regarding the Kinect XBOX 360 and the Kinect v2 are related to a higher resolution of the color stream (1920 x 1080 High-Definition), the depth estimation process, since the Kinect v2 is now a ToF (time-of-flight) sensor, and the overall improvements in the SDK functionalities<sup>10</sup>. Additionally, instead of the typical 20 joints available on Kinect v1, the newer version now tracks 25 joints, as can be depicted in figure 3.15. Table 3.2 presents a table with an overview on the Kinect for XBOX One version 2 sensor.

<sup>9</sup>Kinect for Windows (K4W) v2 Joint List <http://www.codeproject.com/Articles/213034/Kinect-Getting-Started-Become-The-Incredible-Hulk>

<sup>10</sup>Kinect for Windows (K4W) v2 <http://www.microsoft.com/en-us/kinectforwindowsdev/newdevkit.aspx>





Figure 3.14: Kinect for Windows version 2 available for the project thesis.

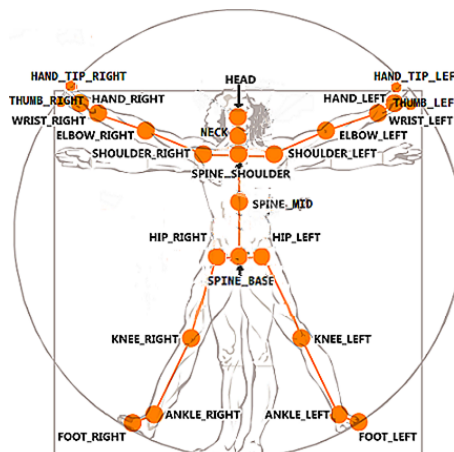


Figure 3.15: Kinect for Windows version 2: 25 Joints Collection Enumeration.

Table 3.2: Kinect v2 overview.

<b>External Power Required</b>	Yes
<b>Sensorization</b>	RGB and Depth Sensors, Microphone Array
<b>Resolution</b>	RGB : 1920 x 1080; Depth, Infrared and BodyIndex: 512 x 424 pixels @ 30 Hz
<b>Platform</b>	4 GB Memory (or more), i7 2.5Ghz (or higher)
<b>Interface</b>	Built-in USB 3.0 host controller
<b>Software</b>	Microsoft Kinect SDK v2
<b>Programing Language</b>	C#, C++, Visual Basic, Java, JavaScript
<b>Dimensions</b>	24.9 cm x 6.6 cm x 6.7 cm

### 3.5 Gait Quantification in Parkinson Disease

Gait disturbances in PD include several features which are not easily quantified in normal observations; these are caught after an effective quantitative evaluation using video-systems that record the gait of the patient. Using this systems, conclusions can be drawn on the left-right gait asymmetry, bilateral coordination, stride-to-stride variability and also the ability of the person to produce a steady gait rhythm. Stride-to-stride variability (inconsistency of stepping) is a characteristic of PD patients and is of interest for numerous reasons. It is a feature that can be seen throughout the disease, and its magnitude tends to increase with time. It can then be assessed in two different moments: the first, where features like gait speed and swing time are measured numerically, and a second moment, independent from the stride length, composed by the gait/stride-to-stride variability [Hausdorff \[2009\]](#).

The quantification of motor signs can be very useful to enhance both PD diagnosis and follow-up [Chen et al. \[2011\]](#); [Cancela et al. \[2011\]](#), and possibly lead to an improvement of treatment and overall life quality of PD patients.

Gait analysis in PD, using motion or vision sensors, has been studied by various authors [Chen et al. \[2011\]](#); [Cancela et al. \[2011\]](#); [Galna et al. \[2014\]](#). In [Cancela et al. \[2011\]](#), the authors proposed a PD monitoring tool, based on six accelerometers and one gyroscope. Based on sensor data collected from PD patients, they extracted parameters that can be useful for distinguishing between on and off states.

A vision-based system for PD assessment (distinction between non-PD, PD drug on and PD drug off states) was proposed in [Chen et al. \[2011\]](#). The authors recorded videos of PD patients and normal subjects while walking. A minimum distance classifier was then built, based on features resulting from gait analysis, which achieved an accuracy of 80.5%.

Recently, the Microsoft Kinect<sup>TM</sup> has been used for gait analysis [Galna et al. \[2014\]](#); [Gabel et al. \[2012\]](#); [Stone and Skubic \[2011\]](#), [Rocha A \[2014\]](#). The Kinect<sup>TM</sup>, as explained in the previous chapter, is a low-cost, portable RGB-D (Red, Green, Blue, Depth) camera that provides color and depth image sequences, as well as skeleton data resulting from 3D tracking. This sensor has the advantage of being less intrusive than marker-based sensors. Moreover, when compared with RGB cameras, it allows motion analysis in less controlled environments, due to the use of infrared light, without losing accuracy [Stone and Skubic \[2011\]](#).

Regarding PD, the validity of the Kinect<sup>TM</sup> for movement measurement in PD patients was recently explored in [Galna et al. \[2014\]](#). When compared with a Vicon system, the sensor was able to accurately measure time and gross spatial characteristics of clinically relevant movements, validating its use for gait analysis in the healthcare context, namely in PD.

### 3.6 Movement Quantification in Epilepsy

It is common that uncoordinated movement is experienced by a patient when an epileptic seizures is induced. This movement is a important clinical factor in seizure identification. Nevertheless,

quantification of this information has not been an object of much attention from the scientific community. The state-of-art approach is analyzing the video-EEG monitoring of such events. Although movement is very important in the diagnosis of epilepsy, for many years, efforts have concentrated on developing quantification algorithms to extract EEG features, which cannot be seen in traditional visual inspection, instead of processing the video information, easily perceived by visual inspection.

The reasons for these rely on the fact that visual analysis allows only a rough estimate of the motion pattern and also the fact that capturing, storing, and processing video data demands enormous throughput from computers. Nevertheless, seizure motion pattern quantification of Epilepsy movements is regarded by the physicians as valuable evidence in the identification of the presence of a seizure and of its source.

To address this complex problem, the common-approaches to human body quantification rely on model-based and model-free methods. Model based approaches use the information from body parts such as joints to reconstruct 3D models, using depth and skeleton information, and perform quantification based on that. On the other hand, most of the model-free approaches use binary silhouette (also known as background subtraction) techniques for human body detection and recognition, and from there predict the body movement [Kumar and Babu \[2012\]](#).

In [Sofuwa et al. \[2005\]](#), a quantitative gait analysis was made during the on-phase of medication cycle and the measures obtained (in terms of spatiotemporal, kinematic, and kinetic gait parameters) were compared to a healthy control group. Gait analysis was conducted using an 8 M-camera Vicon 612 data capturing system set at 120Hz and 3 AMTI forceplates mounted midway on an 8-m walkway. Statistical analysis using a t-student distribution and ANOVA showed lower walking velocity and stride length in PD patients [Sofuwa et al. \[2005\]](#). A gait analysis system that uses a Kinect was developed in [Gabel et al. \[2012\]](#). Regression models were built based on skeleton data, and ground truth measures (using in-shoe pressure sensors and a gyroscope), which were collected from subjects while walking. The obtained models were able to estimate stride duration and arm angular velocity, with an average absolute error in the range between 32 and 71 milliseconds, and 14 and 22 degrees/second, respectively [Gabel et al. \[2012\]](#).

Even though these approaches are suitable for their target applications, they cannot be used to extract quantified information for more complex human motion, such as the epileptic movements. The movement induced by epileptic seizures is complex, uncoordinated, unpredictable and is, thus, extremely difficult to model and quantify. Throughout the time, several works have been done with this purpose. The state-of-art approach to Video-EEG Analysis, performed by Li et al., in a clinical neurophysiology environment, using a monochrome CCD camera with several infrared light mounted right above the bed at an approximate distance of 1.5m is presented in figure [3.16](#).

Infrared reflective markers are attached to landmark points of the body (22 in total) and the setup is assumed that the motion of the seizure will be registered at all times by the video system. Movement quantification is performed by saving the video data files.

The motion information is processed using the QMOVES software, and its divided in two

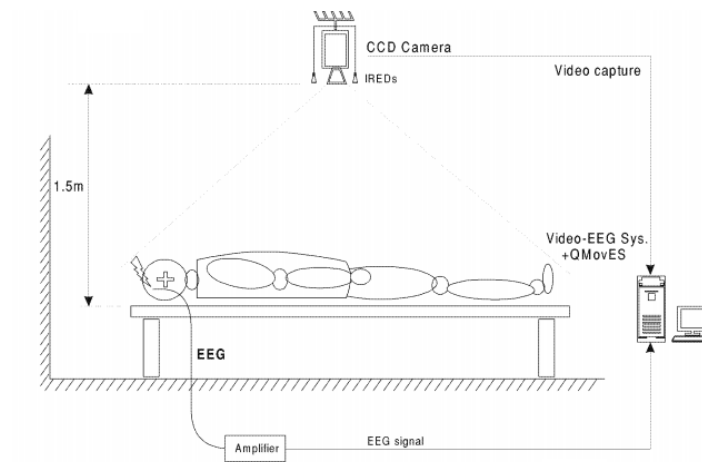


Figure 3.16: The setup of QMovES System. A CCD camera acquires video sequences into a PC where a digital video-EEG system and the QMovES software tool are installed [Li et al. \[2002\]](#).

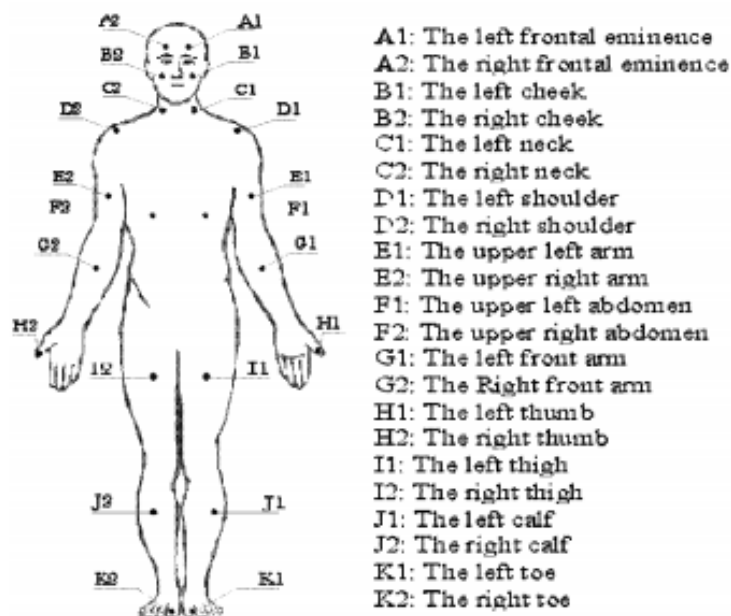


Figure 3.17: 22 landmark positions defined for the full-body marker positioning system [Li et al. \[2002\]](#).

main stages, the initialization and the tracking of the markers. The tracking of the marker is modulated as a two-dimensional (2D) ballistic motion, preceded by a Kalman filter to predict marker positions. Figure 3.18 represents a schematic of the procedure.

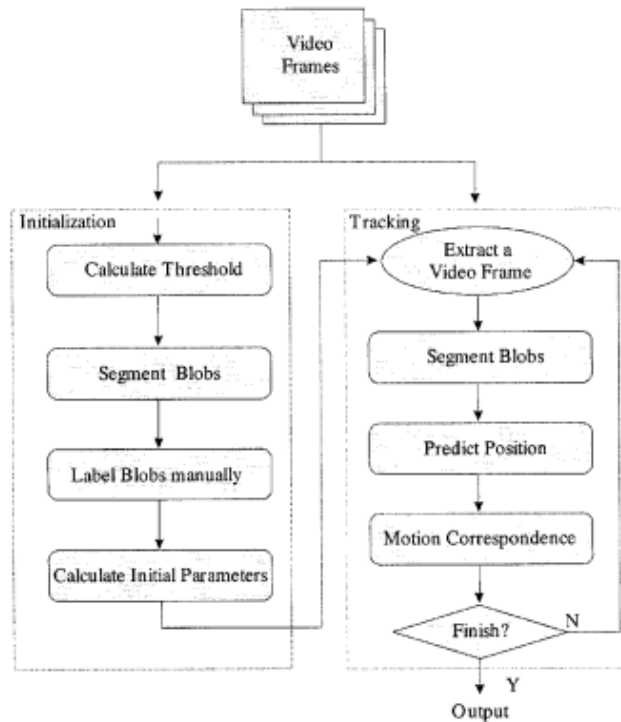


Figure 3.18: Schematic representation of the procedure for movement quantification used in QMovES Li et al. [2002].

The results from QMovES is the 2D movement in both horizontal and vertical axis (X and Y), in terms of pixels units. The authors succeeded in quantifying the motion, in terms of speed and spatial motion patterns, using the markers information Li et al. [2002]. Based on this initial work, Cunha et al. developed a similar approach, to evaluate seizure semiology. The setup for this approach can be seen on figure 3.19.

The setup includes an infrared CCD camera and an infrared LED lamp installed over the bed. Videos from simulation trials and real seizures were recorded and the movement quantification was performed using the pipelines from Li Li et al. [2002] and the MaxTraq software<sup>11</sup>. The authors were able to successfully segment and quantify jerking arm's movements, which are a typical MOI in the late clonic phase of the "tonic-clonic" seizure type Cunha et al. [2003].

Karayiannis et al. proposed the extraction and quantification of temporal motion velocity signals in video recording of neonatal seizures by optical flow methods Karayiannis and Tao [2003]; Karayiannis et al. [2005a,b].

Optical flow is the term used to indicate the velocity field generated by the relative motion between an object and the camera in a frame sequence. Assuming that the optical flow estimations

<sup>11</sup>Software Maxtraq <http://www.innovision-systems.com/Products/MaxTraq.html>

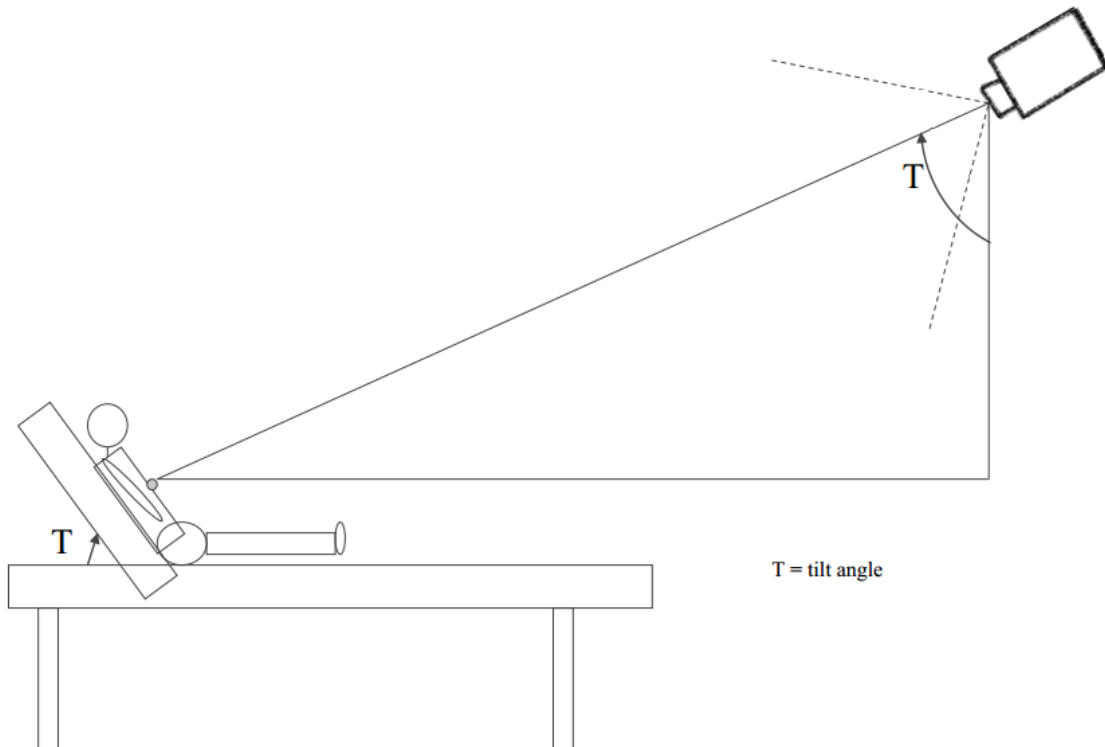


Figure 3.19: Video setup geometric model. Adapted from Cunha et al. [2003].

are a reliable approximation of the two-dimensional image motion, this algorithm can be used in many different applications, such as to recover the three-dimensional motion of the visual sensor as well as determining the three-dimensional surface structure (shape or relative depth), perform motion detection and object segmentation Horn and Schunck [1981] Barron et al. [1994].

Optical Flow can also be referred as the distribution of apparent velocities of movement of brightness patterns in an image, therefore providing important information about the spatial arrangement of the objects viewed and the rate of change of this arrangement Horn and Schunck [1981] Karayiannis and Tao [2003]. Typically, the optical flow computation is based on two successive frames, thereby being an ill-posed problem. An ill-posed problem is characterized by the fact that its solution might not be unique and its solution does not depend continuously on the data Karayiannis and Tao [2003].

Let  $I = I(x, y, t)$  be the continuous space-time frame intensity distribution. If the pixel intensity remains constant along a certain direction, then its derivative is zero:

$$\frac{dI(x, y, t)}{dt} = 0 \quad (3.1)$$

This condition can then be re-written as:

$$\frac{\partial I}{\partial x} * u + \frac{\partial I}{\partial y} * v + \frac{\partial I}{\partial t} = 0 \quad (3.2)$$

where  $u, v$  denote the components of the coordinate velocity vector in terms of the continuous spatial coordinates [Karayiannis and Tao \[2003\]](#).

This equation is also known as the optical flow equation (OFE). The OFE equation is not enough to specify the 2-D velocity field. There are several ways of solving the OFE equation, such as the Phase-Correlation, Block-Based Models, and the most traditional ones (Horn–Schunck and Lucas-Kanade), based on partial derivatives of the image signal and/or the sought flow field and higher-order partial derivatives [Karayiannis and Tao \[2003\]](#).

Global methods (i.e. Horn–Schunck) usually use a smoothness regularization term, to compute dense optical flows over large image regions. Local methods (i.e. Lucas-Kanade) use normal velocity information in local neighborhoods to perform a least squares minimization to find the best fit for the velocity constraint [Barron et al. \[1994\]](#).

[Barron et al. \[1994\]](#) provides an extensive review on the computation of the optical flow algorithms. The Horn–Schunck method advantage is that it yields a high density of flow vectors, even though it can be more sensitive to noise than the local methods. On the other hand, the Lucas-Kanade is a very powerful algorithm for the calculation of the flow, but since it is a local method, it cannot provide the flow information in the interior of uniform region within an image [Horn and Schunck \[1981\]](#); [Barron et al. \[1994\]](#).

In [Karayiannis and Tao \[2003\]](#), the author presents a procedure to quantify seizures, where the motion at a certain frame  $t=t_0$  was quantified by the maximum velocity of the region of the frame that contained the moving body part. After this initial approach, [Karayiannis et al.](#) developed their pipelines in order to recognize and characterize seizures. Their work involved three main tasks: extraction of quantitative motion information from video recordings of seizures, in form of motion-strength and motor-activity signals, selection of quantitative features that convey unique characteristics of neonatal seizures, and finally training artificial neural networks to distinguish neonatal seizures from normal infant motion and also to differentiate myoclonic and focal clonic seizures [Karayiannis et al. \[2005a\]](#). The outcome of their experiments verified that optical-flow methods are indeed a promising tool for quantifying seizures from video recordings.

[O’Dwyer et al.](#) aimed at quantitatively evaluating the lateralizing significance of ictal head movements of patients with temporal lobe epilepsy (TLE), using the same setup from [Cunha et al.](#) This clinical study investigated thirty-eight seizures (31 patients) with TLE. The head movements were quantified by selecting the movement of the nose in relation to a defined point on the thorax in a defined plane facing the camera. Authors statistical analysis showed that ipsilateral movement always preceded contralateral movement, with a 100% positive predictive value in both directions of the head movement. They concluded that there is high lateralizing value of ictal lateral head movements in TLE seizures [O’Dwyer et al. \[2007\]](#).

In the work of [Chen et al.](#), quantitative and trajectory analysis of movement trajectories in supplementary motor area seizures of frontal lobe epilepsy was performed using video analysis from ten patients. From the trajectories, amplitude, frequency, proximal/distal limb amplitude ratios, and shoulder/abdominal amplitude ratios measurements were calculated using MATLAB. The patients used markers, similarly to the setup of [Li et al. \[2002\]](#). Statistically significant



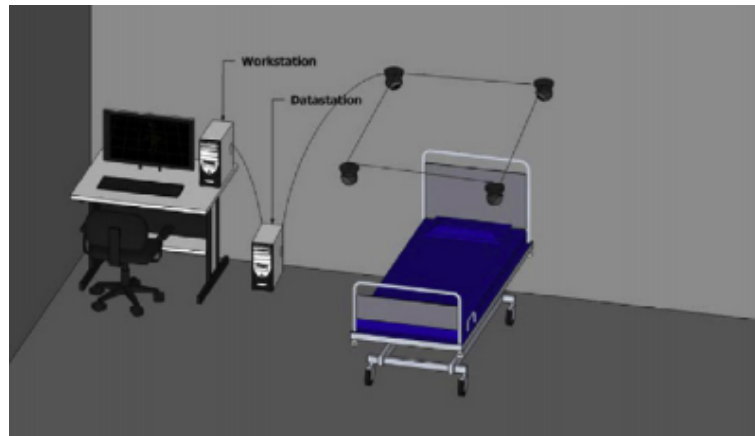


Figure 3.20: System setup with the 4 high-speed SVCams to achieve a 3D motion tracking system for seizure movements. A data-station processes the massive information coming from the cameras and feeds pre-processed data to the workstation where the MOIs are analyzed [Cunha et al. \[2012\]](#).

differences were found in the average amplitude, as well as proximal/distal limb amplitude ratios, in SMA seizures when compared with those of temporal lobe seizures [Chen et al. \[2009\]](#).

Mirzadjanova et al. evaluated the significance of lateralization of ictal upper limb automatisms in TLE seizures, where features like the duration of the automatisms, movement speed, extent, length and predominant frequencies of the movements were analyzed in both upper extremities of the patient body. Results shown that ipsilateral automatisms were more predominant than contralateral automatisms, even though no statistical significance was found in the analysis of the features described above [Mirzadjanova et al. \[2010\]](#). Similar analysis was used in [Rémi et al. \[2011\]](#), where quantitative analysis of movements during epileptic seizures was used to identify objective movement parameters characteristics to distinguish hyperkinetic seizures from other motor (especially automotor) seizures. Recently, a new 3D approach for movement quantification of epileptic seizures was proposed by Cunha et al [Cunha et al. \[2012\]](#). Based on the 2D previous works [Li et al. \[2002\]](#); [Cunha et al. \[2003\]](#), the authors now present a revolutionary approach, using 4 high-speed SVCams to achieve a 3D motion tracking system for seizure movements, as depicted in figure 3.20.

In order to evaluate the feasibility of the 3D approach, both the 2D and the 3D techniques were tested in two different scenarios: a simple motor execution performed by a volunteer and a complex motor motion induced by a real seizure. To quantify the movement of the subject, a set of spherical infrared reflective markers were attached to anatomic points of the patient, and MaxTRAQ 2D software, as well as Vicon Workstation software were used to quantify the 2D and 3D movement, respectively. Results clearly demonstrated the superior ability of the 3D approach, which is expected to have higher impact in the study of more detailed clinical studies in the future, relying in the implemented multimodal synchronized system (3D movement + video + EEG) [Cunha et al. \[2012\]](#).



## Chapter 4

# Summary and Proposed Methodology

Motion detection is the process of detecting a change in the position of an object relative to the surroundings or vice-versa, which can be achieved in several different ways. Accurate motion detection and tracking is then critical, and the movement quantification results are highly-dependable of the detection and tracking stage.

In this thesis, the aim is to make a contribution to the development of a markerless based video-system, based on a low-cost RGB-D camera, that: can be used in the clinical neurology environment, in multiple scenarios; allows the acquisition and tracking of the movement and is also unobstructive to the patients given their health conditions. Thus, systems that use markers or reflectors, for example, attached to the patient's body are out of scope of the goal of this thesis. For this purpose, the type of cameras that fit the best these requirements are RGB-D sensors such as the Kinect<sup>TM</sup> and the Kinect<sup>TM</sup>v2.

This thesis was divided into three major milestones:

1. Development of KiMA software in a multi-disciplinary environment;
2. Implementation and Usage of KiMA in multiple Healthcare scenarios;
3. 3D Quantification of Neurologic Diseases based on MOI's previously segmented using KiMA.



## **Part II**

# **NeuroKinect: A Kinect-based System for Movement Analysis and Quantification in Neurological Diseases**



## Chapter 5

# NeuroKinect: A Kinect-based System for Movement Analysis and Quantification

This chapter will be divided into three major branches: the first part, KiMA software will be addressed; in the second part, attention will be drawn on the different pipelines developed in order to use the streams of information in a different environment (from Microsoft Visual Studio C# to Matlab); and finally, results which derived from the use of KiMA in a healthcare context, for the selection of moments of interest (MOI's), will be presented for the Parkinson's and Epilepsy scenarios.

### 5.1 NeuroKinect, KiT and KiMA

The concept of using Kinect for movement analysis for epilepsy diagnosis was introduced by PhD João Paulo Cunha that developed with Eduardo Dias the KiT, KinecTracker. KiMA, Kinect Motion Analyzer is then a companion software to KiT, currently being continuously developed by a PhD student Ana Rocha, under the supervision of PhD João Paulo Cunha. Figure 5.1 presents the user-interface of KiT.

KiMA developers were Ana Rocha (aprocha@ua.pt) and Hugo Choupina, with constant supervision of both João Paulo Cunha and José Maria Fernandes (IEETA, Aveiro University). A special contribution to KiMA is also attributed to Eduardo Dias.

KiT and KiMA together compose NeuroKinect, a motion analysis system based on a RGB-D Camera, namely a Microsoft Kinect, which connects to a portable computer through an USB connection. Both applications were developed in C#. KiT is used to acquire and save to file information about human motion activity, composed of color, depth and skeleton streams 5.4.

The KinecTracker v1 application allows the acquisition of three different sources:

- Color (1280 × 960 resolution at 12 frames per second (fps), 640 × 480 resolution at 30 fps, or 320 × 240 resolution at 30 fps)

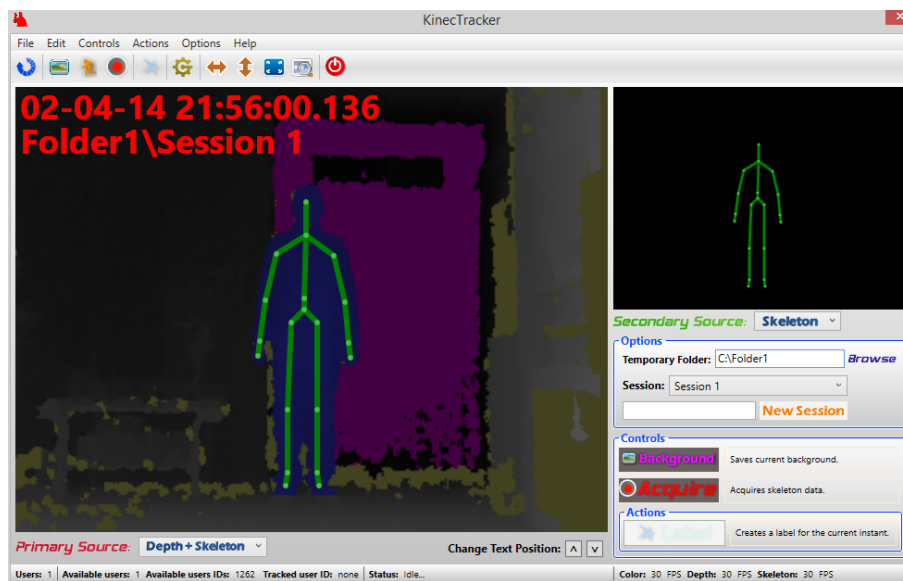


Figure 5.1: KinecTracker v1 UI.

- Depth ( $640 \times 480$ ,  $320 \times 240$ , or  $80 \times 60$  resolution at 30 fps)
- Skeleton of a single subject (20 joints listed in Figure 3.9)

KiMA allows the visualization and the manipulation of the data collected using KinecTracker. This software is expected to fulfill the need for manipulating the data retrieved from KinecTracker and it is thought to become an important tool for the Healthcare Environment where it is already being used.

### 5.1.1 KiMA Requirements

KiMA is a companion tool to KinecTracker that allows the visualization and manipulation of information previously acquired by using the KinecTracker with a Kinect. KiMA runs in Windows Operating Systems, using the Microsoft SDK 1.5. The main requirements defined for KiMA are the following:

1. Offline visualization of previously acquired streams of information (color, depth, skeleton, infrared or body-index) - task attributed to Ana;
2. Video manipulation (play, pause, rewind, next frame, stop, frame-rate speed) - task attributed to Ana;
3. Indication and management of relevant instants(labels) and events (MOIs) - task attributed to Hugo;
4. Exporting of data corresponding to a selected event - task attributed to Hugo.

Consequently, the author's contribution to KiMA were the inception, design and implementation of requirements 3 and 4.

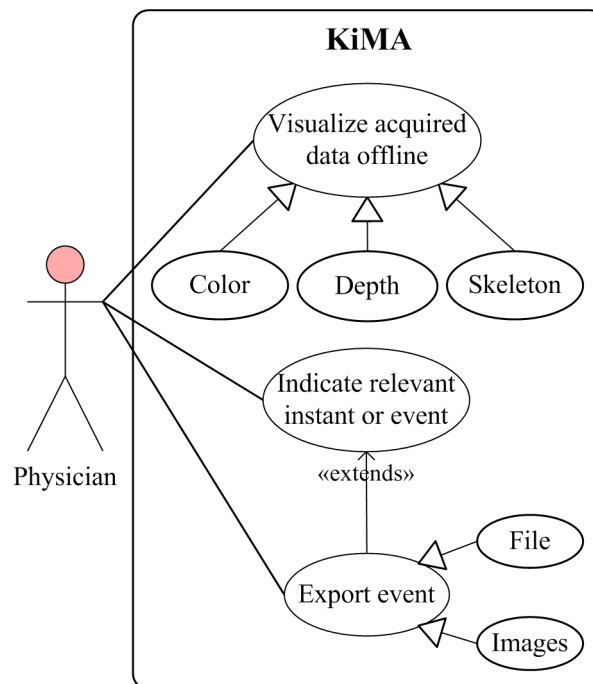


Figure 5.2: KiMA Use-Case Diagram for Kinect v1.

### 5.1.2 NeuroKinect Architecture

KiT (developed by JPC and Eduardo Dias) primary actor is the Kinect sensor, which was addressed previously. Using KiT, multiple streams of information can be saved to file and then use KiMA for the analysis. KiMA (developed by Ana and Hugo) main actor is the physician or the engineer, depending on the aimed task. Inside this analysis, due to the out-breaking and resourceful capabilities of the sensor, the system can be applied in multiple scenarios. Inside the Epilepsy use-case, KiSA (will be addressed in the next chapter) is a prototype of a plug-in for KiMA towards motion analysis in epileptic seizures. One third party of the system might be a remote cloud service, such as ABRiL Tafula S [2014], where information of patient's movement can be stored and then be assessed to use with KiMA (Figure 5.4).

### 5.1.3 KiMA Application

This software is intended to be user-friendly, and so, interacting with it should come naturally. Nevertheless, some concepts need to be understood before beginning data manipulation.

- **Label** → unique moment in time. (i.e: the patient entered the room).
- **Event** → unique moment in time that has a beginning and an end. (Begin → the patient seizure started; End → the seizure ended)
- **Image Flip** → it can be done Horizontally as well as Vertically, just by clicking in the option on the Main Window.

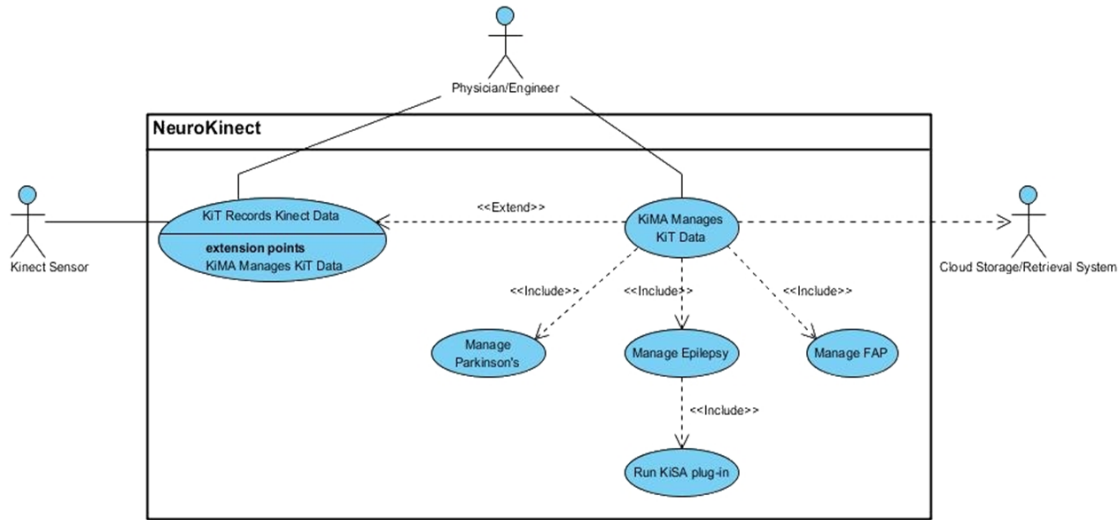


Figure 5.3: NeuroKinect Use-Case Diagram.

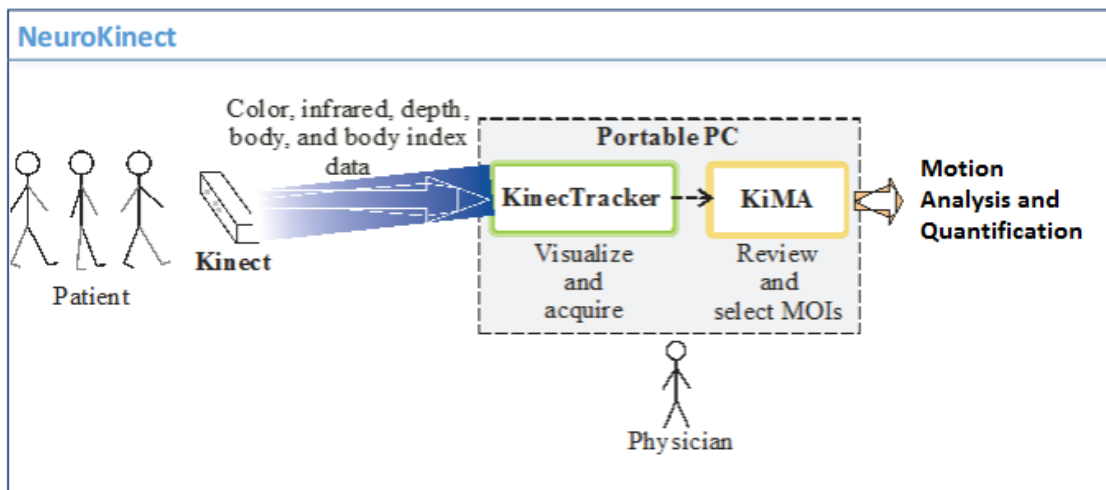


Figure 5.4: NeuroKinect Architecture Rocha A [2014].



- **Video Manipulation Shortcuts** → set of mouse-binding features aimed at ease the interaction with the software.
  - **Play/Pause** – space
  - **Forward Frame** – right arrow
  - **Previous Frame** – left arrow
  - **Stop** - s
- **Tree-View** → Displays in the UI Main-Window all information regarding the Moments of Interest.

Figure 5.5 shows KiMA Main Window, with a loaded acquisition.

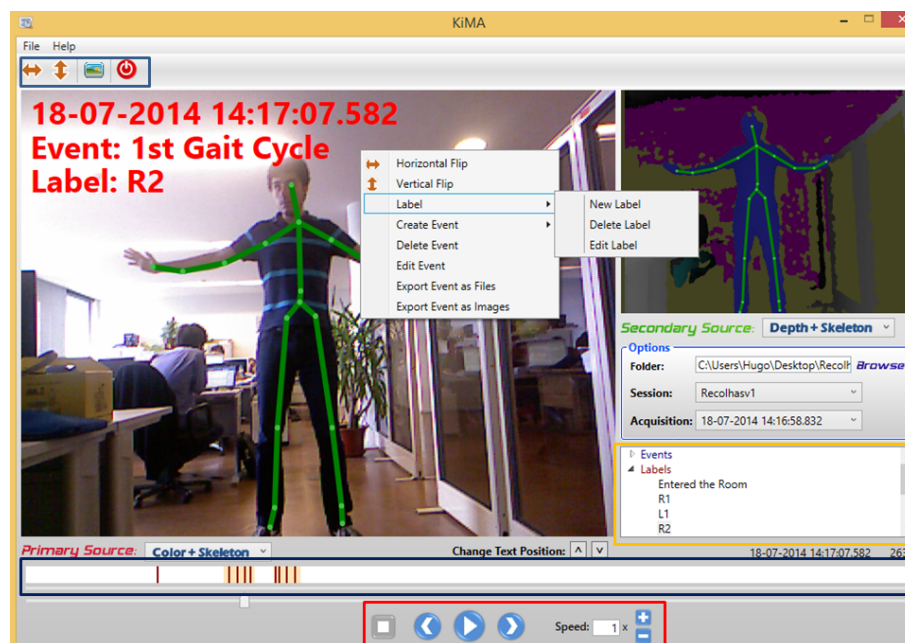


Figure 5.5: Main Window UI of KiMA application, including the display of color, depth and skeleton data and the mouse-binded Context menu.

KiMA's main window UI includes a menu and tool bars, visualization area (with primary and secondary sources), and Options panel. In addition, there are regular video manipulation options (play, pause, stop, rewind, fast forward, previous and next frames, and frame-rate speed). There is also a video progression bar, corresponding to the slider located above the manipulation buttons. The current timestamp and frame number are shown on the right side above the slider.

KiMA allows the indication of labels and events corresponding to MOIs, for further analysis. A label represents a given time instant, and an event has a beginning and an end. They are visually represented in the white rectangular area above the progress bar, using different colors to distinguish between them, as can be seen in Figure 5.7. Furthermore, the associated information (name and description) is displayed in the Tree-view below the Options panel.

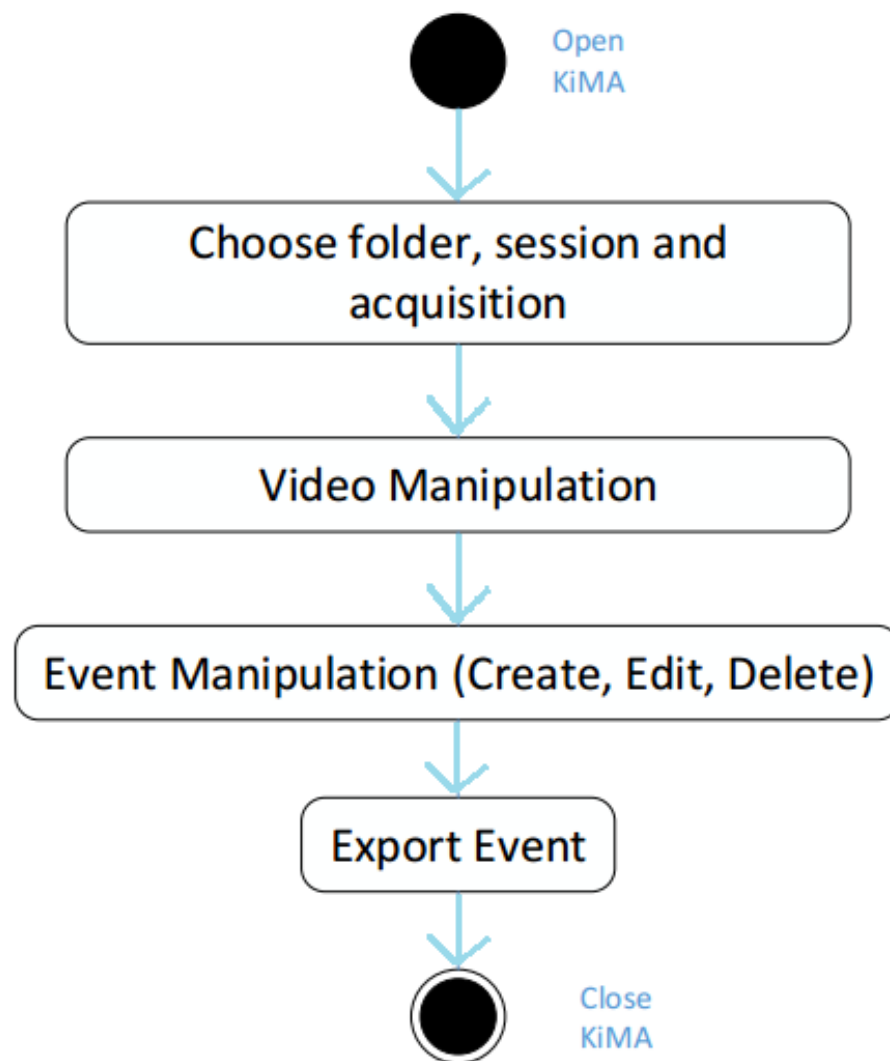


Figure 5.6: KiMA activity diagram.



Figure 5.7: KiMA UI: At the right-side, the tree-view information regarding all labels and events.

The manipulation and creation of MOIs may involve a few steps. For that purpose, the first step consists in choosing an acquisition for offline visualization (requirement 1). This is possible by indicating the location of the folder and the session name containing the desired acquisition, in the Options panel. If there are more than one acquisitions available, the user should select the acquisition via selecting the associated date and time.

When the loading is completed, the information regarding the timestamp of the data collected is placed on the right bottom corner. At this time, you can also see that there is a slider, frame-dependent: you can use this slider to jump frames within the video play.

Analyzing Figure 5.7, in the tree-view it can be seen two events and within each event several labels. The same information is displayed above the video manipulation buttons, with different colors: light orange are the events and dark red the labels. Each label inside each event represents a specific moment, and in this case, each label is synonym of the person step, right or left. Besides the steps, there is also another label that indicates the moment when the person entered the room and the field-of-view of the sensor. This example is the typical analysis performed when partitioning gait cycles within a gait acquisition, using the KiMA software.

After opening an acquisition, it is possible to manipulate the video as in a normal video player, corresponding to requirement 2. Then, the user can save MOIs by creating labels at certain video instants, and events with a given duration, using the context menu shown in Figure 5.5. When creating a label/event, the user must indicate a name and a description (optional). This information is saved to a XML file, and can be viewed in the tree-view of KiMA's main window (see examples shown in Figure 5.7). As can be seen in the Figure 5.5, it is also possible to delete and even edit labels/events. These functionalities address requirement 3. These features of the software are

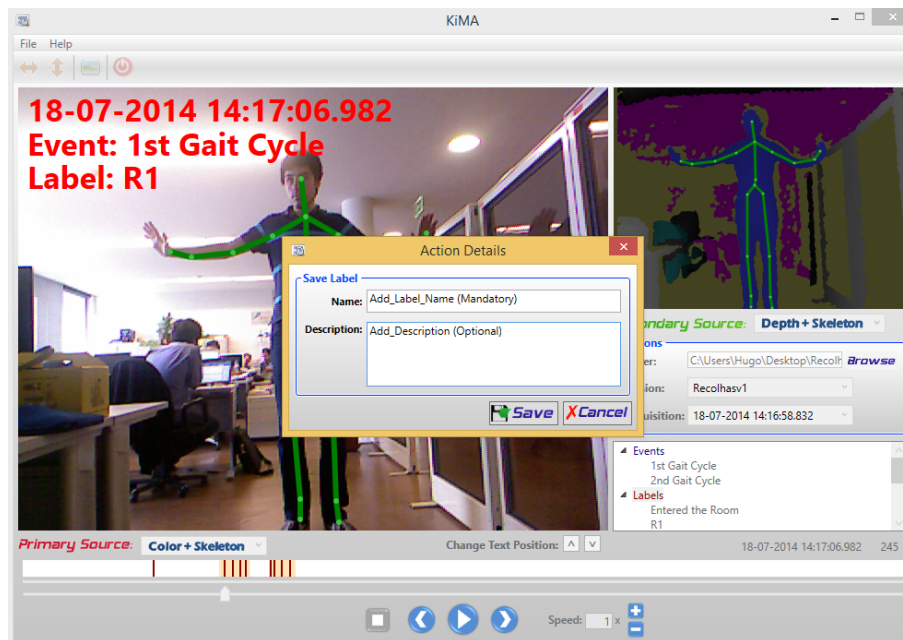


Figure 5.8: KiMA New Label Example: the user must name the event, but an additional description is optional.

binded within the right-button click of the mouse. There is no difference between activating the right-button click on the primary and the secondary source.

For events, it is further possible to export them as files or PNG images, for further analysis (requirement 4). This functionality is expected to be used to select seizures in epilepsy, and to partition gait cycles in PD, for example. To export an Event, the option “Export Event” must be selected within the right-button click and the user is required to create a New Folder, which is where the information regarding that MOI will be stored. If the option was “Export Event as Files”, after the Export is completed, this particular event can be loaded, as it was explained before. These files follow the same structure defined for KiT (header + file content, in bytes or integers, in the case of skeleton). Depending on the kind of stream, the header information can be slightly different. To synchronize all the streams, each different frame corresponds to a different timestamp, equal for all streams.

If the option was “Export Event as Images”, multiple folders will be created, depending on the available information (see Figure 5.13). The name of each created frame matches the timestamp of the moment of acquisition.

Whenever any kind of manipulation is performed (i.e. gait cycles partition), the information is displayed in the tree-view and also saved in a XML file, which can be seen in Figure 5.9. This information is structured two main nodes, Labels and Events. Inside each node, the information regarding each node is stored. The XML organization is fundamental and it allows an enhanced analysis when there is a need to use the information from KiMA in another environment.

```

<?xml version="1.0" encoding="UTF-8"?>
- <Tags>
  - <Label>
    <FrameNumber>159</FrameNumber>
    <Timestamp>20140718141704124</Timestamp>
    <Name>Entered the Room</Name>
  </Label>
  + <Label>
  + <Label>
  + <Label>
  + <Label>
  + <Label>
  + <Label>
  + <Label>
  + <Label>
  - <Event>
    - <Start>
      <FrameNumber>238</FrameNumber>
      <Timestamp>20140718141706748</Timestamp>
    </Start>
    - <End>
      <FrameNumber>275</FrameNumber>
      <Timestamp>20140718141707984</Timestamp>
    </End>
    <Name>1st Gait Cycle</Name>
  </Event>
  + <Event>
</Tags>

```

Figure 5.9: KiMA XML Example: XML organization after the analysis of an acquisition.

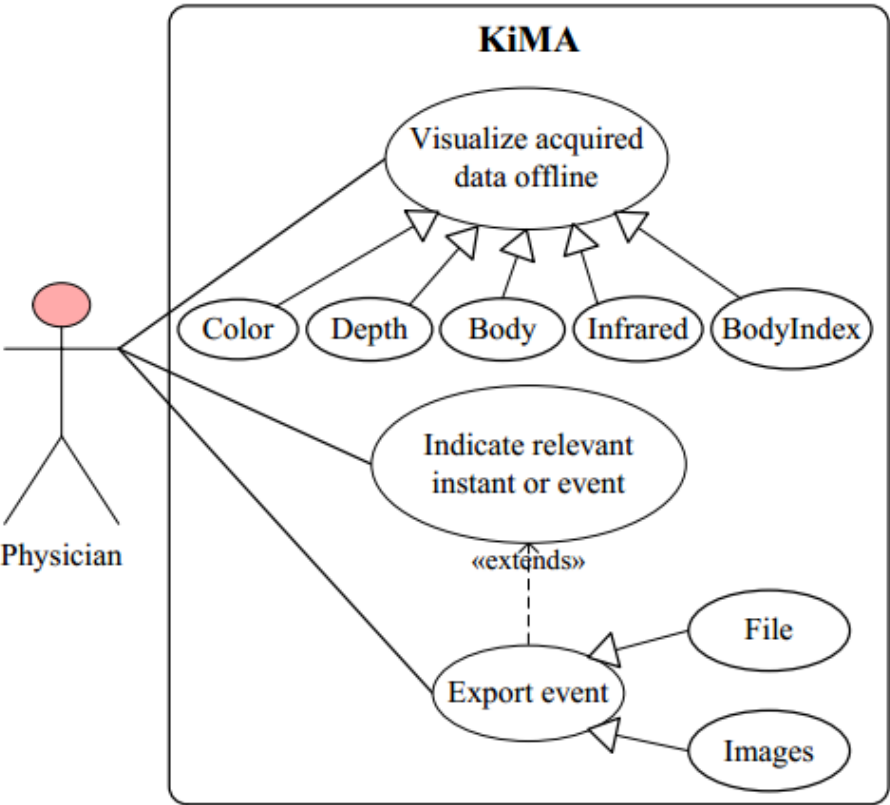


Figure 5.10: KiMA v2 Use-Case Diagram, with the two new streams: Infrared and BodyIndex



Figure 5.11: KiMA v2: Depth, Color and Body streams

#### 5.1.4 KiMA for Kinect v2

Since there are incompatibility issues regarding the use of multiple "Microsoft Kinect".dll components (SDK's) in one single C# solution, KiT and KiMA for Kinect v2 were separately developed from KiT and KiMA for Kinect v1. KiMA v2 was developed once the KiMA for v1 was completed. Since the official SDK for version 2 is not completely developed and available to developers yet, KiMA v2 is being continuously developed, with the monthly releases and updates of the SDK. Figure 5.11 shows the KiMA v2 UI with the depth view on the primary source and the High-Definition color in the secondary source.

Analyzing Figure 5.11, it can be perceived the difference in the depth estimations between the two sensors, as well as the number of joints and the different field-of-view available in the color stream. Comparing KiMA v1 to KiMA v2, there are no major differences: the only noticeable ones are the new previously reported streams available in Kinect v2 (Infrared and BodyIndex, see Figure 5.12), 25 joints available instead of 20, and finally, when exporting an event as images, two new folders will be created, addressing the two new streams (see Figure 5.13).

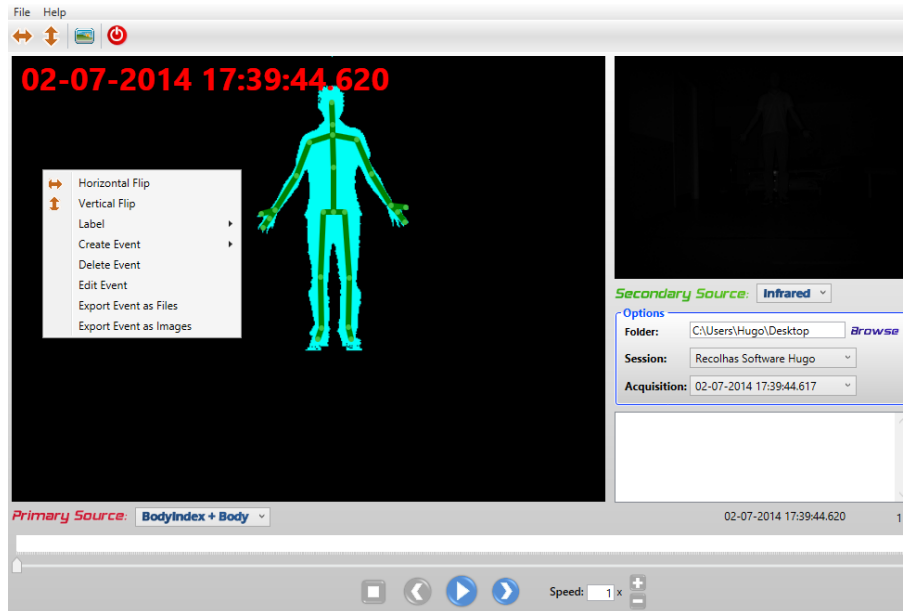


Figure 5.12: KiMA v2: BodyIndex, Infrared and Body streams

Name	Date modified	Type
BodyIndex	18/07/2014 00:30	File folder
Color	18/07/2014 00:30	File folder
Depth	18/07/2014 00:30	File folder
Infrared	18/07/2014 00:30	File folder
20140702154201464#1.kbi	02/07/2014 15:42	KBI File
20140702154201464#1	02/07/2014 15:42	KDPT File
20140702154201464#1.kir	02/07/2014 15:42	KIR File
20140702154201464#1	02/07/2014 15:42	KPOS File
20140702154201464#1.kvid	02/07/2014 15:42	KVID File

Figure 5.13: KiMA v2: Folder data Organization when exporting Events



## 5.2 Kinect 2 Matlab Dynamic Linked Library (DLL)

In this section, the Dynamic Link Libraries (DLL)s of functions (created in order to use the streams of information in a different environment - from Microsoft Visual Studio C#) developed in Microsoft Visual Studio C#, using the Kinect SDK and the Microsoft Libraries will be addressed. The .NET Framework is a development platform for building apps for Windows, Windows Phone, Windows Server, and Microsoft Azure. It consists of the common language runtime (CLR) and the .NET Framework class library, which includes classes, interfaces, and value types that support an extensive range of technologies. The .NET Framework provides a managed execution environment, simplified development and deployment, and integration with a variety of programming languages, including Visual Basic and Visual C#. .NET framework enables the compiling of different pipelines, using public interfaces to interact with the compiled code <sup>1</sup>.

### 5.2.1 KinectforMatlab.dll

Once any event is successfully exported from KiMA, whether in the format of files or images, in some cases it is required to use the Kinect SDK functionalities for the enhancement of the analysis. Developing this pipelines is a need since that the Kinect SDK is incompatible with Matlab and so, for instance, it would be impossible to know per-pixel depth values without this pipelines.

Bearing that in mind, functions for both Kinect v1 and Kinect v2 acquisitions were designed, implemented and fully-tested.

All functions were built-in in one single \*.dll file to ease the user experience in installing the file in the computer. There are three types of functions available inside the \*.dll:

1. functions that return the header information of the files, one for Kinect v1 and one for Kinect v2;
2. functions that return the bytes information of the streams (color, depth, infrared and bodyindex), one for both sensors;
3. functions that return the depth information of the files, one for each sensor;
4. help functions to understand how to use and access each different function.

More details on the installation of the \*.dll and how to access it from Matlab are provided in Appendix A.

---

<sup>1</sup>Microsoft .NET Framework <http://msdn.microsoft.com/en-US/library/zw4w595w.aspx>



## Chapter 6

# NeuroKinect usage in the Healthcare Context: Practical Examples

The developed software throughout the year is suitable to be used as a video-capture and primary analysis system in very different scenarios, such as gait analysis, posture control or even for upper body members tracking. Due to its characteristics, the system (KiT and KiMA) was an integrant part of the developed work in several different scenarios, namely: Parkinson's, Epilepsy, FAP (paramiloidosis) and in the follow-up of rehabilitation strategies on neurological patients. In this chapter we will describe the usage of the resulting system in different neurological diseases.

### 6.1 Parkinson's Disease

Patients that suffer from PD usually show freeze-of-gait, difficulty in maintaining cadence speed and also variability in the stride length. In this scenario, the work developed aimed at, besides the typical quantification of each patient's gait, estimating their clinical gait sub-score (UPDRS motor part sub-score) and differentiate PD from NON-PD (controls), based on the patient's gait analysis. At the same time, since this was an introductory study, another goal was to clearly assess whether the developed system could be used as an important diagnosis tool in supporting the diagnosis and follow-up of PD patients.

For that purpose, an experimental protocol was carried out in a room at São João University Hospital (Porto, Portugal), with the participation of three PD patients (P1, P2 and P3) and three control subjects (N1, N2 and N3). Each PD patient had an implanted DBS stimulator, and performed the experiment twice: with the stimulator on (STIM ON); and a few minutes after turning off the stimulator (STIM OFF). Each control subject performed the experiment only once.

The protocol included the use of the Kinect XBOX 360 and the KiT application, to acquire skeleton data (at a 30 fps rate) from PD patients and control subjects, while they were walking. The walking trajectory of four meters is illustrated by an arrowed dashed line in Figure 6.1. This figure also includes the relevant distances, as well as the Kinect height and tilting angle in relation to the horizontal plane (perpendicular to the gravity force). The chosen setup took into account

the Kinect limitations, and aimed at maximizing the actual tracking area, which is represented by the grey rectangle in Figure 6.1.

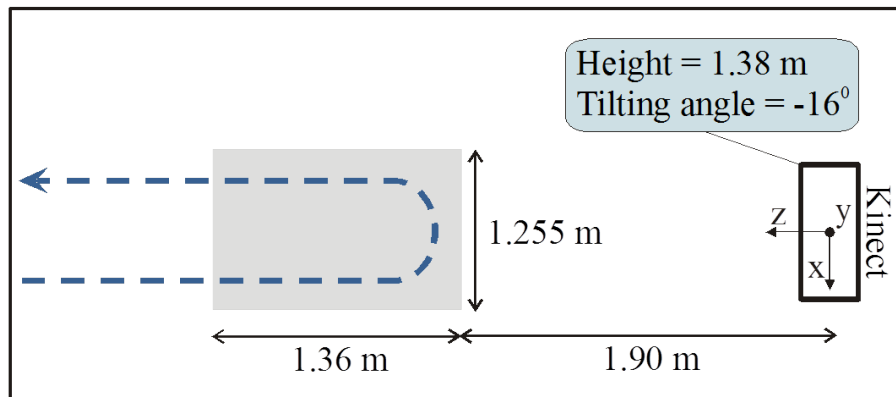


Figure 6.1: Experimental setup used for data acquisition, including the coordinate system associated with the Kinect.

The data acquired within the tracking area were firstly manually selected, and then partitioned into gait cycles, based on depth data acquired at the same time as the skeleton data. The MOI's selection, at this stage, was manually done just due to the fact that KiMA was being developed and so, in order to proceed with the analysis and the software development, the decision was to do it manually.

Among the several quantitative gait parameters calculated, the variance of the center shoulder velocity presented the highest discriminative power to distinguish between non-PD, PD ON and PD OFF states ( $p = 0.004$ ) Rocha A [2014]. In terms of the UPDRS sub-score estimation, the best result was achieved for the average distance between ankles ( $r = -0.85$ ) and also for the median speed of the right ankle Cunha [2014].

Our work here reported contributed to the publication of two very-short papers in two renown Portuguese Medical Conferences and, most importantly, to the publication of an international paper in the world's most credited Biomedical Engineer Conference (EMBC 2014 - see annex).

## 6.2 Epilepsy

KiT was inserted, since 2012, in the routine of "Ludwig-Maximilians-University Munich, Klinikum" that has a specific unit for monitoring and treating epilepsy patients, where the system's feasibility as an epilepsy monitoring tool has already been attested by the medical staff (please see Reference Letter in Appendix). Besides Kinect data, EEG signals synchronized with our system are also acquired, enhancing the information provided to the medical staff. KiMA v1 was inserted in the routine in early February 2014.

In this context, each patient that enters the unit is monitored 24h/7days. The field-of-view of the Kinect sensor is illustrated in Figure 6.2. Analyzing Figure 6.2, it can be perceived that the sensor is perpendicular to the horizontal plane. The setup also took into the Kinect limitations.



Figure 6.2: KiMA v1: Field-of-view of the Epilepsy Room. Typical distances range between 1.9m-2.1m from the sensor to the patient.

Patient's monitoring using KiT and KiMA were authorized by the hospital's Ethics Committee, and all patients signed an informed consent form.

The designed experimental protocol consists in saving the background before initiating the monitoring of a new patient. The next step consists in whenever an epileptic seizure occurred, the moment is marked by creating a label. KiT is always acquiring, with a buffer algorithm continuously running. Whenever a seizure arises, a label is added and is then used as reference to convert the label into a seizure event in KiMA. Then, using this label as reference, a seizure event is created and exported in KiMA. Once the event is created, the seizure information is remotely accessed for the quantification process. The workflow of the process is shown in Figure 6.3.

The data acquired using the KinectTracker includes color and depth data, at 30 fps rate. EEG signals, synchronized with the Kinect, were also collected at the same time.

Based on the RGB-D data correspondent to seizures, extracted by the physicians using KiMA, and the associated background depth frame saved in KinectTracker, background subtraction can be successfully performed over the RGB video. Then, optical flow methods are used with the aim of detecting and quantifying the movement of the seizure.

### 6.2.1 Physical Constraints in the Epilepsy Routine

Epileptic seizures are unpredictable and so, whenever a seizure occurs, immediate response is expected by the physicians which are constantly monitoring the patient. As explained before, there is a practical setup and protocol meticulously designed to get as much seizure information as possible. Nevertheless, there are issues related to the fact that this is a real life situation, and so, most of the times the protocol is not fully respected.

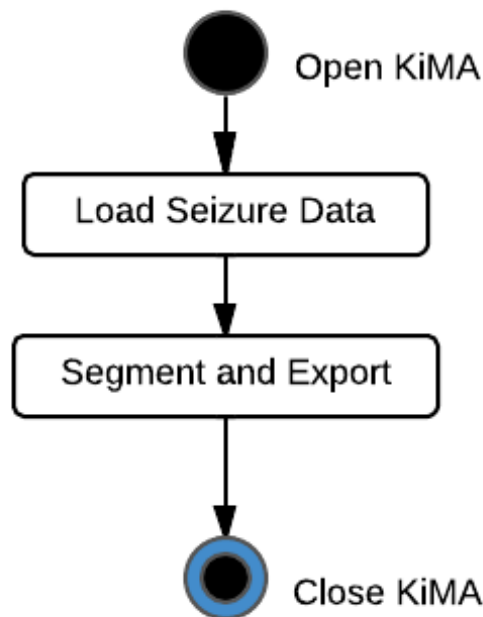


Figure 6.3: Epilepsy Activity Diagram for KiMA: KiMA is used to segment and export the seizure Events, which are then made available via a secure FTP server.

There are two major kinds of limitations in the routine: one is related to the lack of robustness of the skeleton tracking algorithm from the Kinect SDK; the other one is related to the interaction between the patient physical location and the tasks associated to the normal routine of an hospital room.

The Kinect SDK 1.5 and K4W SDK v2, as previously explained, allows the 3D tracking of an individual. In such a complex context as the epilepsy monitoring, accurate estimations of the body joints using this SDK feature could be done and it would be of extreme valuable importance, even though with the known limitations of the sensor. Unfortunately, the Kinect SDK Skeleton Algorithm, in both Kinect v1 and Kinect v2, is not precise enough to provide accurate joints estimations during a seizure occurrence, and so the chosen setup aims at maximizing the resolution of the images.

Nevertheless, for still positions, the K4W v2 sensor seems to provide accurate 3D joints estimations, as it can be depicted in Figure 6.6.

K4W v2 sensor was only recently integrated to the system (Late May/June 2014) and, even with the greater improvement in the skeleton algorithm, it was not able to deal with the presence of the bed lateral components, and so, whenever a patient has a movement too close to the structure, the tracking is not efficient enough in deal with such movement (see Figure 6.5). Figure 6.4 and 6.5 show the field-of-view of KiMA v2 installed in an Epilepsy Monitoring Unit: the first-ever seizure recorded with Kinect v2 sensor.

Even though there have been placed visual markers to set the location of the patient's bed, most of the times the bed is dislocated from the optimal field-of-view point of the Kinect sensor.

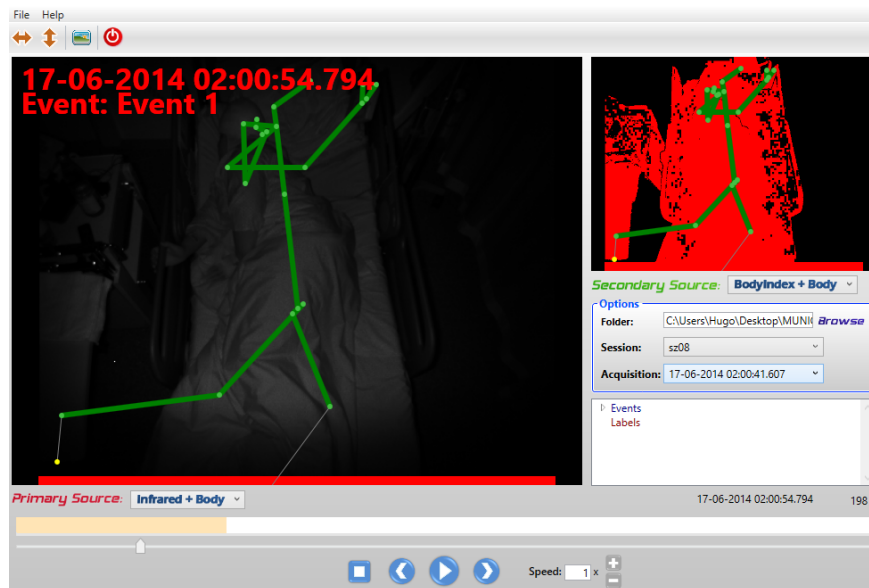


Figure 6.4: KiMA v2 Infrared, Body and BodyIndex.

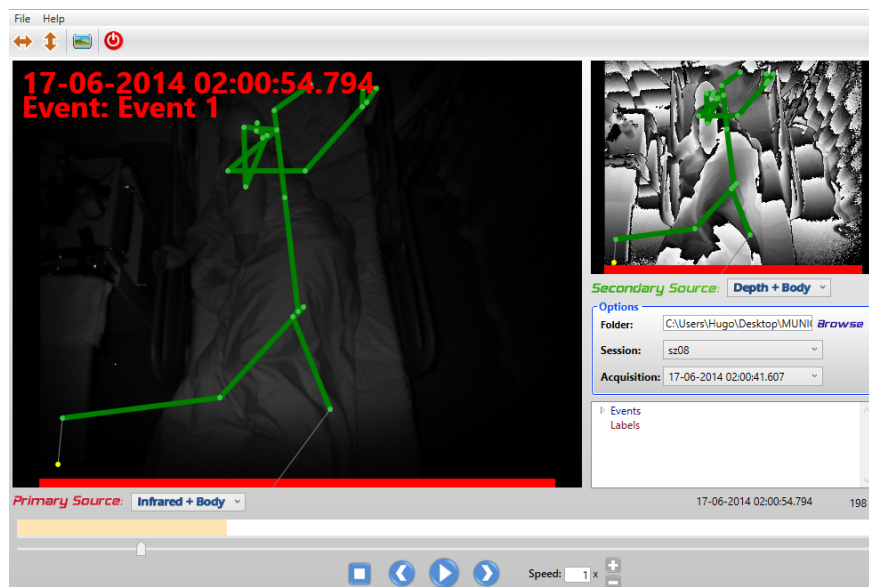


Figure 6.5: KiMA v2 Infrared, Body and Depth.

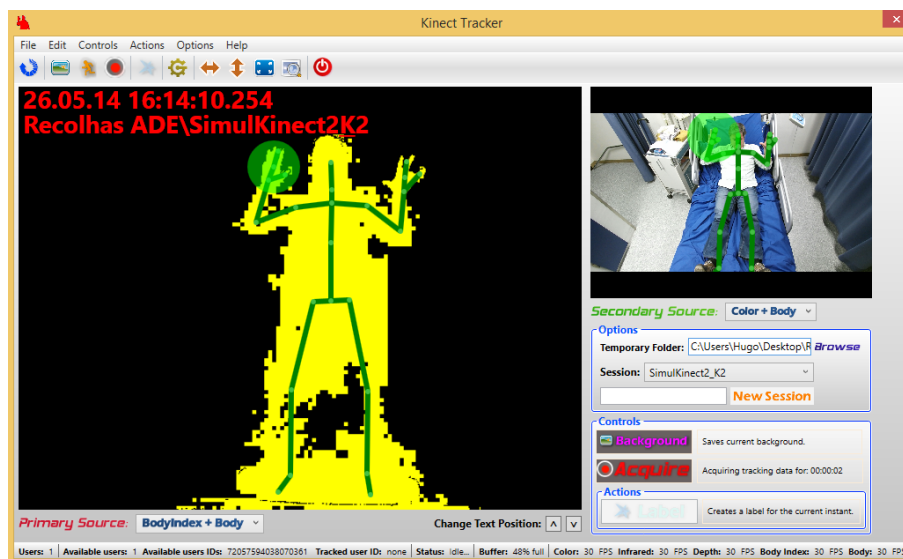


Figure 6.6: KiT v2 from LMU Bed: Trial tests to assess the new sensor robustness.

This dislocation happens due to the fact that there is a need to perform imaging methods to the patients brain (i.e. CT, MRI) and so, the patient needs to be transported. Since this is a routine healthcare environment, when the patient returns to the room, it might not always be in the target area.

Besides the dislocation of the bed, often the background frame is not saved. This issue is critical hence background subtraction of the patient is known as being one of the first methods to be applied when performing human activity motion analysis. When a seizure arises, the physician enters the room to better understand what is going on with the patient, and to help in case of extreme movement acuities. Physicians try to perform a set of activities with the patients to be able to identify whether the patient is already responsive and can perform demanded tasks, such as following the path of a pen. The presence of the physician can sometimes interfere with the field-of-view of the sensor, which contribution would be easily eliminated by the background subtraction algorithm. Nonetheless, this problem was overcome by performing bed subtraction, which is explained in the following section.

## 6.2.2 Bed Subtraction Algorithm

The first frame of each exported event is used to segment the bed. This segmentation is purely based on the depth information. The first important stage of the process begins with the pre-processing, where the depth values are filtered to remove noise and also to segment the bed between known ranges. Depending on the dislocation of the bed from the optimal field-of-view zone, the depth estimations of the bed range between 1300mm - 2100mm. Using the SDK 1.5, each per-pixel depth value is converted to an RGB value in order to create the depth frame, just like in Figure 6.7.





Figure 6.7: Seizure first depth frame.

At this stage, a seed point, thought to be as belonging to the bed, is provided by the user. Based on the intensity-pixel transitions between the initial seed point and the eight neighbors, a region growing algorithm is implemented, where a point is regarded as belonging to the bed if its pixel intensity is within a threshold.

Once the region growing process is completed, the final step consists in matching the color frame to the depth frame. There is a need to do that since both stream sources physical location in the sensor are in different locations (see figure 3.11) and so the two streams need to be re-aligned. The realignment is automatically performed when using the Kinect SDK online, but at this stage, this shift was done using the results in a previous study H [2013].

Very briefly, the aim of the study was to evaluate the misalignment between the depth and color frame of the two streams. To evaluate this misalignment, a script in MATLAB was created. The procedure is shown in figure 6.8, where the user has already chosen several points, one in the mask and another on in the color image, which is where the user believes the mask should be.

Once the labeling of the image points between the two streams was completed, mathematical analysis was done and, two formulas were designed to match the frames:

$$newX(i, j) = oldX(i, j) + \Delta X * \frac{(oldX(i, j))}{imageWidth}; \quad (6.1)$$

$$newY(i, j) = oldY(i, j) - \Delta Y \quad (6.2)$$

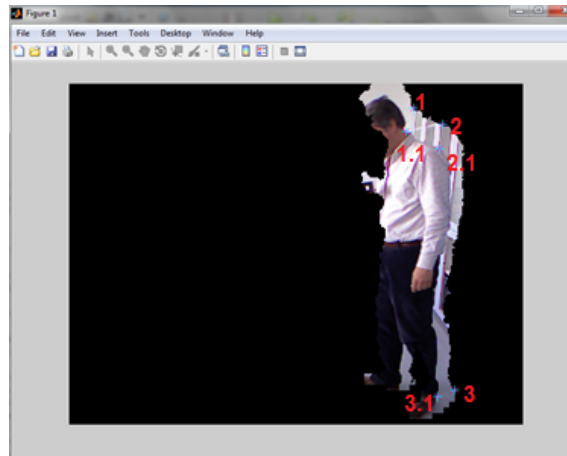


Figure 6.8: Study to evaluate the difference between mask and color image using MATLAB [H \[2013\]](#).

where,  $\Delta X$  and  $\Delta Y$  are the mean variation values calculated. Figure 6.9 presents the relation obtained between the mean variation of the square root distance for each pair of points versus the depth in each frame of the movement.

Based on the obtained results, the bed mask image is shifted in a  $\Delta X$  and  $\Delta Y$  proportion and is then applied to all color frames of the event. One example of a successfully subtracted bed mask is shown in Figure 6.10. Notice that some small black dots arise in the image, inside the bed, which represent noisy depth estimations that are then easily eliminated in Matlab.

The workflow of the procedure is shown in Figure 6.11.

### 6.2.3 Optical Flow Approach

Once bed subtraction is performed, optical flow methods are used for the movement detection and tracking process. Optical flow, as stated before, is the term used to indicate the velocity field generated by the relative motion between an object and the camera in a frame sequence. Since

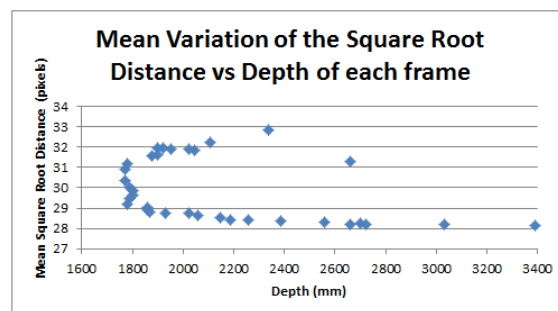


Figure 6.9: Mean Variation of the Square Root Distance vs Depth of each frame of the training image set.

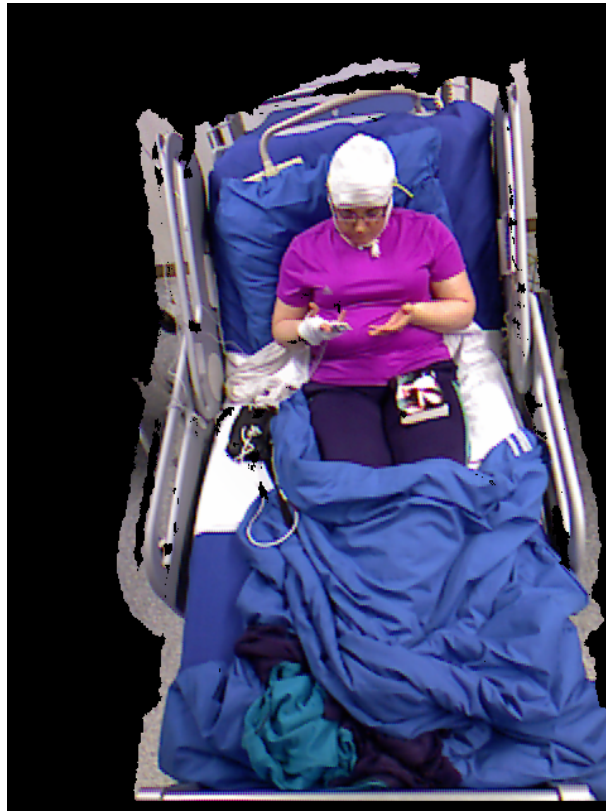


Figure 6.10: Result of Bed Subtraction over the first frame, after alignment between color and depth.

the epileptic movements are mostly unpredictable and uncoordinated, by using the optical flow approach, estimations of which body parts are moving can be achieved.

For this purpose, from the wide range of optical flow algorithms available and already implemented, the choice was to use the Horn-Schunk method. The reasons for this choice were based on the fact that the state-of-art approaches, namely Karayiannis and Tao [2003] Karayiannis et al. [2005a] Karayiannis et al. [2005b], to epilepsy movement quantification also used this method. Furthermore, the Horn-Schunk algorithm is implemented in Matlab<sup>1</sup>, within the *Computer Vision Toolbox*, referred as *vision.OpticalFlow System object*. The algorithm provides us with accurate estimations of the movement boundaries and so, efficient tracking based on that information can be performed.

Briefly, the Horn-Schunk method, by assuming that the optical flow is smooth over the entire image, computes an estimate of the velocity field, that minimizes this equation:

$$E = \iint (I_x u + I_y v + I_t)^2 dx dy + \alpha \iint \left( \frac{\partial u^2}{\partial x} + \frac{\partial u^2}{\partial y} + \frac{\partial v^2}{\partial x} + \frac{\partial v^2}{\partial y} \right) dx dy \quad (6.3)$$

<sup>1</sup>Mathworks <http://www.mathworks.com/>

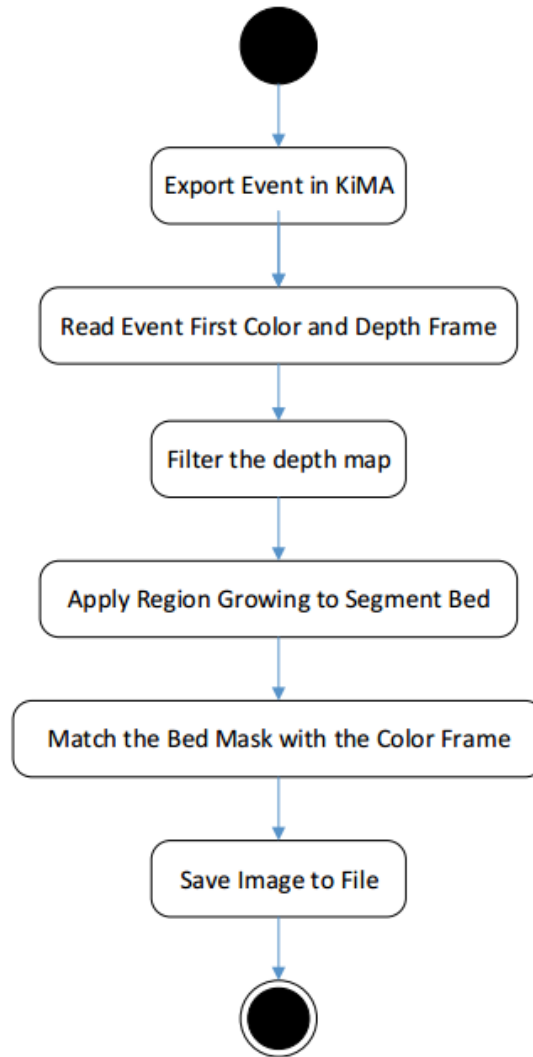


Figure 6.11: UML Activity Diagram of the Bed Subtraction Algorithm.

where  $\alpha$  is the smoothness term of the velocity field,

$$\frac{\partial u}{\partial x} \quad \text{and} \quad \frac{\partial u}{\partial y}$$

are the spatial derivatives of the optical velocity component  $u$ . The  $\alpha$  regularization parameter controls the strength of the smoothness constraint and is usually selected heuristically. The Horn-Schunck method minimizes the previous equation to obtain the velocity field,  $[u \ v]$ , for each pixel in the image, which is given by the following equations:

$$u_{x,y}^{k+1} = u_{x,y}^{-k} - \frac{I_x[I_x u_{x,y}^{-k} + I_y v_{x,y}^{-k} + I_t]}{\alpha^2 + I_x^2 + I_y^2}$$

$$v_{x,y}^{k+1} = v_{x,y}^{-k} - \frac{I_y[I_x u_{x,y}^{-k} + I_y v_{x,y}^{-k} + I_t]}{\alpha^2 + I_x^2 + I_y^2}$$

where

$[u_{x,y}^k v_{x,y}^k]$  is the velocity estimate for the pixel at (x,y) and  $[u_{x,y}^{-k} v_{x,y}^{-k}]$

is the neighborhood average of  $[u_{x,y}^k v_{x,y}^k]$  [Karayiannis and Tao \[2003\]](#).

Matlab implementation has several properties that can be changed, depending on the aimed task. In order to gain more sensitivity with the algorithm, the Horn-Schunk method, besides the Matlab implementation, was manually implemented based on the work of [Kesrarat and Patanavijit \[2011\]](#). Then, a physical test using a golf-ball and the Kinect sensor XBOX 360 was performed.

The aim of this physical test was to clearly assess the behavior of both algorithms. The test consisted in video-recording (color and depth streams) the movement of the ball along an inclined plan, and then track and quantify the ball movement using both Optical Flow algorithms. The algorithm designed for the golf-ball tracking consisted in comparing, frame-by-frame, the optical flow lines within an initial mask, provided by the user. Then, using as reference the optical flow lines drawn in each frame, the mask was continuously shifted based on the differences between the mask centroids. The setup used can be seen in Figure 6.12.

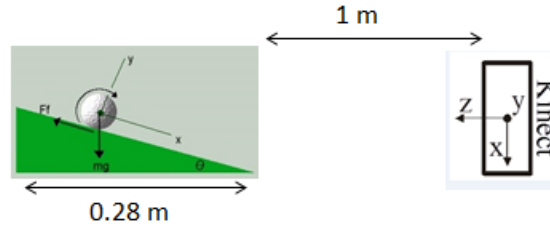


Figure 6.12: Schematic Representation of the conducted trial to perceive and validate the performance of the Optical Flow Algorithms.

Beforehand, the expected result was predicted to be: positive velocities in terms of  $V_y$  (velocity along the Y axis) and  $\pm$  zero velocity along  $V_x$ , since the ball was dropped on the top of the inclined plane, where the ball is only under the gravity force, being zero its initial velocity and acceleration, and the movement would be almost linear. Along the incline plane, conservation of mechanical energy was considered. Three different movements were recorded, with different heights so that the velocities achieved by the ball were different. The results of the tracking are shown in table 6.1.

Table 6.1: Characteristics of the ball movement in terms of initial velocity, acceleration and the angle of the incline plane

h (cm)	$v_0$ (m/s)	$a$ ( $m/s^2$ )	$\alpha$ ( $^\circ$ )
2	0.632	0.069	3.95
5	1	0.174	10
7	1.14	0.242	14

Figure 6.13 presents the 2D movement of the ball, in terms of the X and Y coordinates. Analyzing it, it can be perceived that the movement was not totally uniform as anticipated.

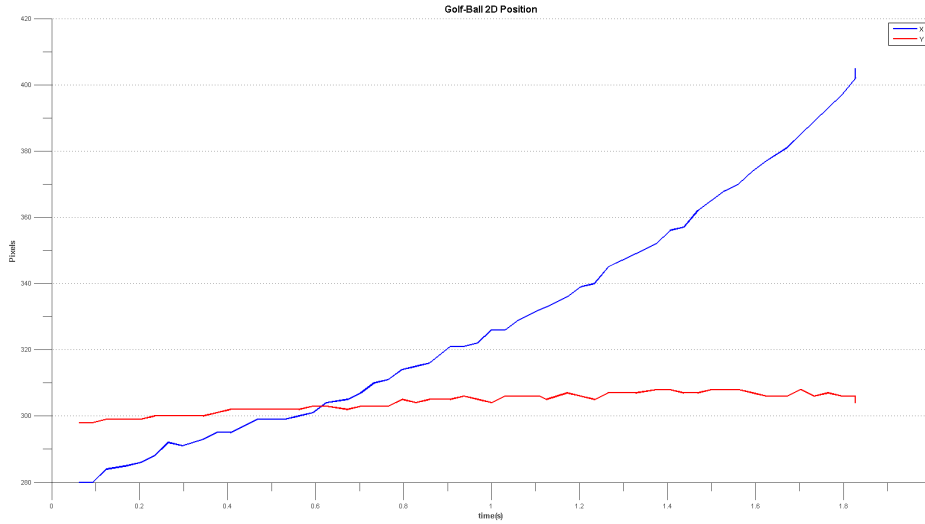


Figure 6.13: Tracings of the 2D golf-ball movement in terms of the X and Y coordinates for the slowest movement.

Figure 6.14 presents the comparison between the real depth value measured by the Kinect sensor and the theoretical value calculated for the position of the ball. The formula used was:

$$3D\text{position} = x_0 + v_0 * t - 0.5 * a * t^2 \quad (6.4)$$

where  $x_0$  is the initial position,  $v_0$  the initial velocity,  $a$  the acceleration and  $t$  the time interval.

We can clearly see that even though there were some noisy estimations, the depth values obtained are pretty accurate when compared to the theoretical values.

Table 6.2: Results obtained on the Optical Flow algorithms: Maximum and Minimum Optical Flow velocities values of the ball, for the two algorithms.

	OF_Matlab				OF_Hugo			
	V <sub>x</sub>		V <sub>y</sub>		V <sub>x</sub>		V <sub>y</sub>	
H (cm)	Max	Min	Max	Min	Max	Min	Max	Min
2	0.094	-0.080	0.1914	0.053	1.712	-1.699	5.676	-0.992
5	0.097	-0.097	0.1824	-0.017	1.969	-1.802	4.856	-1.142
7	0.096	-0.085	0.1622	-0.023	1.409	-1.981	5.8435	-1.682

Analyzing the results obtained, several conclusions can be drawn. Firstly, both algorithms quantified the ball in the expected way, even though the values along  $V_x$  were expected to be considerably lower. Secondly, the output values from the Matlab implementation seem to be normalized between 0 and 1, which is another important conclusion. Besides that, a movement with 0.6 m/s initial velocity was quantified with similar optical flow speed as a movement of 1



Figure 6.14: Tracings of the 3D golf-ball movement in terms of the real depth value (provided by the Kinect) and the calculated theoretical one for the slowest movement.

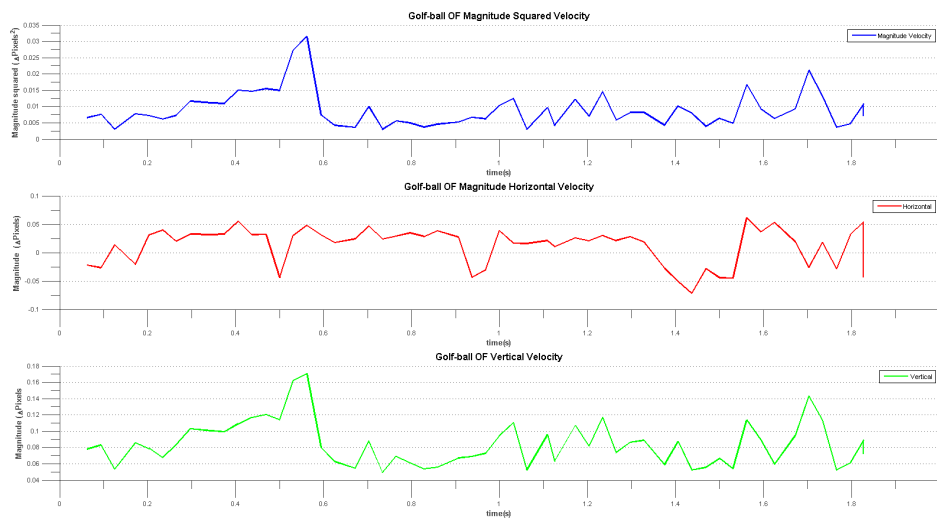


Figure 6.15: Tracings of the 2D golf-ball movement in terms of the Optical flow velocities for the slowest movement.

m/s, which is another relevant conclusion. This similar quantification is related to errors in the ball tracking, even though in visual terms, the output video from the ball tracking seems to be pretty accurate.

In terms of optical flow units, since the results seem to be normalized, an immediate conclusion cannot be drawn, not even when relating to the cited article in the Mathworks website. Nevertheless, there are reasons to believe that the units are  $\Delta pixels/frame$ . Finally, based in this study, for the epilepsy movement detection and quantification, the decision was to use the Matlab

implementation due to the fact that it is more robust and it is not as time-consuming as our own implementation of the algorithm.

#### 6.2.4 3D Motion Tracking Algorithm based on Optical Flow

Based on the main concept of the algorithm developed for the golf-ball tracking, a more robust one was design to track movements within seizures.

Prior to the actual tracking, the Optical Flow velocities are calculated, using a certain gain, being the output value in the form of Horizontal and Vertical Components, which gives us the velocities vectors in both directions. Besides the OF velocities, the OF lines are drawn in each frame. The OF lines are dependent of the gain used for calculating the OF, and so, in order to track a movement with the best accuracy possible, this gain should be as high as necessary to draw the lines on the boundaries of the movement, just like in Figure 6.16. Besides the OF, the Depth data extracted from the Kinect sensor is also used.

The depth estimations, even though with the previously explained problem of misalignment, provides us with the "ground-truth" of the physical position of the aimed ROI and so, that same information is used to automatically correct the algorithm.

The tracking process is initiated with the creation of a mask over the aimed ROI. An initial seed point is also set by the user. In each frame, the lines within the mask are targeted. If there are no lines, it may mean one of two things: 1) the OF gain used is unable to detect the boundaries of the movement; 2) there is no movement. Assuming that the user selected a proper gain, if no lines are find within the mask, it is assumed that there is no optical flow velocity and so, in the next frame, the same mask is used.

In case there are OF lines, it means that movement was detected. The typical state-of-art approach uses the maximum velocity in the area to quantify the movement. For the tracking, we measure which are the "%" highest velocities and we then calculate the median of this values for both the Horizontal and Vertical plane. The median was considered after performing the Jarque-Bera test, which confirmed that the output values obtained did not followed a normal distribution. Furthermore, using a percentage of the highest velocities enables us to filter the tracking for noise. The median values are then multiplied by a certain gain to transform them into pixel dimensions. The original mask is then shifted in the calculated proportion in each direction.

At this stage, a depth criteria is implemented in order to auto-correct the algorithm and also to avoid tracking errors: if the centroid of the new mask is within a certain depth range when compared to the previous positions, the new centroid is labeled as acceptable; else, within the current mask we look for a point of similar depth. If after the auto-correction section, the algorithm is unable to find the next centroid, the user is requested to draw another ROI. The process is repeated until all frames are analyzed.

To avoid high-frequency transitions, each time that the algorithm needs to auto-correct himself and when the user draws another ROI, a spline interpolation is performed over the calculated centroids to smooth the movement. In the end, the Savitzky-Golay FIR smoothing filter is also applied to the movement sequence.





Figure 6.16: Epilepsy Seizure Frame, with bed subtraction performed and OF lines drawn in the frame. The orange arrow represents the actual lines (which represent the detected movement by the algorithm) that are intended to be tracked, whereas the red arrow represents the upper body movement. Note that the original image was rotated  $90^\circ$  for visualization purposes only.

The schematic of the algorithm is presented in Figure 6.17.

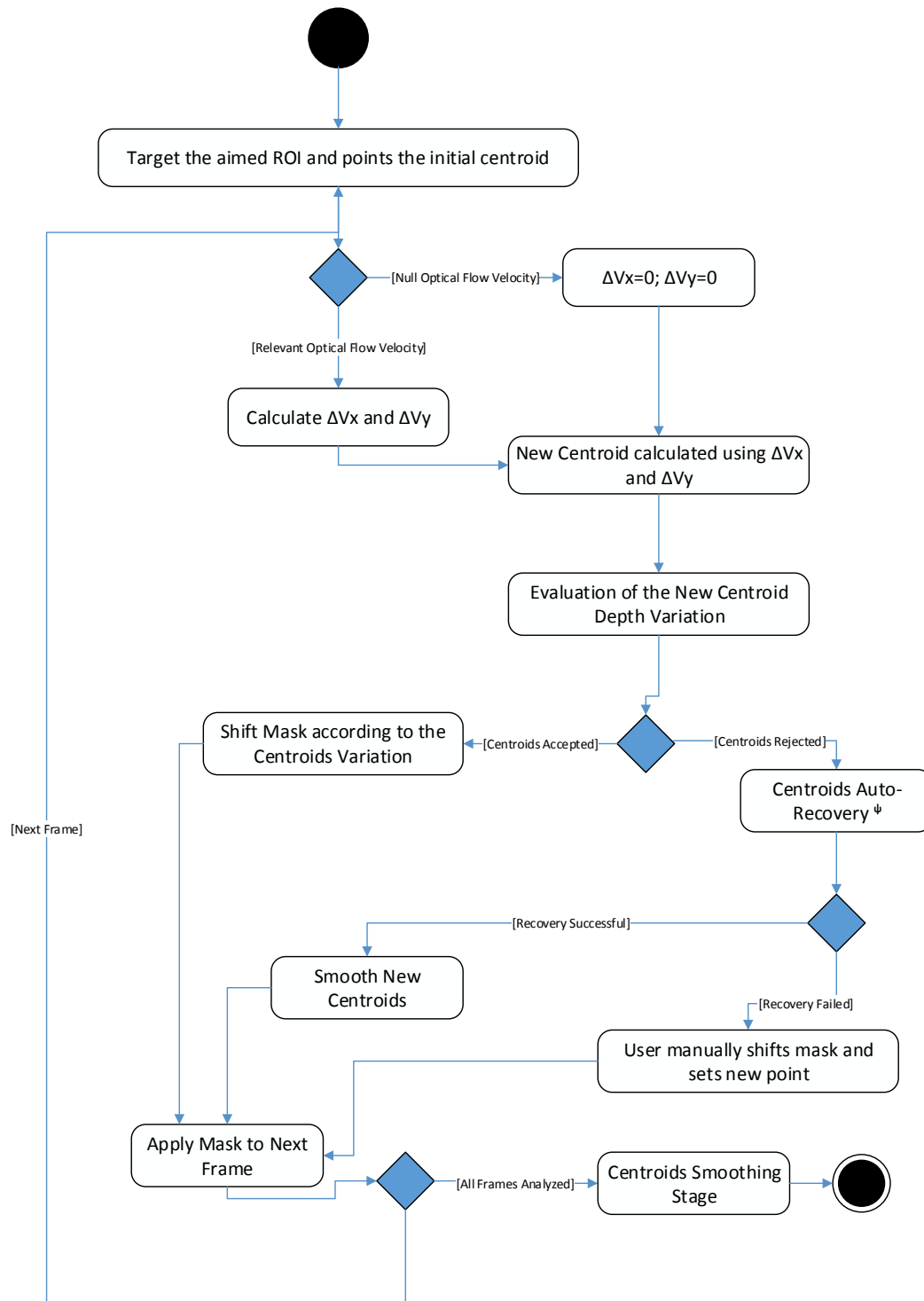


Figure 6.17: UML Activity Diagram of the designed algorithm.

### 6.2.5 Quantification Results



Figure 6.18: KiMA UI: Seizure initial frame.

The proposed semi-automatic approach was applied to an uncoordinated seizure (see figure 6.18), in order to track the head and both hands movement. This seizure, recorded with Kinect XBOX 360 at 30 fps, induced uncoordinated movement in both three body parts, with a duration of twelve seconds (complex motor seizure - hypermotor), and the patient had an IV fluid wire attached to this right-hand, which was also very close to his head.

An overview of the motion pattern presented in the patient seizure can be depicted in Figure 6.19.

The IV wire is a constraint that its contribution cannot be eliminated and it is a source of noisy measurements, since the OF algorithm is extremely sensitive and it detected the wire movement. Nevertheless, the relative error obtained in the head tracking was low. This error was measured by comparing the tracked centroids to the manually labeled ones throughout all frames. The mean relative errors (mean and standard deviation) were:

$$XC_{centroid} : 1.94 \pm 1.14\% \quad (6.5)$$

$$YC_{centroid} : 8.49 \pm 7.32\% \quad (6.6)$$

Comparing our semi-automatic approach, with a state-of-art 2D motion analysis software, MaxTRAQ<sup>2</sup>, not only our approach provides us with 3D information but also the time that it is saved in the task of manually labeling all centroids in each frame is considerable: as an example, for

<sup>2</sup>Software Maxtraq <http://www.innovision-systems.com/Products/MaxTraq.html>

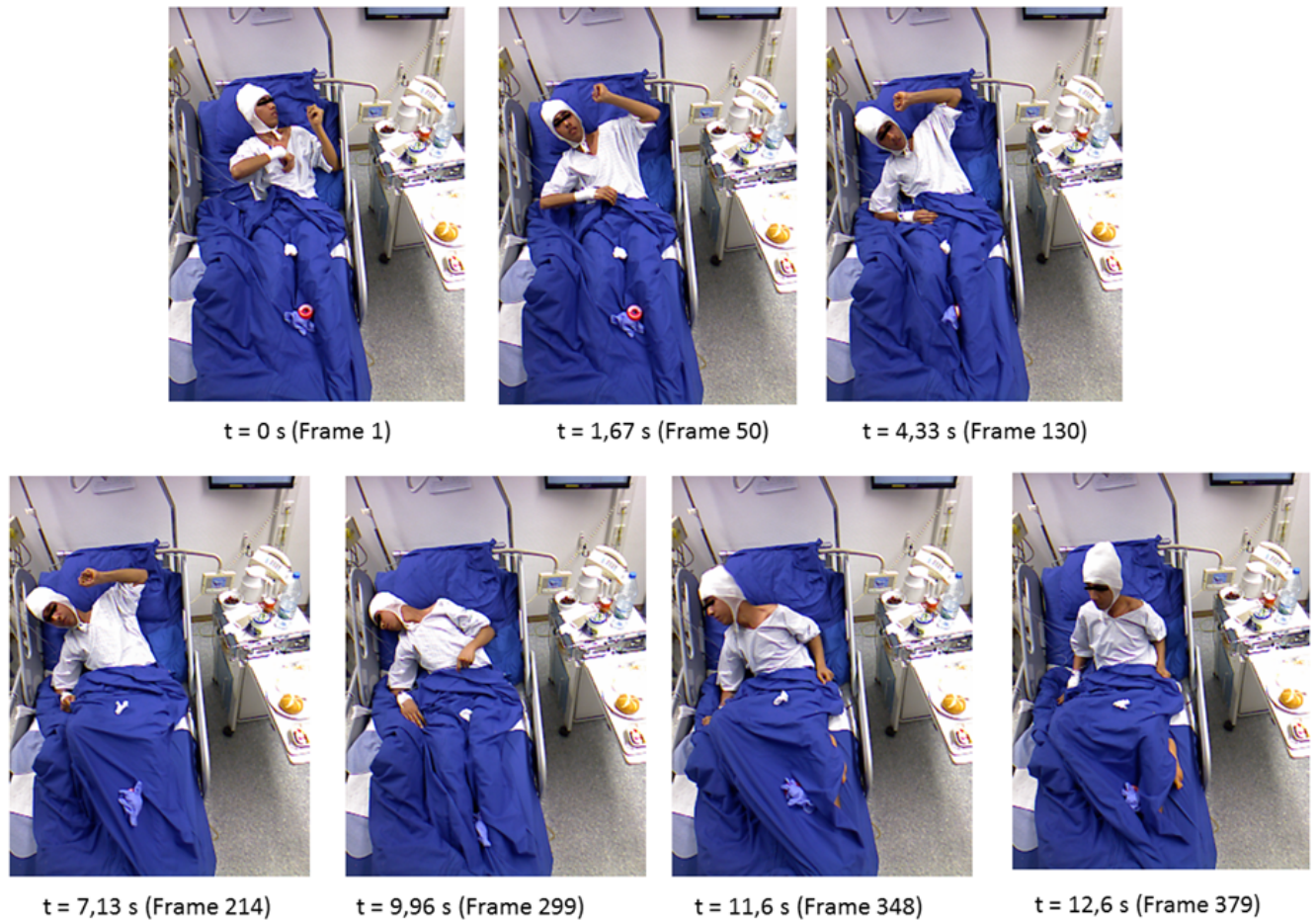


Figure 6.19: Representation of the motion pattern experienced by the patient during the quantified seizure.

the head tracking (378 frames), our semi-automatic algorithm took around 45 seconds whereas in the MaxTRAQ environment, where the user needs to set each centroid manually, it took roughly 3 minutes and 30 seconds. When performing the labeling manually, the user has a much higher control and confidence over the process. Nevertheless, such task is more demanding for the operator, in terms of usability and practicability.

Figure 6.20 presents one snapshot of the manual centroids labeling done to compare the two approaches.

Once the movement tracking is completed, 2D and 3D quantification is performed. It can be quantified in terms of the OF velocities (Magnitude, Horizontal and Vertical); 2D Centroids position variation; Depth variation; and finally, in terms of the 3D Velocity and Acceleration. From Figure 6.21 to Figure 6.26, the blue, red and green points in the time axis represent the moments when the user had to intervene in the tracking process.

The output trajectories of the tracked centroids are shown in Figure 6.21 and Figure 6.22.

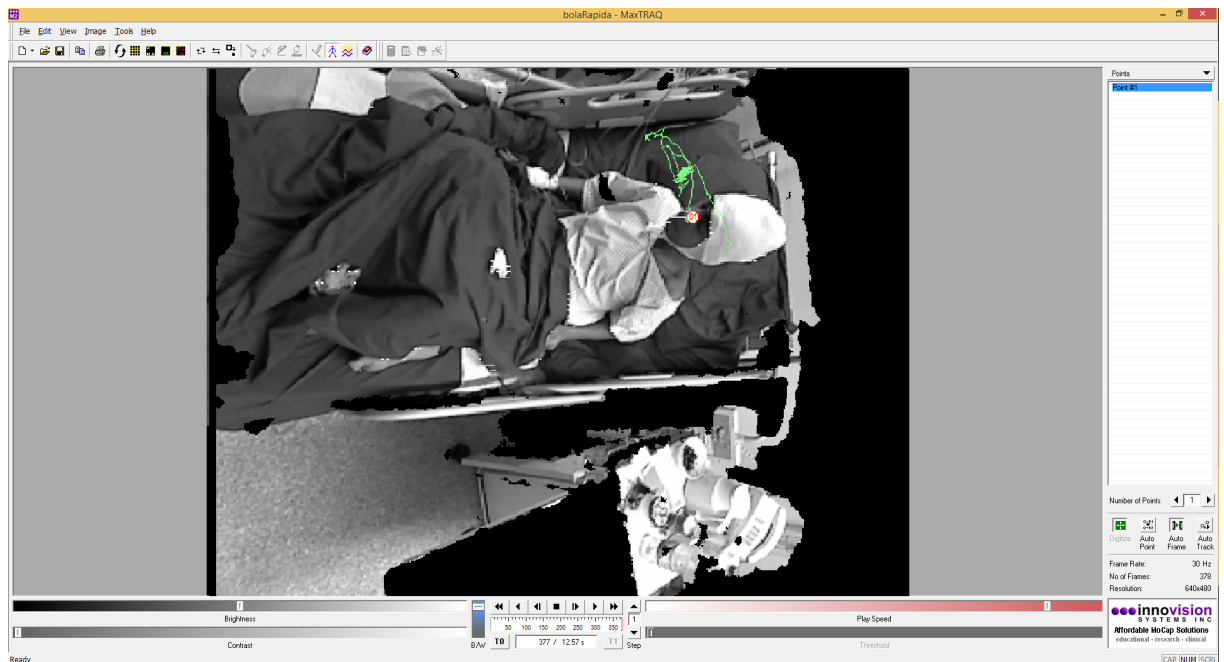


Figure 6.20: MaxTRAQ 2D motion software UI. In the represented frame there is a marker with the centroid of the head at a certain moment in time. The green line represents the head movement throughout the frames.

Figure 6.21 shows the motion of the centroid(pixel unit) in  $x$  axis direction and Figure 6.22 shows similar information in the  $y$  direction.

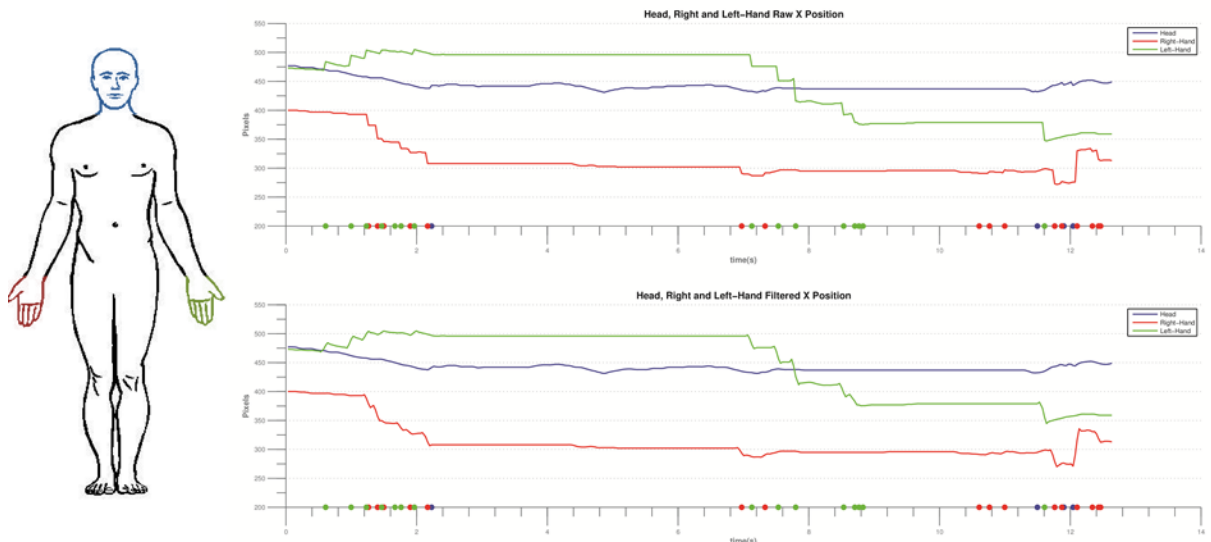


Figure 6.21: Tracings of the body motion in X coordinate (anterior-posterior view), non-filtered and filtered, in function of time with the corresponding body positions.

The optical flow velocities of the tracked centroids are showed in Figure 6.23, Figure 6.24 and Figure 6.25. Figure 6.23 shows the magnitude velocity( $\Delta Pixels^2$  unit). Figure 6.24 and Figure 6.25



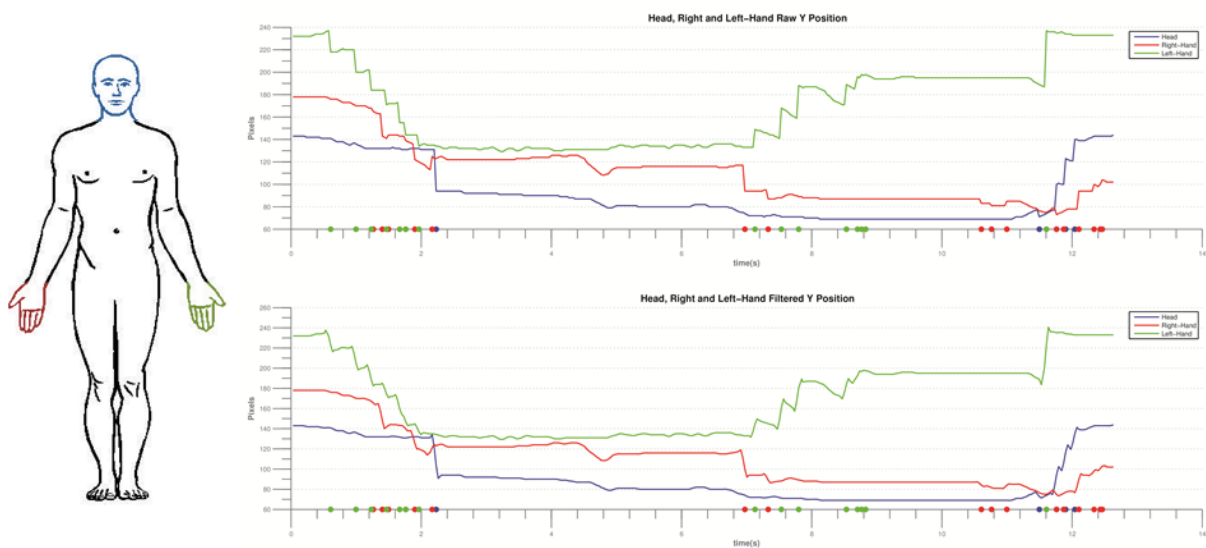


Figure 6.22: Tracings of the body motion in Y coordinate (vertical), non-filtered and filtered, in function of time with the corresponding body positions.

show the horizontal and vertical velocity ( $\Delta Pixels$  unit), respectively.

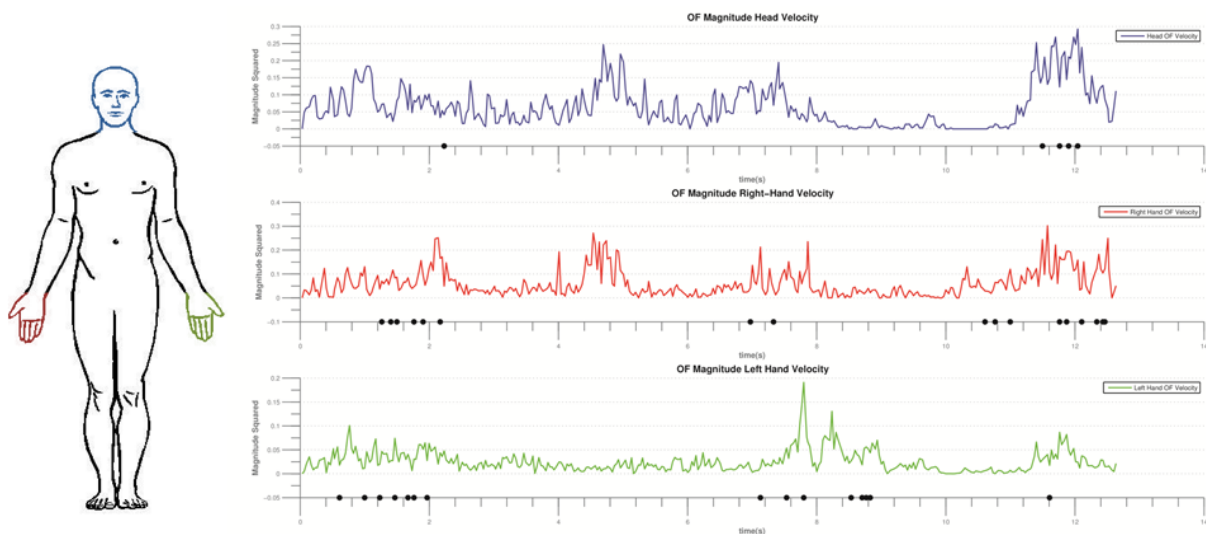


Figure 6.23: Tracings of the optical flow magnitude velocity in function of time with the corresponding body positions.

The depth values of the tracked centroids are showed in Figure 6.26. Figure 6.26 shows the depth values (meters unit) non-filtered and filtered, which were obtained by applying a Butterworth low-pass filter with a cutoff frequency of 6Hz.

Using the depth values and the 2D centroids, it is possible to convert this 2D information  $[x(px), y(px), z(m)]$  to 3D  $[x(m), y(m), z(m)]$  in meters unit. This conversion was performed after mapping the 2D tracked RGB centroids to 2D - Depth centroids, and then convert the 2D-Depth

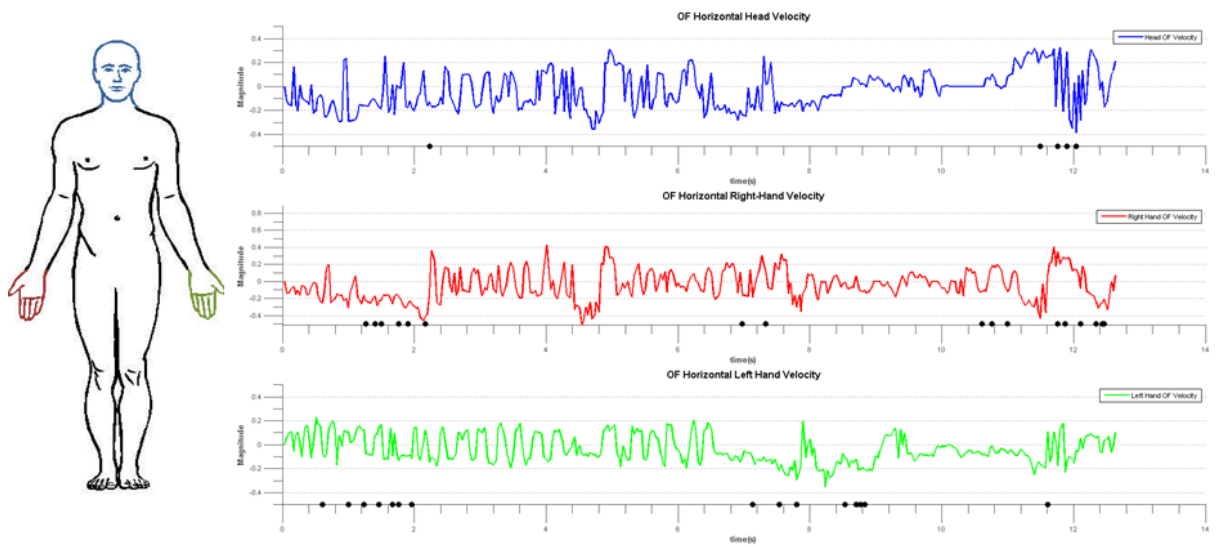


Figure 6.24: Tracings of the optical flow magnitude horizontal velocity in function of time with the corresponding body positions.

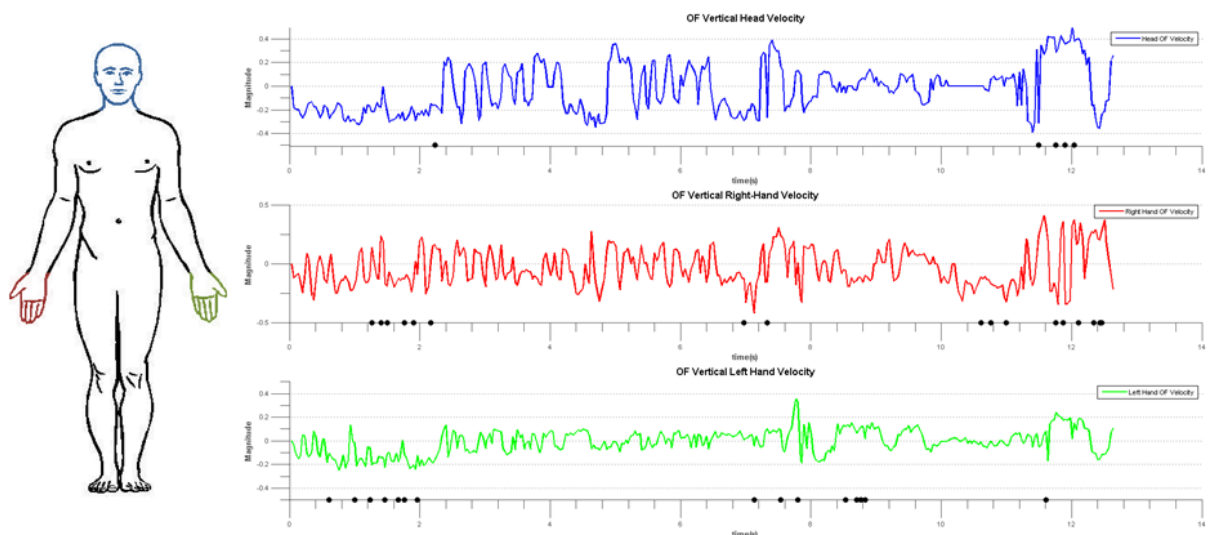


Figure 6.25: Tracings of the optical flow vertical velocity in function of time with the corresponding body positions.

raw values into the third dimension. The formulas to make such a conversion are available online<sup>3</sup>. The 3D velocity and acceleration were calculated using:

$$3Dvelocity = \sqrt{v_x^2 + v_y^2 + v_z^2} \approx \sqrt{\frac{\Delta x^2 + \Delta y^2 + \Delta z^2}{\Delta t^2}} \quad (6.7)$$

$$3Dacceleration = \sqrt{a_x^2 + a_y^2 + a_z^2} \approx \sqrt{\frac{\Delta v_x^2 + \Delta v_y^2 + \Delta v_z^2}{\Delta t^2}} \quad (6.8)$$

<sup>3</sup>Kinect Calibration: converting 2D depth to 3D coordinate space <http://burrus.name/index.php/Research/KinectCalibration>

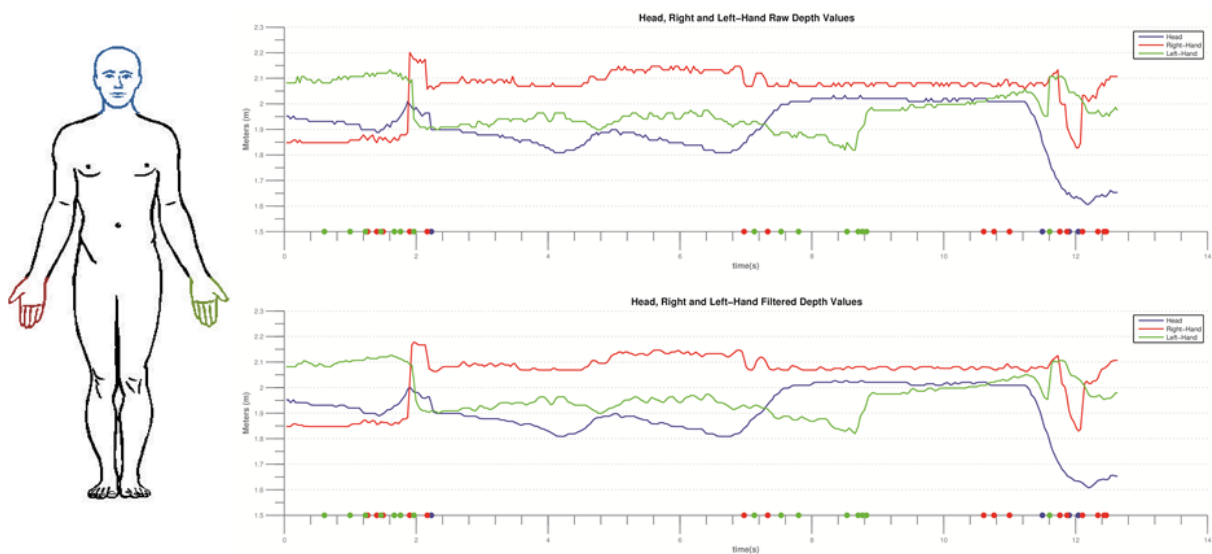


Figure 6.26: Tracings of the depth values, non-filtered and filtered, in function of time with the corresponding body positions.

The velocity of the tracked centroids are showed in Figure 6.27. Figure 6.27 shows the velocity values (meters/s), using the filtered centroids and depth data.

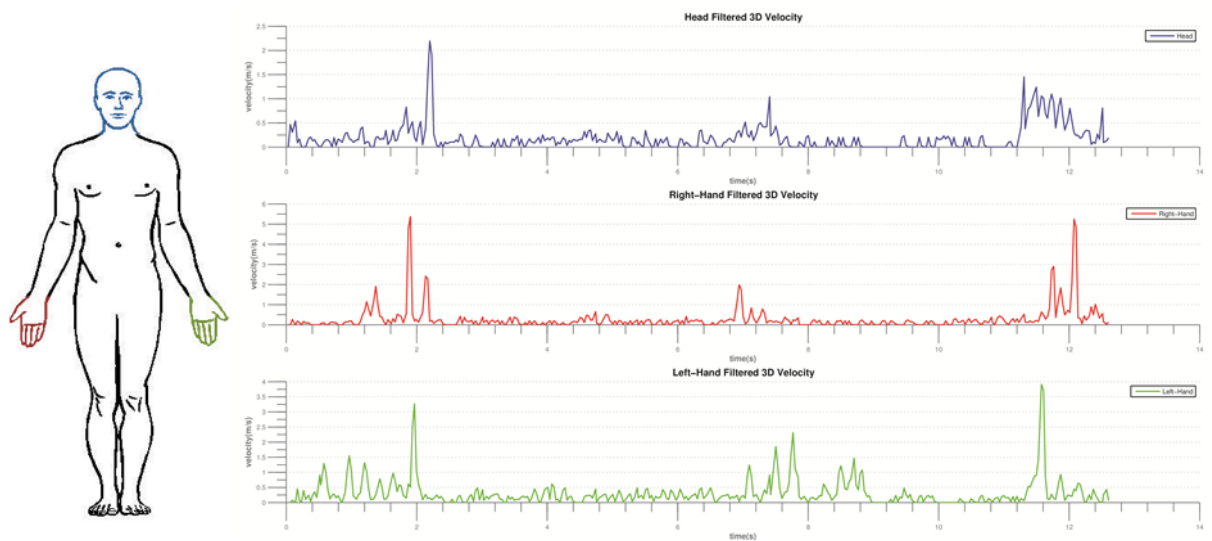


Figure 6.27: Tracings of the velocity values filtered, in function of time with the corresponding body positions.

Figure 6.28 shows the difference between the velocities using the non-filtered and the filtered data, for the Head ROI.

Finally, Figure 6.29 shows the acceleration of the tracked centroids ( $meters/s^2$ ) using the filtered data.



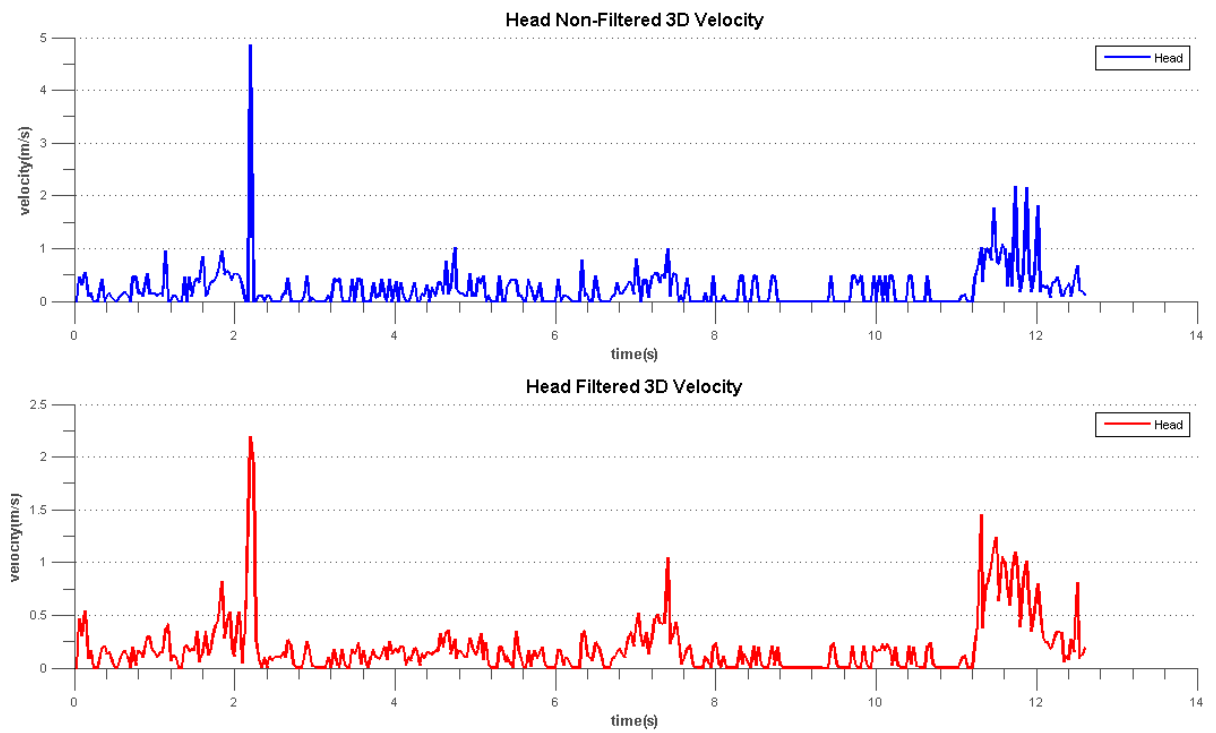


Figure 6.28: Tracings of the velocity values non-filtered and filtered of the Head, in function of time.

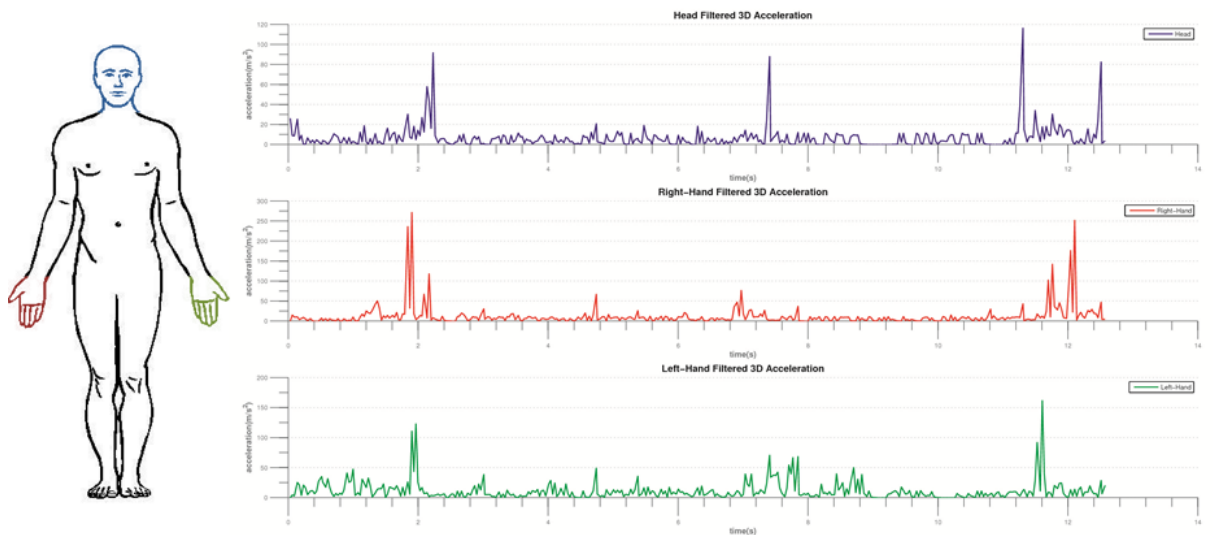


Figure 6.29: Tracings of the acceleration values filtered, in function of time with the corresponding body positions.

### 6.2.6 KiSA: Kinect Seizure Analyzer

A Matlab GUI, named KiSA (Kinect Seizure Analyzer), was developed so that the tracking and quantification process previously reported can be performed in the most user-friendly and intuitive way. KiSA is a motion quantification software that is dependent of KiT and KiMA: KiT saves the seizure information and then, using KiMA, the MOI is segmented and exported to be analyzed in KiSA.

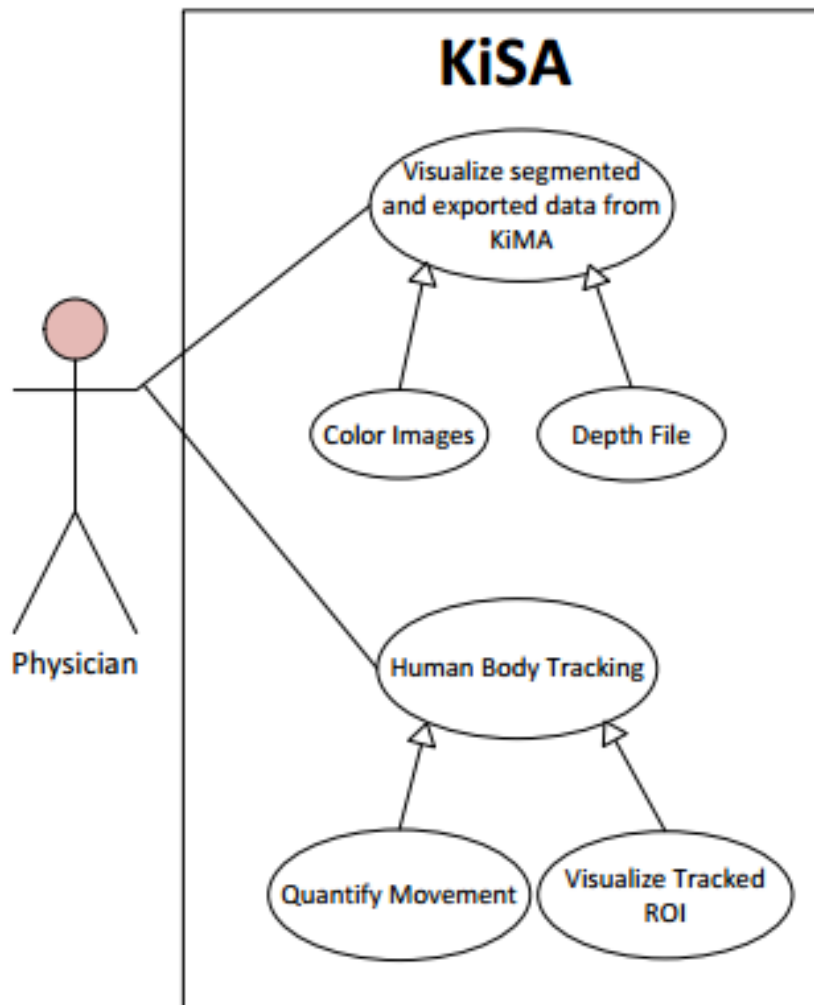


Figure 6.30: KiSA Use-Case Diagram

The main requirements defined for KiSA are the following:

1. Offline visualization of seizures data previously segmented and export data from KiMA (color images, depth file);
2. Video manipulation (play, pause, rewind, next frame, stop);

3. Human body parts tracking based on a semi-automatic approach;
4. Quantification and Visualization of the tracking data.

KiSA's main window UI includes a menu and tool bars, visualization area (with primary and secondary sources), Options and Analysis panel. In addition, there are regular video manipulation options (play, pause, stop, rewind, previous and next frames). There is also a video progression bar, corresponding to the slider located above the manipulation buttons. The current timestamp, the elapsed time and the current frame number are shown on the right side above the slider.

When data regarding a seizure is loaded into the software, the optical-flow is immediately calculated and the two sources of information are instantly available in the two sources. This allows for an immediate visual inspection and comparison of the original RGB information and the Optical Flow analysis. This feature allows requirement 1 and 2. Furthermore, there is an Options panel where several parameters can be adjusted. Also, in the main window, there is a button which initiates the tracking process, addressing requirement 3. Finally, when the tracking process is completed, another window is displayed where the movement quantification results (showed before) are presented, addressing requirement 4.

In the analysis window, the user can immediately load the output video, which is saved once the tracking process is performed. In addition, there is one 2D plot, that addresses the variables calculated before, and one 3D plot for the visualization of the 3D centroids position. Finally, there is a statistics panel for each variable.

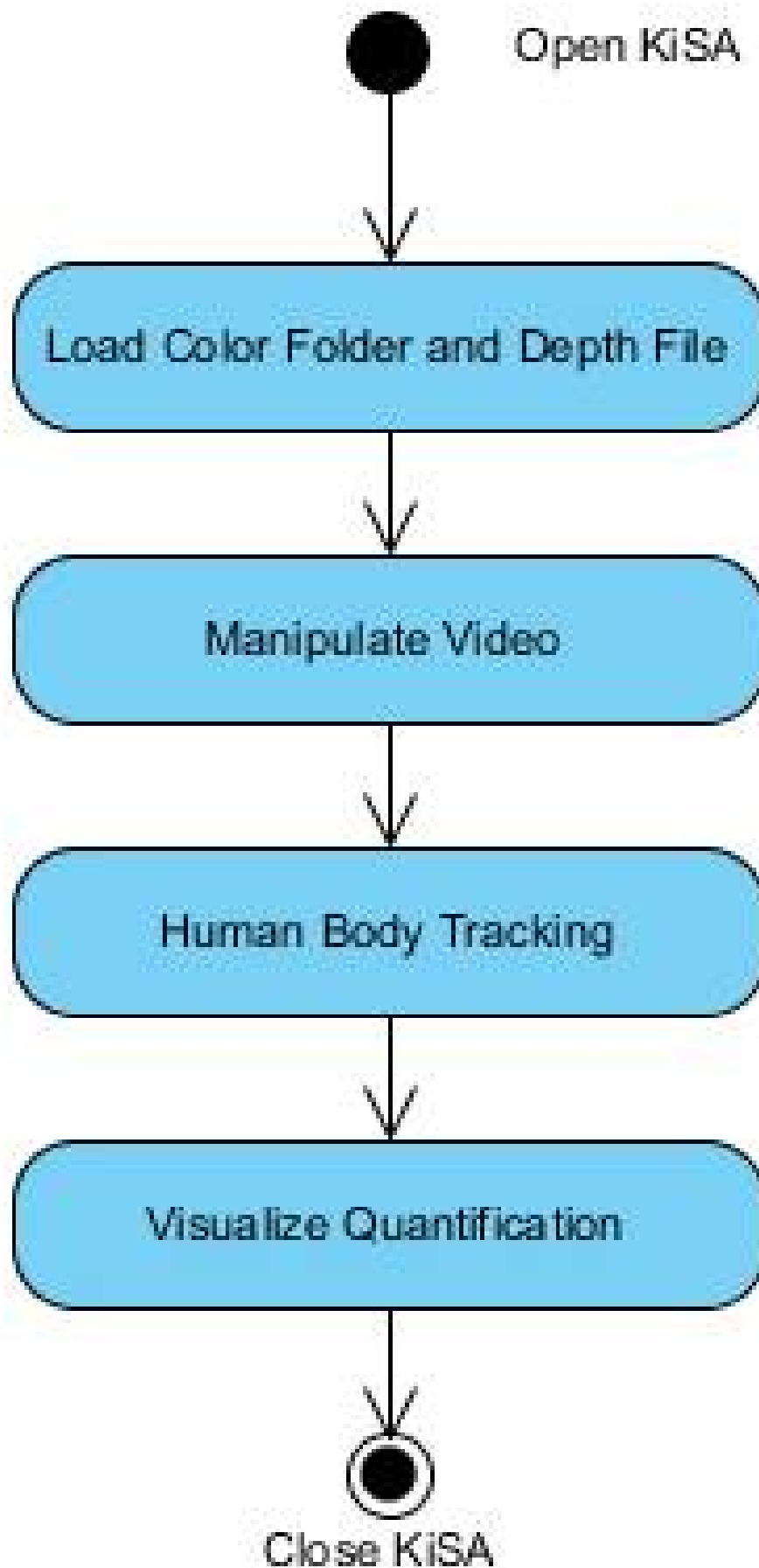


Figure 6.31: KiSA activity diagram.

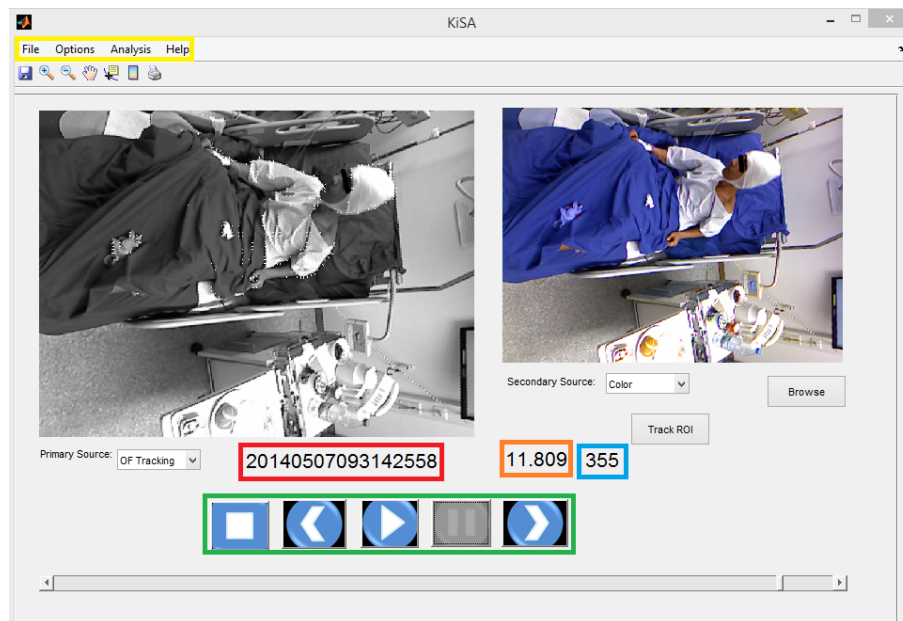


Figure 6.32: Main Window UI of KiSA application, including the display of color and optical flow images. In yellow: the menu bar; In red: the current timestamp; In orange: the elapsed time; In blue: the current frame number; In green: the video manipulation buttons.

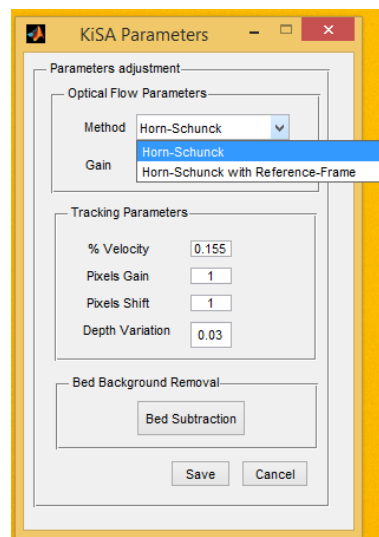


Figure 6.33: UI of KiSA Parameters.

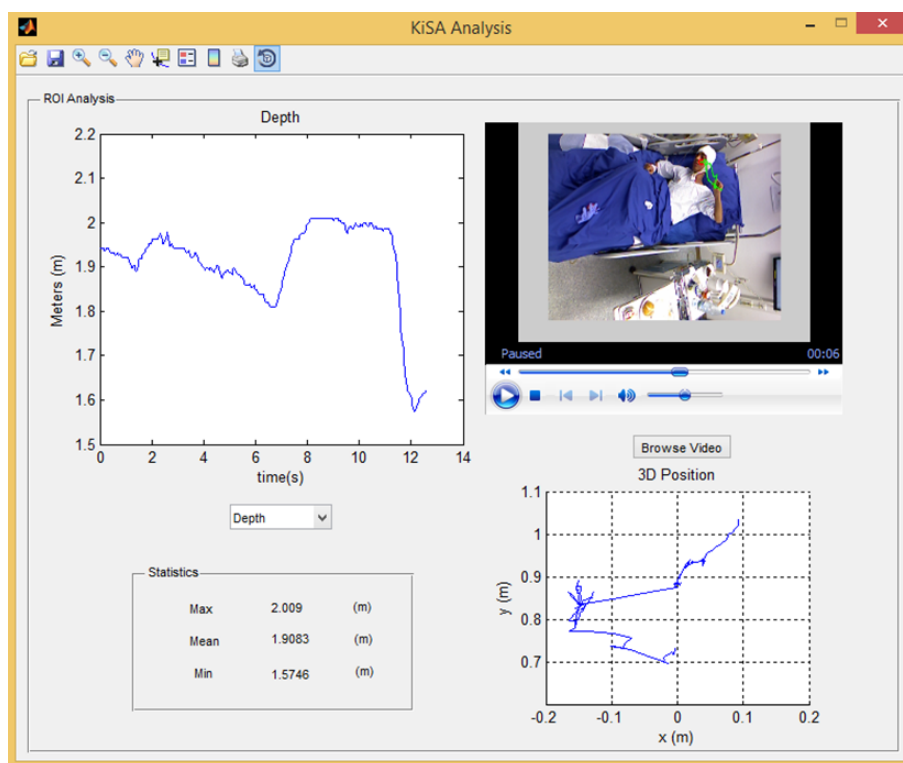


Figure 6.34: UI of KiSA Analysis. Representation of the depth tracing and the 3D position, as well as the statistics of the depth Head variation.

## 6.3 Other usages of NeuroKinect

Besides the collaborations in Parkinson's and Epilepsy, since the KiMA development, collaborations with other neurological movement disorders arose.

### 6.3.1 Familial Amyloid Polyneuropathy (FAP) and Movement Rehabilitation Strategies in Patients that suffered Strokes

Familial Amyloid Polyneuropathy (FAP) is a rare neurologic disease caused by an autosomal dominant genetic mutation that specially affects the peripheral nervous system. It is a highly disabling multisystemic disorder with variable onset and penetrance worldwide.

In Portugal, the largest known affected population, transthyretin (TTR) FAP is the most common type of FAP and it is typically characterized by a nerve length-dependent symmetric polyneuropathy that starts in the feet with loss of temperature and pain sensations and is associated to life-threatening autonomic dysfunction, leading to cachexia and death within 10 years, on average. The motor disorder progresses from difficulty ambulating until the need for walking assistance, wheelchair and total motor disability in latter stages. The gait pattern of TTR-FAP patients is described as similar to the gait pattern of diabetic neuropathy, called steppage (pendent feet and bent knee), but it has never been quantified.

This project aims at describing and quantifying the motor impairment of this population, focusing on gait. The goal is to describe in detail the gait pattern of TTR-FAP patients and to detect inter and intra-individual parameters for the development of a tool to support earlier clinical diagnose using the Kinect<sup>TM</sup> v.2.0 from Microsoft. At this moment, the gait of five patients and five controls were already acquired using KiT, and results on this quantification are being at the moment processed using KiMA for gait cycles partition and then Matlab for the mathematical analysis.

In terms of the interaction with the software, the person responsible for the project provided us with this **feedback**: "The KineTracker and KiMA (Kinect Motion Analyzer) were the applications used for data collection and analysis of the gait pattern alterations of Transthyretin Familial Amyloid Polyneuropathy (TTR-FAP) patients and mutation carriers. Both applications are fast and very intuitive.

On site, it was easy to get everything ready and perform the planned set up at the Neurophysiology Clinical Service of Hospital Santo Antonio, Porto, Portugal. Subjects reacted very well to the paraphernalia and were curious regarding skeleton tracking. During data collection it is truly important to be able to assess skeleton tracking in loco and quickly optimize the setup; moreover, during data processing, it is very useful to be able to mark moments of interest with labels and events to better compute measures of interest for specific research.

These applications have great potential on assessing movement alterations at the clinical yard without wasting clinicians and patients' time and without the need of special environment. We will keep using this software and helping to improve its performance. "“.

Besides supporting the Familial Amyloid Polyneuropathy (FAP) project, both software's are also being used to support the influence of postural control in the mid phase of gait support in patients that suffered strokes.

The goal is to objectively assess the influence of the postural control in the gait of the patients, undergoing rehabilitation strategies. Using KiT and KiMA, the treatment strategies, as well as the progress of the patient, will be evaluated in a 6 weeks window, using the recent Kinect™ v.2.0 from Microsoft. At the moment, the two moments were already acquired and the gait cycles partitions were already performed using KiMA. Currently, the mathematical analysis is being done using Matlab and MokkA.

In terms of the interaction with the software, the person responsible for the project provided us with this **feedback**:" The system is quite interesting and has as main advantage the fact of being portable, enabling this way taking it to the Healthcare context, namely ADE Rehabilitation Clinic, Famalicão, Portugal. It is also very easy to get everything ready and perform the planned set up. The majority of the patients thought the idea quite interesting and even shown curiosity in understanding the processes being performed. In terms of the software, KiMA is user-friendly and, with its continuous development, it will be very useful in the analysis of the data collected with the sensor."



## Chapter 7

# Discussion and Future Work

The Microsoft Kinect is certainly a remarkable piece of technology that truly is one of a kind. Despite its original intention being far different than ending up in scientific research, it is a fact that the inherent specifications and characteristics of the device makes it very attractive to several fields of research. The device has several limitations, but can be used as a low-cost effective solution for motion capture. The main advantage of the RGB-D sensors reviewed is the fact that they all are a novel motion analysis tool which allows markerless tracking, making them suitable for our quest in implementing a low-cost markerless video-system for movement tracking and analysis.

Kinect sensor breakthrough functionalities, with the skeletal joints in addition to the RGB and depth (plus infrared and bodyindex in the K4W v2) images, have potentialized the human activity analysis. The body joints representation provided by the skeletal tracking have tremendous importance and relevance, since that body parts are very difficult to be obtained from the normal RGB video data.

This representation simplifies the human tracking and activity recognition, and since the 3D skeleton poses are viewpoint and appearance invariant, it allows for more robust pose estimation and action recognition. The majorities of the works using the Kinect sensor take advantage of the skeletal joints and design models on top of them. Nevertheless, some issues arise when doing this: detected body joints tend to be noisy and unreliable in some situations (occluded scenes).

NeuroKinect embraces the majority of the Kinect SDK features in a package of software that, since its first official release in February 2014, has been continuously improved and has already been used in multiple healthcare scenarios.

Prior to the release of the March release of K4W v2, there was (as far as known) none available software that allowed not only gathering the streams of information acquired but also the manipulation of the acquired data in a user-friendly UI like ours. KiMA answers this need, even though it is oriented to a certain file structure.

NeuroKinect is more than just a software package: it is a markerless RGB-D video capturing system that has the possibility of being used barely everywhere; in less than ten minutes, the software (KiT) is already acquiring and the analysis in KiMA, if intended, can start immediately after

the acquisition of the first patient. In addition, by immediately reviewing the acquired data, on-the-spot changes to the planned setup can be performed in order to maximize the data acquisition.

NeuroKinect strengths rely in its portability and in being markerless, which make it suitable for the healthcare environment. The K4W v2 sensor, when compared to the previous one, is undoubtedly more robust and overall much better than the previous one. With the two new available streams, the amount of information acquired is critical (about 4GB/min for Kinect v1, 12 GB/min for Kinect v2) when acquiring all available streams.

At the moment, KiMA only allows a primary segmentation of the collected data, and the analysis is performed elsewhere, mainly in C# and Matlab. For that purpose, pipelines were created that allow using the raw information acquired with the sensor in Matlab. The critical information are the depth raw values, since that, using KiMA, the color, depth, bodyindex and infrared images can be quickly created. Using the raw depth values enhances any kind of image processing intended to be performed afterward.

Besides KiMA development, interesting work was developed in multiple healthcare scenarios, as explained before. The focus are neurological diseases with movements impairments (Neuro from Neurological, Kinect from movement analysis).

Gait impairments in Parkinson's disease are known to evolve with the progression of the disease. The importance of a correct diagnosis is then critical: the sooner the problem is detected, the faster it can be handled. This is where our method enters, with a low-cost markerless video system that aims at being able to provide important and relevant information to the clinicians in order to assess the disease and its progress throughout time.

An interesting number of gait acquisitions were performed over the last year, in São João University Hospital (Porto, Portugal), from which resulted three publications, one international and two national. Even though the national publications are important, the international paper, submitted for the most credited Biomedical Engineering Conference in the world, is a milestone that validates our approach to movement quantification using the Kinect sensor. At this moment, on-going work is being done, using now both Kinect XBOX 360 and also K4W for the patients gait acquisition, and KiMA for the gait cycles partition and also for the on-the-spot visual inspection of the patients gait.

With this work, we have shown that our low-cost portable system can be easily mounted in any hospital environment for evaluating patients' gait/updrs and, besides that, it was very well accepted by the patients, since it is markerless and non-intrusive. On average, a normal recording of a patients gait, with the stimulator ON and OFF, takes around five minutes. Besides PD, the on-going collaborations using the NeuroKinect system will also show the superior ability in the proposed approach in being used in multiple scenarios, with the outstanding fact that FAP gait has never been quantified before.

So far, all this projects were based in the acquired skeleton data and the analysis and quantification process is designed over that information. In the Epilepsy disease, the skeleton data is not accurate enough to perform a quantification process and so, the proposed method is based on image processing. KiMA, at the moment, only provides the physicians the possibility of review-

ing the seizure and that visual analysis allows only a rough estimate of the motion pattern of the seizure.

From the clinicians perspective, uncoordinated seizure motion pattern of the patient's body is considered as a valuable evidence in the identification not only of the presence of a seizure but also its source. Using the optical-flow as a reference for the motion pattern, and based on the physical test with a golf-ball, a semi-automatic approach was designed with interesting results.

The algorithm is highly dependent of accurate depth estimations and since that the two streams are misaligned, the tracking task is extremely difficult. Nevertheless, with the manual shift introduced, the results are quite interesting since that, for the head movement, the user only had to intervene in the process five times throughout the total number of frames(378). In terms of the efficiency of the proposed approach, we have compared our analysis with the one that would be done by using a state-of-art 2D motion analysis software, Maxtraq, and the results were significant: not only our approach saves physicians critical time but also provides them with 3D information, which using MaxTraq would require the use of at least 3 RGB cameras.

Efforts are currently being done so that this color-depth mapping (can only be performed using the sensor online) can be saved to file and used to have 100% certainties that the two streams are correctly aligned. Once this information is available, the robustness of this approach is highly enhanced and can definitely be used for markerless tracking and quantification of uncoordinated seizure movements. Also, the algorithm designed needs validation in other seizures information since that it was only applied for this one seizure. Comparing the results obtained for the three movements with the video analysis, even though there might be some noisy measurements, especially in both hands tracking, the overall values obtained are accordant with the movement characteristics.

With the development of KiSA, physicians can now perform qualitative as well as quantitative movement analysis using KiT+KiMA+KiSA. As a proof of concept, the decision then was to design a similar KiMA UI in Matlab (to ease the interaction of the familiarized physicians to KiMA for KiSA) but with different requirements, as it was explained before.

KiSA is a prototype which, as well as the proposed semi-automatic approach, will be continuously developed, with the hope of becoming an important tool in the epilepsy scenario. The idea is to integrate the developed approach into a plug-in for KiMA.

With the recent introduction of Kinect v2 in the Epilepsy Monitoring Unit, seizures can now be tracked during day and night by using the infrared stream. To our knowledge, there is no similar system like ours, built-in inside an hospital routine. Nevertheless, using the infrared and depth information from Kinect v2 to track and quantify, without using color (becomes too expensive in terms of amount of information gathered), will definitely be a possibility to consider and explore in a very short time.

Very recently, nonprofit EIC BBK-Dravet Syndrome Foundation developed the "Night Seizure Monitor"<sup>1</sup>, that detects seizures patterns during kids sleep, using the Kinect for Windows v2 sen-

---

<sup>1</sup>Microsoft Uses Kinect to Create Epilepsy Night Seizure Monitor <http://news.softpedia.com/news/Microsoft-Uses-Kinect-to-Create-Epilepsy-Night-Seizure-Monitor-447470.shtml>

sor, which proves that what is being done at the moment is extremely valuable and we hope that accurate scientific research can result from this straight cooperation between the university and the hospitals.

KiMA, which was developed inside a multi-disciplinary environment (Biomedical, Informatics and Electro engineering), has already proven that it has the possibility of becoming an important tool in movement analysis.

Future work includes transforming our current file structure to make it compatible for \*.C3D files, as well as transforming KiMA from its current role (primary source of data segmentation) to a movement analysis quantification software, with the integration of KiSA features and also with features important for gait analysis, such as cadence, speed or angles between joints.

KiMA efforts were not only appreciated and validated from the physicians, but they were as well accepted by the scientific community. In addition, KiMA was also presented in a Portuguese Biomedical Student Conference and most importantly, it was presented in the Kinect for Windows v2 Developer Program Preview Conference in Berlin, Germany (April 2014). The feedback from the Microsoft engineers was absolutely overwhelming and it motivate us to work even further to continue the development of the software.

# Bibliography

- W. H. O. WHO, *Neurological disorders: public health challenges*. World Health Organization, 2006.
- S. Noachtar and A. S. Peters, “Semiology of epileptic seizures: a critical review,” *Epilepsy & Behavior*, vol. 15, no. 1, pp. 2–9, 2009.
- C. Rathore, A. Radhakrishnan, S. D. Nayak, and K. Radhakrishnan, “Teaching video neuroimage: electroclinical characteristics of micturition-induced reflex epilepsy,” *Neurology*, vol. 70, no. 20, pp. e86–e86, 2008.
- N. Specchio, A. Carotenuto, M. Trivisano, S. Cappelletti, F. Vigeveno, and L. Fusco, “Ictal yawning in a patient with drug-resistant focal epilepsy: Video/eeg documentation and review of literature reports,” *Epilepsy & Behavior*, vol. 22, no. 3, pp. 602–605, 2011.
- S. S. Spencer, “The relative contributions of mri, spect, and pet imaging in epilepsy,” *Epilepsia*, vol. 35, no. s6, pp. S72–S89, 1994.
- V. Castaneda and N. Navab, “Time-of-flight and kinect imaging,” *Computer Aided Medical Procedures and Augmented Reality, Technische Universität München*, 2011.
- S. Fuchs and G. Hirzinger, “Extrinsic and depth calibration of tof-cameras,” in *Computer Vision and Pattern Recognition, 2008. CVPR 2008. IEEE Conference on*. IEEE, 2008, pp. 1–6.
- M. Zollhöfer, M. Martinek, G. Greiner, M. Stamminger, and J. Süßmuth, “Automatic reconstruction of personalized avatars from 3d face scans,” *Computer Animation and Virtual Worlds*, vol. 22, no. 2-3, pp. 195–202, 2011.
- M. R. Andersen, T. Jensen, P. Lisouski, A. K. Mortensen, M. K. Hansen, T. Gregersen, and P. Ahrendt, “Kinect depth sensor evaluation for computer vision applications,” Århus Universitet, Tech. Rep., 2012.
- Z. Li, A. M. da Silva, and J. P. S. Cunha, “Movement in epileptic seizures: a new approach to video-eeg analysis,” *Biomedical Engineering, IEEE Transactions on*, vol. 49, no. 6, pp. 565–573, 2002.
- J. S. Cunha, C. Vollmar, Z. Li, J. Fernandes, B. Feddersen, and S. Noachtar, “Movement quantification during epileptic seizures: a new technical contribution to the evaluation of seizure semiology,” in *Engineering in Medicine and Biology Society, 2003. Proceedings of the 25th Annual International Conference of the IEEE*, vol. 1. IEEE, 2003, pp. 671–673.
- J. P. S. Cunha, L. M. Paula, V. F. Bento, C. Bilgin, E. Dias, and S. Noachtar, “Movement quantification in epileptic seizures: a feasibility study for a new 3d approach,” *Medical engineering & physics*, vol. 34, no. 7, pp. 938–945, 2012.

- F. J. R. M. V. R. C. J. Rocha A, Choupina H, “Parkinson’s disease assessment based on gait analysis using an innovative rgb-d camera system - accepted for publication,” in *Annual International Conference of the IEEE Engineering in Medicine and Biology Society (EMBC)*, 2014.
- C. H, “Neurokinect: 3d gait quantification in neurological diseases - monography,” 2013.
- J. P. S. Cunha, B. Cunha, A. S. Pereira, W. Xavier, N. Ferreira, and L. Meireles, “Vital-jacket®: A wearable wireless vital signs monitor for patients’ mobility in cardiology and sports,” in *Pervasive Computing Technologies for Healthcare (PervasiveHealth), 2010 4th International Conference on-NO PERMISSIONS*. IEEE, 2010, pp. 1–2.
- M. Swan, “The quantified self: Fundamental disruption in big data science and biological discovery,” *Big Data*, vol. 1, no. 2, pp. 85–99, 2013.
- S. Wu, B. Chaudhry, J. Wang, M. Maglione, W. Mojica, E. Roth, S. C. Morton, and P. G. Shekelle, “Systematic review: impact of health information technology on quality, efficiency, and costs of medical care,” *Annals of internal medicine*, vol. 144, no. 10, pp. 742–752, 2006.
- J. James Parkinson Essay, *An essay on the shaking palsy*. Printed by Whittingham and Rowland for Sherwood, Neely, and Jones, 1817.
- H. Bernheimer, W. Birkmayer, O. Hornykiewicz, K. Jellinger, and F. . Seitelberger, “Brain dopamine and the syndromes of parkinson and huntington clinical, morphological and neurochemical correlations,” *Journal of the neurological sciences*, vol. 20, no. 4, pp. 415–455, 1973.
- W. Schultz, “Multiple dopamine functions at different time courses,” *Annu. Rev. Neurosci.*, vol. 30, pp. 259–288, 2007.
- J.-M. Fellous and R. Suri, “Dopamine, roles of.”
- E. Dorsey, R. Constantinescu, J. Thompson, K. Biglan, R. Holloway, K. Kieburtz, F. Marshall, B. Ravina, G. Schifitto, A. Siderowf *et al.*, “Projected number of people with parkinson disease in the most populous nations, 2005 through 2030,” *Neurology*, vol. 68, no. 5, pp. 384–386, 2007.
- N. C. C. f. C. C. G. B. NCC, “Parkinson’s disease: national clinical guideline for diagnosis and management in primary and secondary care.” Royal College of Physicians, 2006.
- J. M. Hausdorff, “Gait dynamics in parkinson’s disease: common and distinct behavior among stride length, gait variability, and fractal-like scaling,” *Chaos: An Interdisciplinary Journal of Nonlinear Science*, vol. 19, no. 2, p. 026113, 2009.
- J. Jankovic, “Parkinson’s disease: clinical features and diagnosis,” *Journal of Neurology, Neurosurgery & Psychiatry*, vol. 79, no. 4, pp. 368–376, 2008.
- G. Ebersbach, M. Sojer, F. Valldeoriola, J. Wissel, J. Müller, E. a. Tolosa, and W. Poewe, “Comparative analysis of gait in parkinson’s disease, cerebellar ataxia and subcortical arteriosclerotic encephalopathy,” *Brain*, vol. 122, no. 7, pp. 1349–1355, 1999.
- M. E. Morris, R. Ianssek, T. A. Matyas, and J. J. Summers, “Stride length regulation in parkinson’s disease normalization strategies and underlying mechanisms,” *Brain*, vol. 119, no. 2, pp. 551–568, 1996.

- M. E. Morris, F. E. Huxham, J. McGinley, and R. Iansek, "Gait disorders and gait rehabilitation in parkinson's disease." *Advances in neurology*, vol. 87, pp. 347–361, 2000.
- S. Fahn, D. Oakes, I. Shoulson, K. Kieburtz, A. Rudolph, A. Lang, C. Olanow, C. Tanner, K. Marek, P. S. Group *et al.*, "Levodopa and the progression of parkinson's disease." *The New England journal of medicine*, vol. 351, no. 24, p. 2498, 2004.
- R. Fisher and M. Saul, "Overview of epilepsy," *Book of Comprehensive Epilepsy Center*, 1997.
- H. Lüders, J. Acharya, C. Baumgartner, S. Benbadis, A. Bleasel, R. Burgess, D. Dinner, A. Ebner, N. Foldvary, E. Geller *et al.*, "Semiological seizure classification\*," *Epilepsia*, vol. 39, no. 9, pp. 1006–1013, 1998.
- S. Warach, J. Ives, G. Schlaug, M. Patel, D. Darby, V. Thangaraj, R. Edelman, and D. Schomer, "Eeg-triggered echo-planar functional mri in epilepsy," *Neurology*, vol. 47, no. 1, pp. 89–93, 1996.
- K. A. McNally, A. L. Paige, G. Varghese, H. Zhang, E. J. Novotny, S. S. Spencer, I. G. Zubal, and H. Blumenfeld, "Localizing value of ictal–interictal spect analyzed by spm (isas)," *Epilepsia*, vol. 46, no. 9, pp. 1450–1464, 2005.
- S.-K. Kim, D. S. Lee, S. K. Lee, Y. K. Kim, K. W. Kang, C. K. Chung, J.-K. Chung, and M. C. Lee, "Diagnostic performance of [18f] fdg-pet and ictal [99mtc]-hmpao spect in occipital lobe epilepsy," *Epilepsia*, vol. 42, no. 12, pp. 1531–1540, 2001.
- D. M. Gavrilu, "The visual analysis of human movement: A survey," *Computer vision and image understanding*, vol. 73, no. 1, pp. 82–98, 1999.
- L. Lee and W. E. L. Grimson, "Gait analysis for recognition and classification," in *Automatic Face and Gesture Recognition, 2002. Proceedings. Fifth IEEE International Conference on.* IEEE, 2002, pp. 148–155.
- R. B. Davis III, S. Ounpuu, D. Tyburski, and J. R. Gage, "A gait analysis data collection and reduction technique," *Human Movement Science*, vol. 10, no. 5, pp. 575–587, 1991.
- R. Baker, "The history of gait analysis before the advent of modern computers," *Gait & posture*, vol. 26, no. 3, pp. 331–342, 2007.
- M. E. Morris, J. McGinley, F. Huxham, J. Collier, and R. Iansek, "Constraints on the kinetic, kinematic and spatiotemporal parameters of gait in parkinson's disease," *Human Movement Science*, vol. 18, no. 2, pp. 461–483, 1999.
- O. Sofuwa, A. Nieuwboer, K. Desloovere, A.-M. Willems, F. Chavret, and I. Jonkers, "Quantitative gait analysis in parkinson's disease: comparison with a healthy control group," *Archives of physical medicine and rehabilitation*, vol. 86, no. 5, pp. 1007–1013, 2005.
- T. B. Moeslund, A. Hilton, and V. Krüger, "A survey of advances in vision-based human motion capture and analysis," *Computer vision and image understanding*, vol. 104, no. 2, pp. 90–126, 2006.
- X. Chen and J. Davis, "Camera placement considering occlusion for robust motion capture," *Computer Graphics Laboratory, Stanford University, Tech. Rep.*, vol. 2, no. 2.2, p. 2, 2000.
- M. Hansard, S. Lee, O. Choi, and R. Horaud, *Time-of-flight cameras.* Springer, 2013.

- E. R. Melgar and C. C. Diez, *Arduino and Kinect Projects: Design, Build, Blow Their Minds*. Apress, 2012.
- J. Webb and J. Ashley, *Beginning Kinect Programming with the Microsoft Kinect SDK*. Apress, 2012.
- D. Catuhe, *Programming with the Kinect for Windows software development kit*. O'Reilly Media, Inc., 2012.
- K. Khoshelham and S. O. Elberink, "Accuracy and resolution of kinect depth data for indoor mapping applications," *Sensors*, vol. 12, no. 2, pp. 1437–1454, 2012.
- J. Han, L. Shao, D. Xu, and J. Shotton, "Enhanced computer vision with microsoft kinect sensor: A review," 2013.
- S.-W. Chen, S.-H. Lin, L.-D. Liao, H.-Y. Lai, Y.-C. Pei, T.-S. Kuo, C.-T. Lin, J.-Y. Chang, Y.-Y. Chen, Y.-C. Lo *et al.*, "Quantification and recognition of parkinsonian gait from monocular video imaging using kernel-based principal component analysis," *Biomedical Engineering Online*, vol. 10, no. 1, pp. 1–21, 2011.
- J. Cancela, M. Pastorino, M. Arredondo, M. Pansera, L. Pastor-Sanz, F. Villagra, M. Pastor, and A. Gonzalez, "Gait assessment in Parkinson's disease patients through a network of wearable accelerometers in unsupervised environments," in *Annual International Conference of the IEEE Engineering in Medicine and Biology Society (EMBC)*, 2011, pp. 2233–2236.
- B. Galna, G. Barry, D. Jackson, D. Mhiripiri, P. Olivier, and L. Rochester, "Accuracy of the Microsoft Kinect sensor for measuring movement in people with Parkinson's disease," *Gait & Posture*, 2014.
- M. Gabel, R. Gilad-Bachrach, E. Renshaw, and A. Schuster, "Full body gait analysis with Kinect," in *Annual International Conference of the IEEE Engineering in Medicine and Biology Society (EMBC)*, 2012, pp. 1964–1967.
- E. E. Stone and M. Skubic, "Passive in-home measurement of stride-to-stride gait variability comparing vision and Kinect sensing," in *Annual International Conference of the IEEE Engineering in Medicine and Biology Society (EMBC)*, Aug 2011, pp. 6491–6494.
- M. Kumar and R. V. Babu, "Human gait recognition using depth camera: a covariance based approach," in *Proceedings of the Eighth Indian Conference on Computer Vision, Graphics and Image Processing*. ACM, 2012, p. 20.
- N. B. Karayiannis and G. Tao, "Extraction of temporal motion velocity signals from video recordings of neonatal seizures by optical flow methods," in *Engineering in Medicine and Biology Society, 2003. Proceedings of the 25th Annual International Conference of the IEEE*, vol. 1. IEEE, 2003, pp. 874–877.
- N. B. Karayiannis, G. Tao, Y. Xiong, A. Sami, B. Varughese, J. D. Frost, M. S. Wise, and E. M. Mizrahi, "Computerized motion analysis of videotaped neonatal seizures of epileptic origin," *Epilepsia*, vol. 46, no. 6, pp. 901–917, 2005.
- N. B. Karayiannis, B. Varughese, G. Tao, J. D. Frost Jr, M. S. Wise, and E. M. Mizrahi, "Quantifying motion in video recordings of neonatal seizures by regularized optical flow methods," *Image Processing, IEEE Transactions on*, vol. 14, no. 7, pp. 890–903, 2005.



- B. K. Horn and B. G. Schunck, "Determining optical flow," in *1981 Technical Symposium East*. International Society for Optics and Photonics, 1981, pp. 319–331.
- J. L. Barron, D. J. Fleet, and S. S. Beauchemin, "Performance of optical flow techniques," *International journal of computer vision*, vol. 12, no. 1, pp. 43–77, 1994.
- R. O'Dwyer, J. P. Silva Cunha, C. Vollmar, C. Mauerer, B. Feddersen, R. C. Burgess, A. Ebner, and S. Noachtar, "Lateralizing significance of quantitative analysis of head movements before secondary generalization of seizures of patients with temporal lobe epilepsy," *Epilepsia*, vol. 48, no. 3, pp. 524–530, 2007.
- L. Chen, X. Yang, Y. Liu, D. Zeng, Y. Tang, B. Yan, X. Lin, L. Liu, H. Xu, and D. Zhou, "Quantitative and trajectory analysis of movement trajectories in supplementary motor area seizures of frontal lobe epilepsy," *Epilepsy & Behavior*, vol. 14, no. 2, pp. 344–353, 2009.
- Z. Mirzadjanova, A. S. Peters, J. Rémi, C. Bilgin, J. P. Silva Cunha, and S. Noachtar, "Significance of lateralization of upper limb automatisms in temporal lobe epilepsy: a quantitative movement analysis," *Epilepsia*, vol. 51, no. 10, pp. 2140–2146, 2010.
- J. Rémi, J. P. Silva Cunha, C. Vollmar, Ö. Bilgin Topçuoğlu, A. Meier, S. Ulowetz, P. Beleza, and S. Noachtar, "Quantitative movement analysis differentiates focal seizures characterized by automatisms," *Epilepsy & Behavior*, vol. 20, no. 4, pp. 642–647, 2011.
- R. V. C. J. Tafula S, Moreira N, "Abril - advanced brain imaging lab.: a cloud based computation environment for cooperative neuroimaging projects," in *Annual International Conference of the IEEE Engineering in Medicine and Biology Society (EMBC)*, 2014.
- R. A. C. H. F. J. M. V. R. R. M. J. Cunha, João, *Sistema de quantificação 3D de movimento portátil e de baixo custo para estimativa do sub-score de marcha em doentes parkinsónicos*. Portuguese Neurology Society, 2014.
- D. Kesrarat and V. Patanavijit, "Tutorial of motion estimation based on horn-schunck optical flow algorithm in matlab," *IEEE AU JT*, vol. 15, no. 1, pp. 8–16, 2011.



## **Appendix A**

# **Steps for KinectforMatlab.dll instalation**



In order to use the \*.dll file, .NET framework needs to be installed in the computer. The steps for installation of the pipeline are as follow:

1. Run Windows Command Line (i.e. CMD) as Administrator;
2. Copy the .NET Framework folder path to the CMD window, command:

```
cd C:\Windows\Microsoft.NET\Framework64\setminusv4.???????
```

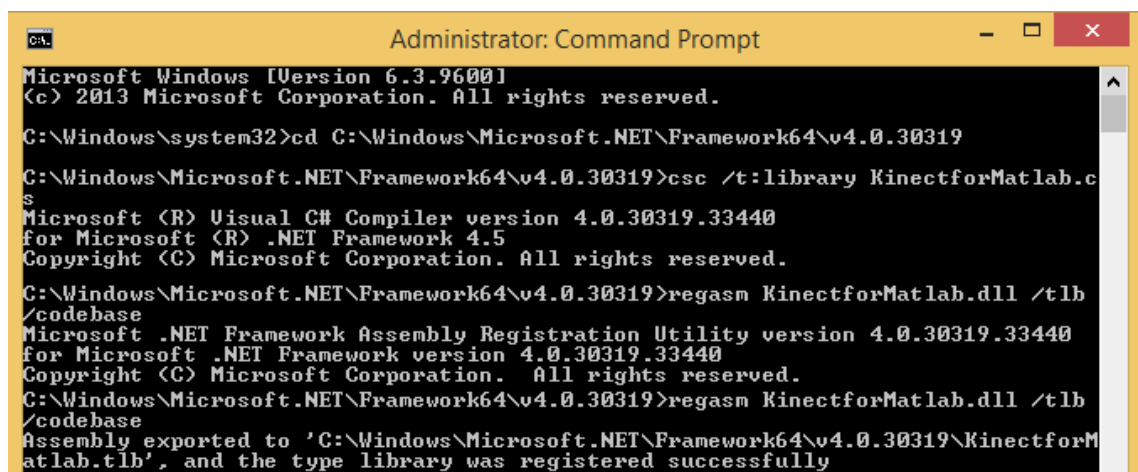
3. Copy "KinectforMatlab.cs" to the .NET Framework folder;
4. Compile the KinectforMatlab.cs file to a \*.dll, command:

```
\csc /t:library KinectforMatlab.cs
```

5. Register the KinectforMatlab.cs Active X control, command:

```
regasm KinectforMatlab.dll /tlb /codebase
```

The procedure is showed in figure A.1, where the final message states that the pipeline was successfully compiled.



```
Administrator: Command Prompt
Microsoft Windows [Version 6.3.9600]
(c) 2013 Microsoft Corporation. All rights reserved.
C:\Windows\system32>cd C:\Windows\Microsoft.NET\Framework64\v4.0.30319
C:\Windows\Microsoft.NET\Framework64\v4.0.30319>csc /t:library KinectforMatlab.cs
Microsoft (R) Visual C# Compiler version 4.0.30319.33440
for Microsoft (R) .NET Framework 4.5
Copyright (C) Microsoft Corporation. All rights reserved.
C:\Windows\Microsoft.NET\Framework64\v4.0.30319>regasm KinectforMatlab.dll /tlb
/codebase
Microsoft .NET Framework Assembly Registration Utility version 4.0.30319.33440
for Microsoft .NET Framework version 4.0.30319.33440
Copyright (C) Microsoft Corporation. All rights reserved.
C:\Windows\Microsoft.NET\Framework64\v4.0.30319>regasm KinectforMatlab.dll /tlb
/codebase
Assembly exported to 'C:\Windows\Microsoft.NET\Framework64\v4.0.30319\KinectforM
atlab.tlb', and the type library was registered successfully
```

Figure A.1: KinectforMatlab.dll Pipeline Procedure

Once the source code pipeline is compiled, in order to use it on Matlab, the following commands should be used: firstly, load the .NET library. Then, for example, to access the depth information of a \*.kdpt (depth) file, the following command should be used:

$$\text{depthValue} = \text{net.depthKinectvOne}('filename', 'kdpt', 'pixelY', 'pixelX', 'frameNumber');$$

(A.1)



## **Appendix B**

# **Portuguese Annual Biomedical Students Conference**

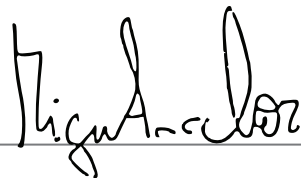




CERTIFICATE

**IX ENEEB**

It is hereby certified that ***Hugo Choupina*** presented "Neurokinetic" in the ENEEB Open Stage Panel of the IX Encontro Nacional de Estudantes de Engenharia Biomédica (IX National Meeting of Biomedical Engineering Students), which took place in Porto, Portugal on March 7th 2014.



Miguel Amador  
(Organization IX ENEEB - Porto 2014)





## **Appendix C**

# **Microsoft Kinect for Windows Developer Preview Conference**





Re: Kinect for Windows Developer Preview Program

Date: April 11, 2014

This letter confirms that Hugo Choupina (University Porto, Portugal) took part in the Kinect for Windows 24-hour hack-a-thon in Berlin, Germany April 11 – 12, 2014. This event was hosted by the Microsoft Kinect for Windows team as part of their developer preview program, which gives developers, students, and researchers worldwide the ability to participate in the beta test of the Kinect for Windows v2 sensor and software development kit (SDK).

Sincerely,

Heather Mitchell  
Business Development and Strategy Manager  
Microsoft Kinect for Windows



## **Appendix D**

### **Reference Letter from LMU**







**KLINIKUM**  
DER UNIVERSITÄT MÜNCHEN

**NEUROLOGISCHE KLINIK UND POLIKLINIK  
MIT FRIEDRICH-BAUR-INSTITUT**

**Direktorin: Prof. Dr. med. M. Dieterich**



in Assoziation mit dem Institut für Neuroimmunologie und dem  
Institut für Schlaganfall- und Demenzforschung

Prof. Dr. S. Noachtar □ Klinikum der Universität München – Großhadern  
Neurologische Klinik, Marchioninstr. 15 □ D-81377 München

Prof. Dr. med. Soheyl Noachtar  
Leiter, Epilepsie-Zentrum

Telefon: +49 (0)89 7095 – 3691/2685  
Telefax: +49 (0)89 7095 – 6691  
Email: noa@med.uni-muenchen.de

[www.klinikum.uni-muenchen.de](http://www.klinikum.uni-muenchen.de)

Postanschrift:  
Marchioninstr. 15  
D-81377 München

Ihr Zeichen:

Unser Zeichen:  
Noa/st

München, den 17.7.2014

To whom it may concern:

The KinecTracker (KiT) and Kinect Motion Analyzer (KiMA) software developed at professor João Paulo Cunha's lab, are being used at the Epilepsy Monitoring Unit of the University of Munich by our technicians and neurophysiologists. Quantification of movement patterns in epilepsy patients is a demanding task and, so far, based on this cooperation, interesting results are being achieved.

Both applications are very user-friendly and intuitive, which is critical to our staff to be able to operate them in the routine of the unit.

These applications have great potential on assessing movement patterns in the Epilepsy context without wasting physicians' time and without much change to the routine environment of our EMU.

We will keep using this software and we look forward to help in improving its performance.

Yours sincerely

Prof. Soheyl Noachtar  
Head, Epilepsy Center



## **Appendix E**

# **Parkinson's Disease Assessment Based on Gait Analysis Using an Innovative RGB-D Camera System - EMBC 2014**



# Parkinson's Disease Assessment Based on Gait Analysis Using an Innovative RGB-D Camera System

Ana Patrícia Rocha, *Student Member, IEEE, EMBS*, Hugo Choupina, José Maria Fernandes, Maria José Rosas, Rui Vaz, João Paulo Silva Cunha, *Senior Member, IEEE, EMBS*

**Abstract**—Movement-related diseases, such as Parkinson's disease (PD), progressively affect the motor function, many times leading to severe motor impairment and dramatic loss of the patients' quality of life. Human motion analysis techniques can be very useful to support clinical assessment of this type of diseases. In this contribution, we present a RGB-D camera (Microsoft Kinect) system and its evaluation for PD assessment. Based on skeleton data extracted from the gait of three PD patients treated with deep brain stimulation and three control subjects, several gait parameters were computed and analyzed, with the aim of discriminating between non-PD and PD subjects, as well as between two PD states (stimulator ON and OFF). We verified that among the several quantitative gait parameters, the variance of the center shoulder velocity presented the highest discriminative power to distinguish between non-PD, PD ON and PD OFF states ( $p = 0.004$ ). Furthermore, we have shown that our low-cost portable system can be easily mounted in any hospital environment for evaluating patients' gait. These results demonstrate the potential of using a RGB-D camera as a PD assessment tool.

## I. INTRODUCTION

Parkinson's disease (PD) is an idiopathic neurodegenerative disease, which results from the death of brain cells that produce dopamine [1]. The lack of dopamine typically leads to characteristic motor symptoms, such as bradykinesia (i.e. slowness of movement), shuffling gait, and freezing of gait (i.e. sudden and brief motor blocks).

An estimated seven to ten million individuals worldwide have PD [2]. This number is expected to rise significantly in the future [3], with 60,000 new cases being currently reported every year only in the U.S. [2]. Even though PD has presently no cure, there is available treatment that can improve functional capacity. A possible treatment is deep brain stimulation (DBS), which consists in implanting stimulating electrodes in the brain, and a pulse generator.

To provide the best possible treatment, both an early diagnosis and regular evaluations are essential. The diagnosis of PD is currently based mainly on clinical criteria [1]. During

This work was supported by EU funds through COMPETE and by national funds through the Portuguese Science Foundation (FCT) within the projects PTDC/EEI-ELC/2760/2012 and PTDC/NEU-SCC/0767/2012.

Ana Patrícia Rocha, and José Maria Fernandes are with IEETA and the Department of Electronics, Telecommunications and Informatics, University of Aveiro, Aveiro, Portugal (e-mail: aprocha@ua.pt, jfernan@ua.pt).

Hugo Choupina is with FEUP, University of Porto, Porto, Portugal (e-mail: meb12027@fe.up.pt).

Maria José Rosas, and Rui Vaz are with the Movement Disorders Group, S. João University Hospital, Porto, Portugal (e-mail: rosas.mariajose@gmail.com, ruimcvaz@gmail.com).

João Paulo Silva Cunha is with INESC-TEC Porto, and FEUP, University of Porto, Porto, Portugal (e-mail: jcunha@ieee.org).

PD follow-up, the monitoring of the disease's progression and treatment outcome is usually based on a rating scale, such as the Unified Parkinson Disease Rating Scale (UPDRS) [4]. In both cases, the assessment typically includes visual examination of motor symptoms by physicians, which tends to be rather subjective. So, the quantification of motor signs can be very useful to enhance both PD diagnosis and follow-up [5], [6], and possibly lead to an improvement of treatment and overall life quality of PD patients.

Gait analysis in PD, using motion or vision sensors, has been studied by various authors [5], [6], [7]. In [6], the authors proposed a PD monitoring tool, based on six accelerometers and one gyroscope. Based on sensor data collected from PD patients, they extracted parameters that can be useful for distinguishing between on and off states.

A vision-based system for PD assessment (distinction between non-PD, PD drug on and PD drug off states) was proposed in [5]. The authors recorded videos of PD patients and control subjects while walking. A minimum distance classifier was then built, based on features resulting from gait analysis, which achieved an accuracy of 80.5%.

Recently, the Microsoft Kinect<sup>TM</sup> has been used for gait analysis [7], [8], [9]. The Kinect is a low-cost, portable RGB-D (Red, Green, Blue, Depth) camera [10] that provides color and depth image sequences, as well as skeleton data resulting from 3D tracking. This camera has the added advantage of being less intrusive than marker-based sensors. Moreover, when compared with RGB cameras, it allows motion analysis in less controlled environments, due to the use of a depth sensor based on infrared light, without losing accuracy [9].

A gait analysis system that uses a Kinect was developed in [8]. Regression models were built based on skeleton data, and ground truth measures (using in-shoe pressure sensors and a gyroscope), which were collected from subjects while walking. The obtained models were able to estimate stride duration and arm angular velocity, with an average absolute error in the range between 32 and 71 milliseconds, and 14 and 22 degrees/second, respectively.

Regarding PD, the validity of the Kinect for movement measurement in PD patients was recently explored in [7]. When compared with a Vicon system, the sensor was able to accurately measure timing and gross spatial characteristics of clinically relevant movements, validating its use for gait analysis in the health care context, namely in PD.

Considering the potential of RGB-D camera systems to constitute a low-cost and portable solution for assessing movement-related diseases, we explore in this contribution

the possibility of using such a system as a PD assessment tool. We carried out an evaluation of both PD patients and control subjects, during a walking task, which consisted in the extraction of several gait parameters from skeleton data acquired by using our *KinecTracker* application. Moreover, the usefulness of those parameters for supporting both PD diagnosis and follow-up was studied.

## II. MATERIALS AND METHODS

An experimental protocol was carried out in a room at São João University Hospital (Porto, Portugal), with the participation of three PD patients (P1, P2 and P3) and three control subjects (C1, C2 and C3). Each PD patient had an implanted DBS stimulator, and performed the experiment twice: with the stimulator on (STIM ON); and a few minutes after turning off the stimulator (STIM OFF). Each control subject performed the experiment only once.

The protocol included the use of the *KinecTracker* application, developed in C# by our group using the Kinect Software Development Kit v1.5 [11], to acquire skeleton data (at a 30 fps rate) from PD patients and control subjects, while they were walking. The walking trajectory of four meters is illustrated by an arrowed dashed line in Fig. 1. This figure also includes the relevant distances, as well as the Kinect height and tilting angle in relation to the horizontal plane (perpendicular to the gravity force). The chosen setup took into account the Kinect limitations [12], and aimed at maximizing the actual tracking area, which is represented by the grey rectangle in Fig. 1.

The demographics of the control subjects and PD patients are presented in Table I. For the PD patients, disease-related details are shown in Table II, including the number of months since DBS surgery, and the UPDRS scores for the motor examination section and the specific gait item [4]. The study was authorized by the hospital's Ethics Committee, and all subjects signed an informed consent form.

Each acquired frame data corresponds to a skeleton of twenty joints, illustrated in Fig. 2 (a). Fig. 2 (b) shows an example of depth and skeleton data, as displayed in *KinecTracker* (user interface shown in Fig. 3). Each joint corresponds to a 3D position, considering the coordinate system associated with the Kinect [12] (depicted in Fig. 1).

The data acquired within the tracking area were firstly manually selected, and then partitioned into gait cycles, based on depth data acquired at the same time as the skeleton data.

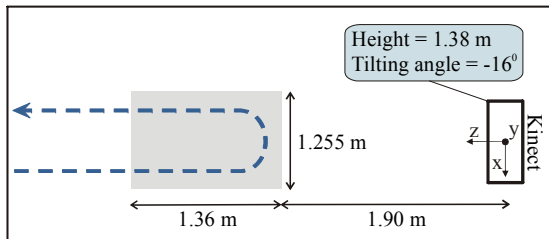


Fig. 1. Experimental setup used for data acquisition, including the coordinate system associated with the Kinect.

TABLE I  
SUBJECTS' CHARACTERIZATION (AVERAGE AND [MINIMUM, MAXIMUM] VALUES FOR AGE, WEIGHT, AND HEIGHT).

	Control subjects	PD patients
Gender (male/female)	2/1	2/1
Age	49 [46, 54]	53.7 [47, 59]
Height (m)	1.65 [1.58, 1.72]	1.68 [1.59, 1.8]
Weight (kg)	83.3 [54, 118]	82.7 [78, 90]

TABLE II  
PARKINSON'S DISEASE PATIENTS' CHARACTERIZATION REGARDING DBS AND UPDRS SCORES.

PD patient	Months after DBS surgery	UPDRS III <sup>a</sup> (gait <sup>b</sup> )	
		STIM ON	STIM OFF
P1	6	13 (1)	31 (1)
P2	1.5	7 (1)	26 (1)
P3	10	11 (0)	42 (2)

<sup>a</sup> UPDRS motor score (part III). The maximum score is 108. [4]

<sup>b</sup> UPDRS gait sub-score (item 29). Score ranges between 0 (normal) and 4 (cannot walk). [4]

We considered that a gait cycle begins when the left/right foot initiates contact with the ground ( $IC_{L/R}$ ), and ends when the same foot initiates again contact with the ground. In the data analysis presented below, we used only the data corresponding to the portion of the walking sequence where the subject is walking towards the camera, since we verified that the remaining data were much noisier.

As indicated in Fig. 1, the Kinect was tilted by rotating  $-16^\circ$  around its x-axis, with the aim of obtaining the optimum field of view. In order to simplify comparison between results obtained with different angles, and facilitate interpretation of results, the joints' 3D positions were converted into a coordinate system corresponding to a non-tilted camera (angle of  $0^\circ$ ).

Based on the resulting data we created two different datasets: unfiltered and filtered. The filtered dataset was

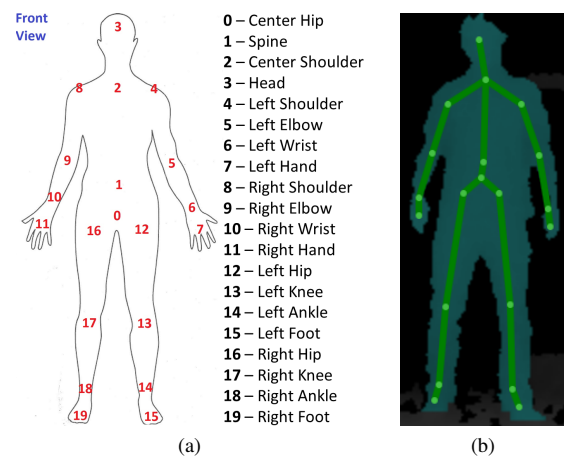


Fig. 2. Skeleton joints provided by the Kinect (a), and depth and skeleton data as displayed in the *KinecTracker* application (b).

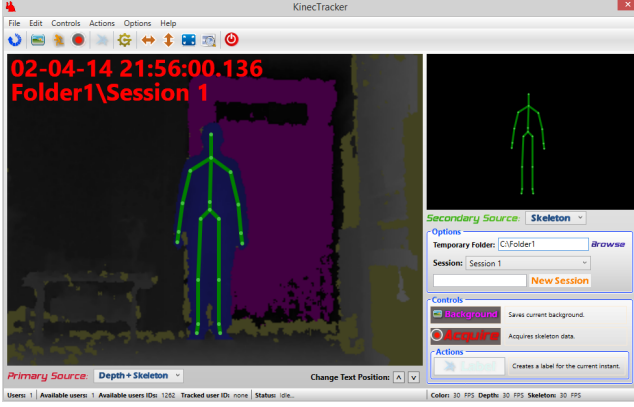


Fig. 3. User interface of the *KineTracker* application.

obtained by using a first order low-pass Butterworth filter, with a cutoff frequency of 5 Hz, over the unfiltered data. For both datasets, the following 34 measures were computed, for each frame of each left/right gait cycle:

- Velocity of the left/right foot, ankle, knee and hip, right/left hand, wrist, elbow and shoulder, central hip and shoulder, spine, and head, using (1);
- Acceleration of the left/right foot, ankle, knee and hip, right/left hand, wrist, elbow and shoulder, central hip and shoulder, spine, and head, using (2);
- Distance between feet, ankles, knees, hands, wrists, and elbows, using (3);
- Angle at left/right knee (defined by hip, knee and ankle joints), right/left elbow (defined by wrist, elbow and shoulder joints), center shoulder (defined by spine, center shoulder and head joints), and spine (defined by center hip, spine and center shoulder joints), using (4).

$$\text{velocity} = \sqrt{v_x^2 + v_y^2 + v_z^2} \approx \sqrt{\frac{\Delta x^2 + \Delta y^2 + \Delta z^2}{\Delta t^2}} \quad (1)$$

$$\text{acceleration} = \sqrt{a_x^2 + a_y^2 + a_z^2} \approx \sqrt{\frac{\Delta v_x^2 + \Delta v_y^2 + \Delta v_z^2}{\Delta t^2}} \quad (2)$$

$$\text{distance} = \|\mathbf{P}_{\text{left}} - \mathbf{P}_{\text{right}}\| \quad (3)$$

$$\text{angle} = \arccos\left(\frac{\mathbf{P}_2 \mathbf{P}_1 \cdot \mathbf{P}_2 \mathbf{P}_3}{\|\mathbf{P}_2 \mathbf{P}_1\| \times \|\mathbf{P}_2 \mathbf{P}_3\|}\right) \quad (4)$$

In (1),  $v_x$  is the component of the velocity vector on the x-axis for a given joint, and  $\Delta x$  corresponds to the difference between the x-coordinate values considering two consecutive frames. In (2),  $a_x$  is the component of the acceleration vector on the x-axis for a given joint, and  $\Delta v_x$  refers to the difference between velocities, on the x-axis, considering two consecutive frames. Similar notations are used for the y- and z-axis. In both (1) and (2),  $\Delta t$  is the time elapsed between two consecutive frames.

In (3),  $\mathbf{P}_{\text{left}}$  and  $\mathbf{P}_{\text{right}}$  refer to the left and right joint 3D positions, respectively. In (4),  $\mathbf{P}_1$ ,  $\mathbf{P}_2$  and  $\mathbf{P}_3$  correspond to three different joint 3D positions. For example, considering the angle at left knee, these points correspond

to the coordinates of the left hip, knee and ankle joints, respectively.

A set of parameters, for each gait cycle, was then computed over the obtained velocities, accelerations, distances and angles: average, median, variance, and variance divided by the average (normalized variance). This resulted in 136 different parameters.

Additionally, the following four parameters were obtained, for each gait cycle: gait cycle duration, stride length, stride average velocity, and cadence. For the right leg, these parameters were computed using (5), (6), (7) and (8), respectively. In (5) and (6),  $k$  corresponds to the gait cycle number. In (6),  $\mathbf{P}_{\text{IC}_R(k)}$  and  $\mathbf{P}_{\text{IC}_R(k+1)}$  refer to the right ankle 3D positions at instants  $\text{IC}_R(k)$  and  $\text{IC}_R(k+1)$ , respectively. Similar equations were used for the left leg.

$$k\text{th gait cycle duration} = \text{IC}_R(k+1) - \text{IC}_R(k) \quad (5)$$

$$k\text{th stride length} = \|\overrightarrow{\mathbf{P}_{\text{IC}_R(k)} \mathbf{P}_{\text{IC}_R(k+1)}}\| \quad (6)$$

$$\text{stride average velocity} = \text{stride length} / \text{gait cycle duration} \quad (7)$$

$$\text{cadence} = 1 / \text{gait cycle duration} \quad (8)$$

### III. RESULTS

In order to evaluate which parameters can be used to statistically distinguish between non-PD subjects, PD patients in the STIM ON state and PD patients in the STIM OFF state, we performed the Kruskal-Wallis test [13] for each different parameter. The results ( $p < 0.05$ ) for each dataset (unfiltered and filtered) are presented in Table III, where the lowest value for each case is indicated in bold.

Fig. 4 shows an example of the center shoulder velocity versus the elapsed time, during a single gait cycle carried out by subject C2 and patient P2 in the STIM OFF state, when considering the filtered data. The corresponding variance values are also indicated in Fig. 4.

TABLE III  
KRUSKAL-WALLIS TEST RESULTS ( $p < 0.05$ ), WHEN COMPARING NON-PD, PD STIM ON AND PD STIM OFF STATES, FOR THE UNFILTERED AND FILTERED DATASETS.

Parameter			p-value <sup>a</sup>	
			Unfiltered	Filtered
Variance	Velocity	Head	N.S.	0.011
		Center shoulder	0.027	<b>0.004</b>
		Shoulder	N.S.	0.021
	Acceleration	Center shoulder	0.042	0.016
	Distance	Elbows	0.019	0.024
Normalized variance	Velocity	Elbow	N.S.	0.046
		Center shoulder	<b>0.009</b>	0.006
		Shoulder	N.S.	0.039
	Acceleration	Center shoulder	0.041	0.008
Distance	Elbows	0.024	0.024	
Average	Acceleration	Center shoulder	N.S.	0.041
Stride duration			0.045	0.045
Cadence			0.045	0.045

<sup>a</sup> N.S. means non-significant ( $p \geq 0.05$ ).

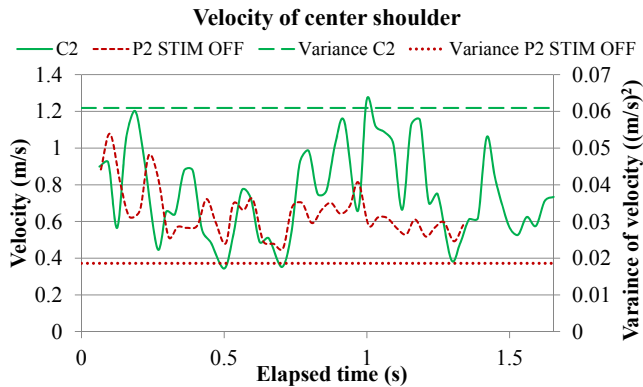


Fig. 4. Velocity of the center shoulder versus the elapsed time, for a gait cycle performed by subject C2 and patient P2 in STIM OFF state, considering the filtered dataset. The associated variance values are also included.

#### IV. DISCUSSION AND CONCLUSION

In this contribution, we used a system based on a single sensor that minimizes intrusiveness, when compared with the use of several sensors attached to the body in [6]. Similarly to [5], we explored the possibility of both PD diagnosis and follow-up based on gait analysis. However, in contrast with [5], we relied on depth images and skeleton data based on infrared light instead of common RGB images, which allowed a less controlled environment (background color, lighting, and subject clothing). Comparing with [8], we analyzed a greater number of gait parameters, associated with all skeleton joints provided by the Kinect. Moreover, we identified the most appropriate parameter for PD assessment.

From Table III, we can see that filtering contributes to an overall improvement of the parameters' ability to statistically distinguish between three different states: non-PD, PD STIM ON, and PD STIM OFF. It can also be seen that the variance of the center shoulder velocity seems to be the most appropriate parameter for discriminating between the three considered states ( $p = 0.004$ ). From the example depicted in Fig. 4, we can see that the value of this parameter is smaller for the PD patient, when compared with the control subject. This can be explained by the fact that PD patients tend to walk slower, and therefore their walking speed does not reach values as large as for healthy subjects.

The presented results show the potential of using a low-cost RGB-D camera-based system for supporting both PD diagnosis and follow-up, which can be very important for early detection of PD and treatment outcome improvement. Consequently, it can contribute to an increase of the patients' quality of life, and a reduction of health care costs.

#### V. FUTURE WORK

Although the obtained results provide indications for using RGB-D cameras to support PD assessment, more data are

required to confirm these preliminary indications. Acquisition sessions with new subjects are already scheduled and the associated results will be included in the next contribution. Furthermore, we have now integrated the pre-release version of the new Kinect for Windows v2 [14], which is expected to have better overall characteristics, into the *KinecTracker* application. This pre-release camera was awarded to our R&D group as a "Developer Preview Program" member, and will be used in the present system evolution.

#### ACKNOWLEDGMENT

The authors wish to thank the subjects that participated in the study. A special thanks to Microsoft, and to Eduardo Dias for contributions in the *KinecTracker* application.

#### REFERENCES

- [1] The National Collaborating Centre for Chronic Conditions, *Parkinson's disease: National clinical guideline for diagnosis and management in primary and secondary care*. Royal College of Physicians, 2006.
- [2] Parkinson's Disease Foundation. (2014, April) Statistics on Parkinson's. [Online]. Available: [http://www.pdf.org/en/parkinson\\_statistics](http://www.pdf.org/en/parkinson_statistics)
- [3] E. Dorsey, R. Constantinescu, J. Thompson, K. Biglan, R. Holloway, K. Kieburtz, F. Marshall, B. Ravina, G. Schifitto, A. Siderow *et al.*, "Projected number of people with Parkinson disease in the most populous nations, 2005 through 2030," *Neurology*, vol. 68, no. 5, pp. 384–386, 2007.
- [4] S. T. Gancher, "The unified Parkinsons disease rating scale," in *Parkinson's Disease: Diagnosis and Clinical Management*, S. A. Factor and W. J. Weiner, Eds. Demos Medical Publishing, 2002. [Online]. Available: <http://www.ncbi.nlm.nih.gov/books/NBK27754/>
- [5] S.-W. Chen, S.-H. Lin, L.-D. Liao, H.-Y. Lai, Y.-C. Pei, T.-S. Kuo, C.-T. Lin, J.-Y. Chang, Y.-Y. Chen, Y.-C. Lo *et al.*, "Quantification and recognition of parkinsonian gait from monocular video imaging using kernel-based principal component analysis," *Biomedical Engineering Online*, vol. 10, no. 1, pp. 1–21, 2011.
- [6] J. Cancela, M. Pastorino, M. Arredondo, M. Pansera, L. Pastor-Sanz, F. Villagra, M. Pastor, and A. Gonzalez, "Gait assessment in Parkinson's disease patients through a network of wearable accelerometers in unsupervised environments," in *Annual International Conference of the IEEE Engineering in Medicine and Biology Society (EMBC)*, 2011, pp. 2233–2236.
- [7] B. Galna, G. Barry, D. Jackson, D. Mhiripiri, P. Olivier, and L. Rochester, "Accuracy of the Microsoft Kinect sensor for measuring movement in people with Parkinson's disease," *Gait & Posture*, 2014.
- [8] M. Gabel, R. Gilad-Bachrach, E. Renshaw, and A. Schuster, "Full body gait analysis with Kinect," in *Annual International Conference of the IEEE Engineering in Medicine and Biology Society (EMBC)*, 2012, pp. 1964–1967.
- [9] E. E. Stone and M. Skubic, "Passive in-home measurement of stride-to-stride gait variability comparing vision and Kinect sensing," in *Annual International Conference of the IEEE Engineering in Medicine and Biology Society (EMBC)*, Aug 2011, pp. 6491–6494.
- [10] J. Han, L. Shao, D. Xu, and J. Shotton, "Enhanced computer vision with Microsoft Kinect sensor: A review," *IEEE Transactions on Cybernetics*, vol. 43, no. 5, pp. 1318–1334, Oct 2013.
- [11] Microsoft. (2014, April) Kinect for Windows SDK v1.5. [Online]. Available: <http://www.microsoft.com/en-us/download/details.aspx?id=29866>
- [12] Microsoft. (2014, April) Coordinate spaces. [Online]. Available: <http://msdn.microsoft.com/en-us/library/hh973078.aspx>
- [13] W. H. Kruskal and W. A. Wallis, "Use of ranks in one-criterion variance analysis," *Journal of the American Statistical Association*, vol. 47, no. 260, pp. 583–621, 1952.
- [14] Microsoft. (2014, April) Kinect for Windows v2 Developer Preview Program. [Online]. Available: <http://www.microsoft.com/en-us/kinectforwindowsdev/newdevkit.aspx>